Title
Genetic analysis of Omi/HtrA2 and MUL1 in the PINK1/Parkin pathway

Author
Yun, Jina

Publication Date
2013

Peer reviewed|Thesis/dissertation

UNIVERSITY OF CALIFORNIA

Los Angeles

Genetic analysis of *Omi/HtrA2* and *MUL1* in the PINK1/Parkin pathway

A dissertation submitted in partial satisfaction of the

requirements for the degree Doctor of Philosophy

in Molecular and Medical Pharmacology

by

Jina Yun

2013

ABSTRACT OF THE DISSERTATION

Genetic analysis of *Omi/HtrA2* and *MUL1* in the PINK1/Parkin pathway

By

Jina Yun

Doctor of Philosophy in Molecular and Medical Pharmacology

University of California, Los Angeles, 2013

Professor Ming Guo, Chair

Parkinson's disease (PD) is the second most common neurodegenerative disorder. Poor understanding of PD pathogenesis has limited the development of effective therapies. Recently, studies on PD associated genes have linked mitochondrial dysfunction to underlying causes of PD. Mutations in the mitochondrial Ser/Thr kinase PINK1 or the Ubiquitin E3 ligase Parkin cause early onset hereditary PD. Genetic studies indicate that *PINK1* and *parkin* function in the same pathway to regulate mitochondrial dynamics through Mitofusin (MFN). This dissertation aims to identify other components in the PINK1/Parkin pathway. In chapter two, we investigate genetic interaction between *PINK1* and *Omi/HtrA2 in vivo*. Previously, mutations in the mitochondrial protease Omi/HtrA2 were identified in PD patients, and *in vitro* studies show that phosphorylation of Omi/HtrA2 is PINK1-dependent, suggesting that *Omi/HtrA2* acts downstream of *PINK1*. However, our work suggests that *Omi/HtrA2* does not function in the same genetic pathway as *PINK1*. *Omi/HtrA2* null mutants in *Drosophila* do not share any of *PINK1* mutant phenotypes. Furthermore, *Omi/HtrA2* and *PINK1* fail to modify each other's

mutant phenotypes. Based on our results, we do not favor a hypothesis in which Omi/HtrA2 plays an essential role in *PINK1/parkin* mediated PD pathogenesis. These data are also consistent with recent human genetics studies that show no association between *Omi/HtrA2* and PD. In chapter three, we identify MUL1, a mitochondrial ubiquitin E3 ligase, as a novel suppressor of *PINK1* mutants. MUL1 suppresses *PINK1* and *parkin* phenotypes including mitochondrial morphology, muscle degeneration, and dopaminergic neuronal phenotypes. MUL1 suppresses *PINK1* phenotypes by reducing MFN levels through ubiquitination. Further genetic epistasis studies indicate that *MUL1* acts in parallel to the PINK1/parkin pathway to regulate mitochondrial integrity. In mammalian cells, the PINK1/Parkin pathway has been shown to mediate the selective degradation of damaged mitochondria called mitophagy. We found that although MUL1 regulates MFN levels, Parkin-mediated mitophagy is not affected. In consistent with our genetic studies in *Drosophila*, these data support that MUL1 acting in parallel to PINK1/Parkin is conserved. Our work suggests that reduction of MFN by MUL1 is sufficient to reverse *PINK1*/*parkin* deficiency phenotypes and proposes MUL1 as a potential therapeutic target to modulate PD pathology.

The dissertation of Jina Yun is approved.

Heather R. Christofk

Daniel L. Kaufman

Alexander M. van der Bliek

Yibin Wang

James Akira Wohlschlegel

Ming Guo, Committee Chair

University of California, Los Angeles

2013

TABLE OF CONTENTS

LIST OF FIGURES

ACKNOWLEDGEMENTS

I would like to first thank my thesis advisor Ming Guo for the endless amount of support and encouragement she has provided. Her sympathy to patients and passion for a cure as a doctor have continuously inspired me. I am also thankful for her patience and effort to help me become a better scientist. I consider myself extremely lucky to have had Ming as a role model early on in my career. I am surely going to miss the many hours we spent discussing science and preparing manuscripts.

For great advice and mentorship, I would like to thank my committee members Heather Christofk, Daniel Kaufman, Alexander van der Bliek, Yibin Wang, and James Wohlschlegel. I really appreciate their time, help and advice to guide me.

I thank my parents Na-hyug Yun and Eun-kyu Park for their unlimited love and support. They have made many sacrifices so that I can pursue my dream, and have always been there to support me. I can never thank them enough for what they have done for me. I would also like to thank my sister Jung-ah Yun and my brother Jae-hyun Yun for their love and support.

I would also like to thank Atish Ganguly, Jin-chul Kim, Hakeem Lawal, Lok Kwan Leung, Michael Lizzio, Young-suk Nam, Prajal Patel, Ji-yeon Seo, and Yu Sun for their help, advice, and friendship.

Last but not least, I would like to acknowledge UCLA dissertation year fellowship and Glenn Family Foundation Scholarship through which this work was funded.

Chapter 2 is a version of Jina Yun, Joseph H. Cao, Mark W. Dodson, Ira E. Clark, Pankaj Kapahi, Ruhena B. Chowdhury, Ming Guo. "Loss-of-function analysis suggests that Omi/HtrA2 is not an essential component of the pink1/parkin pathway *in vivo*." J Neurosci. 28:14500-14510 (2008). We are very grateful to M. Miura for antibodies, J. Belote for fly strains, N. Tapon and A. Whitworth for communicating unpublished results, and A. Yamaguchi for generating one transgenic fly strain, B.A. Hay for insightful comments on the manuscript, F. Laski for use of his microtome, L. Cruz, H. Deng and J. Olson for technical help, and the Guo lab members for discussions.

Chapter 3 is a version of manuscript prepared for submission. Jina Yun, Huan Yang, Rajat Puri, Chunlai Wu, Michael Lizzio, Zuhang Sheng, and Ming Guo. "*MUL1*, a novel suppressor of *PINK1*, acts in parallel to the PINK1/parkin pathway to regulate mitochondrial integrity and body fat." We are very grateful to A. Whitworth for antibodies and DNA constructs, A. Courey for antibodies and fly strains, H. Bellen for fly strains, D. Chan and M. Cookson for stable cell lines, A. van der Bliek for reagents, H. Mcbride for communicating unpublished results, Rainbow transgenic for generating transgenic fly strains, P. Patel and L. Leung for insightful comments on the manuscript, F. Laski for use of his microtome, L. Dreier for use of his microscope, N. Freimer for use of his CO_2 incubators, H. Deng, B. Al-Anzi, H. Huang and Y. Sun for technical help and the Guo lab members for discussions.

BIOGRAPHICAL SKETCH

Jina Yun

University of California, Los Angeles
695 Charles E. Young Drive, Gonda, Rm 3309A
Los Angeles, CA 90095
Email: jinayun@ucla.edu
Tel: (310) 966-7523

Education

2007-present	University of California, Los Angeles, CA Ph.D. candidate, *Department of Molecular and Medical Pharmacology*
2006-2007	University of California, Los Angeles, CA Graduate student, *ACCESS program*
2002-2004	Yonsei University, Seoul, South Korea M.S., *Department of Biotechnology*
1998-2002	Yonsei University, Seoul, South Korea B.S., *Department of Biotechnology*

Awards

2011-2012	University of California, Los Angeles, Dissertation Year Fellowship
2009	Glenn Family Foundation Scholarship
2002-2004	Honors Tuition Waiver Scholarship
2002	Graduate Yonsei University with Highest Honors
1998-2002	Education Scholarship from Ministry of Patriots and Veterans Affairs

Research Experience

2006-present	Doctorial Research (Thesis Advisor: Ming Guo, M.D., Ph.D.) *Department of Molecular and Medical Pharmacology, UCLA, CA*
2004-2006	Research Assistant (Advisor: Jong Won Oh Ph.D.) *Department of Biotechnology*, Yonsei University, Seoul, Korea

2002 – 2004 Masters research (Thesis Advisor: Jong Won Oh Ph.D.)
Department of Biotechnology, Yonsei University, Seoul, Korea
Thesis: Functional Analysis of Recombinant PKR-like ER Kinase (PERK)

2000-2002 Undergraduate Research Assistant (Advisor: Jong Won Oh Ph.D.)
Department of Biotechnology, Yonsei University, Seoul, Korea

Publications

Yun, J., Lizzio, M.A. and Guo, M. *MUL1* as a novel suppressor of *PINK1* mutants and its regulation of mitochondrial dynamics through MFN. *In preparation*

Yun, J., Cao, J.H., Dodson, M.W., Clark, I.E., Kapahi, P., Chowdhury, R.B. and Guo, M. (2008) Loss-of-function analysis suggests that *Omi/HtrA2* is not an essential component of the *pink1/parkin* pathway *in vivo*. *Journal of Neuroscience* 28: 14500-14510.

Yun, J., Chung, H., Kim, S., Cho, H., and Oh, J.W. (2006) Purification and characterization of the functional catalytic domain of PKR-like Endoplasmic Reticulum Kinase expressed in *E. coli. J. Microbiol. Biotechnol.* 16, 9:1453-1458

Presentations

Yun, J., Lizzio, M and Guo, M. (2012) Identification of *MUL1* as a novel suppressor of the *pink1/parkin* null mutants. Poster presentation – Mitochondrial Trafficking and Function in Neuronal Health and Disease, Boston, MA

Yun, J., Cao, J.H., Dodson, M.W., Clark, I.E., Kapahi, P., Chowdhury, R.B. and Guo, M. (2009) Mutational Analysis of the mitochondrial protease Omi/HtrA2 and its interaction with the Parkinson's disease gene *pink1 in vivo.* Poster presentation – Annual Neurology Science Day, The department of Neurology, UCLA

Yun, J., Cao, J.H., Dodson, M.W., Clark, I.E., Kapahi, P., Chowdhury, R.B. and Guo, M. (2008) Mutational Analysis of the mitochondrial protease Omi/HtrA2 and its interaction with the Parkinson's disease gene *pink1 in vivo.* Poster presentation – Mitochondrial Biology in Cardiovascular Health & Diseases Conference, Bethesda, Maryland

Kim S.J., Yun, J., and Oh, J.W. (2005) Combination of a PRK2 inhibitor and interferon- a synergistically suppresses Hepatitis C Virus RNA replication. Poster presentation – The Annual Meeting & International Symposium of the Korean Society for Micorbiology and Biotechnology, Korea University, Seoul, Korea

Yun, J., Chung, H., Kim, J.H., and Oh, J.W. (2003) Modulation of endoplasmic reticulum stress-induced signaling pathway by Hepatitis C Virus nonstructural proteins. Poster presentation – The

International Symposium on the Korean Society of Medical Biochemistry and Molecular Biology, Seoul, Korea

Teaching Experience

Spring 2010	Life Sience 3 (LS3) teaching assistant *Department of Molecular, Cell and Developmental Biology*, *UCLA, CA*
Spring 2009	MCDB104 teaching assistant *Department of Molecular, Cell and Developmental Biology*, *UCLA, CA*
Fall 2002	Applied Microbiology teaching assistant *Department of Biotechnology*, *Yonsei University, Seoul, Korea*
Spring 2002	General Microbiology teaching assistant *Department of Biotechnology, Yonsei University, Seoul, Korea*

CHAPTER 1

INTRODUCTION

Parkinson's Disease

Parkinson's disease (PD), first reported by James Parkinson, is the second most common neurodegenerative disorder. The incidence of PD increases with age, affecting about 0.3%, 1%, and 4% of the population over the age of 40, 65, and 80 respectively (Dexter and Jenner, 2013). Symptoms of PD are largely divided into motor and non-motor symptoms. Motor symptoms include resting tremor, rigidity (stiffness), bradykinesia (slowness of movement), and postural instability. Non-motor symptoms include autonOmic dysfunction, cognitive impairment, neurobehavioral disorders such as depression and anxiety, and sensory and sleep abnormalities (Caballol et al., 2007; Jankovic, 2008). Pathological characteristics are preferential loss of dopmaminergic (DA) neurons in substantia nigra and presence of cytoplasmic protein aggregates called Lewy bodies (Dauer and Przedborski, 2003). Currently, there is no cure for PD available. Most PD treatments focus on relieving symptoms by replacing dopamine. However, the dompamine replacement therapies have several limitations which include no effect on the disease progression, relief of motor symptoms only, and loss of efficacy over time. In order to develop therapies that alter disease progression or address non-motor symptoms, better understanding of the pathogenesis is necessary. Our current studies suggests that the mitochondrial dysfunction and oxidative stress underlie PD pathogenesis (Dauer and Przedborski, 2003).

Mitochondrial dysfunction and PD

Mitochondrial dysfunction in sporadic PD

Early evidence of mitochondrial dysfunction in PD came from the discovery that MPTP (1-methyl-4-phenyl-1,2,3,6-tetrahydropyridine), a neurotoxin that inhibits complex I of mitochondrial respiratory chain causes parkinsonism in humans (Langston et al., 1983) and several animal models (Chiueh et al., 1984; Kolata, 1983; Langston et al., 1984a; Langston et al., 1984b). MPP+, an oxidized product of MPTP, is selectively taken up by DA neurons where it accumulates in mitochondria and inhibits complex I activity of mitochondrial respiratory chain (Nicklas et al., 1985; Ramsay et al., 1986). In addition to MPTP, rotenone, a complex I inhibitor, also causes highly selective nigrostriatal dopaminergic degeneration as well as cytoplasmic inclusions in rats (Betarbet et al., 2000; Sherer et al., 2003). The link between inhibition of complex I and parkinsonism was further substantiated by observations that complex I activity is reduced in the substantia nigra of PD patients (Parker et al., 1989; Schapira et al., 1989) (Hattori et al., 1991) as well as muscles (Bindoff et al., 1991; Shoffner et al., 1991), lymphocytes and platelets (Yoshino et al., 1992) of PD patients. Inhibition of complex I is believed to cause a reduction of ATP production and an increase in reactive oxygen species (ROS) (Abou-Sleiman et al., 2006), suggesting increased oxidative damage as a possible explanation for neuronal cell death. Indeed, protein carbonyls are increased in complex I from PD patients' brains, which is reproduced by treatment of rotenone (Keeney et al., 2006). Furthermore, paraquat, a pesticide that increases ROS, reproduces similar PD features of MPTP in frogs (Barbeau et al., 1985). Taken together, these studies strongly implicate the role of mitochondrial dysfunction and oxidative stress in PD pathogenesis.

Mitochondrial dysfunction in hereditary PD

PD was once believed to be caused only by exposure to environmental toxins. However, discoveries of genes associated with hereditary PD have changed the belief. Starting with

discovery of *SNCA* (*PARK1* and *PARK4)* that causes autosomal dOminant form of PD, linkage analyses have indentified five more genes associated with hereditary forms of PD – *parkin (PARK2), DJ-1 (PARK7), pten-induced kinase 1 (PINK1,PARK6), Leucine-rich repeat kinase 2 (LRRK2, PARK8),* and *ATP13A2 (PARK9).* Mutations in *SNCA* and *LRRK2* cause autosomal-dOminant PD whereas mutations in *parkin*, *PINK1, DJ-1,* and *ATP13A2* cause autosomal-recessive PD (Dexter and Jenner, 2013). Subsequently, studies of *parkin, PINK1,* and *DJ-1* have provided strong evidence that mitochondrial dysfunction and oxidative stress are important in the pathogenesis of hereditary PD.

Linkage analysis of autosomal recessive juvenile parkinsonism (AR-JP) reveal that deletions in *parkin* is responsible for the pathogenesis of AR-JP (Kitada et al., 1998). *Parkin* encodes an E3 uibiquitin ligase that contains a ubiquitin-like (UBL) domain, the first RING finger domain, a in-between RING (IBR), and the second RING finger domain. The RING finger and IBR domains confer on Parkin an E3 ubiquitin ligase activity that transfers ubiquitin moieties to target proteins (Shimura et al., 2000; Zhang et al., 2000). Studies of neuronal cells overexpressing Parkin suggest that Parkin has protective roles against various stresses induced by drug treatment, and the function is dependent on E3 ligase acitivty (Darios et al., 2003). The same study also reported that Parkin delays mitochondrial swelling and localizes to mitochondria upon stress, providing an early hint of Parkin's role in mitochondria. Direct evidence of Parkin's role in mitochondria came from an *in vivo* study using *Drosophila*. *parkin* null mutants show muscle degeneration and male sterility due to mitochondrial dysfunction (Greene et al., 2003). Subsequently, studies in *parkin* knockout mice reported decreased protein levels of complex I and IV subunits and reduced respiratory capacity (Palacino et al., 2004). Parkin's protective roles

against various stressors provide possible explanation why loss of *parkin* causes early onset of PD.

Another study from autosomal recessive PD identified *PINK1*as a PD associated gene (Valente et al., 2004a). *PINK1* encodes a Ser/Thr kinase that has mitochondrial targeting sequence (MTS) in its N-terminus followed by a transmembrane domain (TM) and a kinase domain. PINK1 mainly localizes to mitochondria and protects against stress-induced mitochondrial dysfunction. Several mutations within *PINK1* in PD patients suggest that loss of kinase activity contributes to the PD pathology (Corti et al., 2011). Similar to Parkin, overexpression of *PINK1* has protective roles against diverse stress inducers (Haque et al., 2008; Petit et al., 2005; Pridgeon et al., 2007; Wood-Kaczmar et al., 2008). In *Drosophila*, *PINK1 null* mutants show sensitivity toward stressors, muscle degeneration, and defects in mitochondrial integrity (Clark et al., 2006b; Park et al., 2006; Yang et al., 2006). Studies in *PINK1* knockout mice report decreased mitochondrial respiration in the brains (Gautier et al., 2008). PINK1's mitochondrial localization and mitochondrial phenotypes further strengthen the importance of mitochondrial function in PD.

PINK1 and parkin in the same pathway

The shocking phenotypic similarity between *PINK1* and *parkin* null mutants in *Drosophila* lead to further genetic interaction studies between these genes. These genetic studies have shown that *PINK1 parkin* double null mutants show the same phenotypes as single null mutants, indicating that these two PD genes act in the same genetic pathway (Clark et al., 2006b; Park et al., 2006; Yang et al., 2006). Furthermore, the observation that *parkin* overexpression suppresses *PINK1* mutant phenotypes, but not vice versa, places *parkin* downstream of *PINK1*. This pathway is also conserved in mammalian cells, and pathology of PD patients' fibroblasts

with mutations in *PINK1* is suppressed by wildtype *parkin* (Exner and Hartemann, 2009; Exner et al., 2007). These studies have important meanings in that 1) they place two PD associated genes in a pathway, strongly suggesting that deregulation of the pathway might cause early onset PD and 2) pathology of *PINK1* could be rescued by *parkin*, providing a therapeutic opportunity for patients with *PINK1* mutations. The studies also evoke an interesting question. How does the PINK1/Parkin pathway regulate mitochondrial integrity?

Role of the PINK1/Parkin pathway in mitochondrial dynamics

Mitochondria undergo constant changes in their shape, size, and subceullar localization in response to cellular energy demands, developmental processes, and environmental stimuli (Exner et al., 2012; Palmer et al., 2011). Mitochondrial morphology and size are determined through a balance between mitochondrial fusion and fission (Ferree and Shirihai, 2012; Palmer et al., 2011). The main regulators of mitochondrial fusion and fission are dynamin-like GTPases. Mitochondrial fusion is regulated by Mitofusin 1 and 2 (MFN1 and MFN2) whereas mitochondrial fission is mediated by Drp1 (Detmer and Chan, 2007). Studies show that excessive mitochondrial fusion or fission induced by loss of function or overexpression of the main regulators cause changes in mitochondrial morphology, size, and localization as well as changes in mitochondrial function (Bach et al., 2003; Frank et al., 2001; Lee et al., 2004; Misko et al., 2010; Otsuga et al., 1998; Santel and Fuller, 2001; Smirnova et al., 1998; Varadi et al., 2004). Abnormal mitochondrial morphologies observed in *parkin* and *PINK1* null mutant flies suggest a possibility of deregulation in mitochondrial dynamics. Genetic studies in *Drosophila* show that modulation of mitochondrial dynamics by *drp1* overexpression or *MFN* knockdown is

sufficient to suppress *PINK1* or *parkin* null mitochondrial phenotypes (Deng et al., 2008a; Poole et al., 2008b; Yang et al., 2008a). The studies suggest that the role of the PINK1/Parkin pathway is to regulate mitochondrial dynamics by inhibiting mitochondrial fusion and/or promoting mitochondrial fission. Although role of the PINK1/Parkin pathway in mitochondrial dynamics is maintained in mammalian cell culture systems, *parkin* or *PINK1* knockdown causes mitochondrial fragmentation that is suppressed by overexpression of *MFN* or dOminant negative form of *drp1* (*drp1K38A)* (Cui et al., 2010; Dagda et al., 2009; Lutz et al., 2009; Sandebring et al., 2009). This suggests that the PINK1/Parkin pathway in mammalian systems promotes fusion and/or inhibits fission. Reasons and explanations of the discrepancies between *Drosophila* and mammalian systems need to be further elucidated. Evidence directly connecting mitochondrial dynamics and the PINK1/Parkin pathway came from studies reporting that Parkin directly binds to and ubiquitinates MFN in *Drosophila* (Poole et al., 2008b; Ziviani et al., 2010). Consistently, MFN levels are increased in both *parkin* and *PINK1* null mutants, indicating that Parkin is dependent on PINK1 function to regulate MFN. The same regulation of MFN by Parkin is also shown in human dopaminergic neuronal cells (Gegg et al., 2010; Gegg and Schapira, 2011), suggesting that the regulation has relevance to the PD pathogenesis. Based on these observations, it was expected that mutations in *parkin* or *PINK1* comprOmise the regulation of MFN. Indeed, *parkin* and *PINK1* mutant fibroblasts from PD patients fail to show decrease in MFN levels and ubiquitination of MFN in response to stressors (Rakovic et al., 2011). These findings prove that deregulation of mitochondrial dynamics is associated with the PD pathology.

The PINK1/Parkin pathway in mitochondrial transport

Efforts to find proteins that interact with PINK1 identified mitochondrial Rho-GTPase (Miro) and Milton (Weihofen et al., 2009). Milton associates with mitochondria and regulates axonal transport of mitochondria to synapses (Stowers et al., 2002). The role of Miro in mitochondrial trafficking was characterized by studying *miro* mutants in *Drosophila* (Guo et al., 2005). In *miro* mutant muscles and neurons, mitochondria abnormally accumulate in cell bodies instead of axons and dendrites, suggesting that Miro controls the transport and distribution of mitochondria. Further studies have reveal that microtubule-dependent transport of mitochondria is mediated by Milton acting as an adaptor that binds to both kinesin heavy chain (KHC) and Miro (Glater et al., 2006). Based on the function of Miro and Milton in the transport and distribution of mitochondria, complex formation among PINK1, Miro, and Milton proposes an intriguing hypothesis that PINK1 regulates mitochondrial transport together with Miro and Milton. Recent studies prove that the PINK1/Parkin pathway regulates mitochondrial transport in rat hippocampal neurons and *Drosophila* larval neurons (Liu et al., 2012; Wang et al., 2011). PINK1 or *parkin* overexpression arrests mitochondrial movement. The control of mitochondrial movement is achieved by sequential events - phosphorylation of Miro by PINK1 that targets Miro for ubiquitination by Parkin, proteasomal degradation of Miro, and dissociation of kinesin from mitochondria. These studies show that the PINK1/Parkin pathway is not only involved in mitochondrial dynamics but also regulates mitochondrial transport and distribution.

The PINK1/Parkin pathway in mitophagy and quality control

In addition to mitochondrial morphology and transport, the PINK1/Parkin pathway functions in mitochondrial quality control via the selective autophagic degradation of mitochondria, called mitophagy. Mitophagy was previously described in cultured rat hepatocytes

and *Saccharomyces cerevisiae* (Kissova et al., 2004; Rodriguez-Enriquez et al., 2006). However, Richard Youle's group first linked the PINK1/Parkin pathway to mitophagy using human cell culture (Narendra et al., 2008). In HeLa cells overexpressing *parkin*, dissipation of mitochondrial membrane potential using the mitochondrial uncoupler CCCP causes the accumulation of PINK1 in the mitochondria, which triggers recruitment of Parkin onto mitochondria resulting in autophagic degradation of the mitochondria (Matsuda et al., 2010; Narendra et al., 2008; Narendra et al., 2010b). Further studies have demonstrated that recruited Parkin ubiquitinates a broad range of mitochondrial outer membrane proteins including MFN (Chan et al., 2011; Tanaka et al., 2010). The massive ubiquitination on mitochondria recruits the autophagic adaptor protein p62/SQSTM1, which in turn brings the autophagic machinery to the mitochondria (Ding et al., 2010; Geisler et al., 2010; Narendra et al., 2010a). Based on these studies, one can speculate that PD patients have defects in the clearance of mitochondria. Indeed, Parkin-mediated mitophagy is impaired in *PINK1* mutant fibroblasts from PD patients (Rakovic et al., 2013)

Drosophila as a model organism to study the PINK1/Parkin pathway

Drosophila melanogaster is an advantageous system to study biological processes and diseases. Most genes involved in crucial biological processes and diseases are conserved in *Drosophila*, but there is less redundancy in genes (Rubin, 2000), reducing the complexity of studying gene function. Generation time is relatively short (~10 days), and maintenance is easy and inexpensive. In addition, numerous genetic tools are available for gene expression, knockdown, deletion, as well as mutagenesis. Combination of techniques, great numbers of flies

accumulated for decades, and short generation time facilitates forward and reverse genetic screening (Guo, 2010; Guo, 2012).

When it comes to studying the PINK1/Parkin pathway *in vivo*, the advantages are greater. Although *PINK1* or *parkin* loss of function has been studied in other *in vivo* model systems (Anichtchik et al., 2008; Flinn et al., 2009; Kitada et al., 2007; Palacino et al., 2004; Ved et al., 2005), *Drosophila* shows the strongest phenotypes among all. Due to its strong phenotypes and easy genetic manipulation, important studies that first placed *PINK1* and *parkin* in the same pathway (Clark et al., 2006b; Park et al., 2006; Yang et al., 2006) and revealed its roles in mitochondrial dynamics (Deng et al., 2008a; Poole et al., 2008b; Yang et al., 2008a) and mitochondrial transport (Liu et al., 2012; Wang et al., 2011) were done using *Drosophila*. Furthermore, unbiased genetic screens exploiting several phenotypes of *PINK1* mutants in *Drosophila* identified multiple modifiers (Fernandes and Rao, 2011; Imai et al., 2010; Liu and Lu, 2010; Tain et al., 2009; Vo et al., 2012), providing hints of potential other roles of the PINK1/Parkin pathway.

REFERENCES

Abou-Sleiman, P.M., M.M. Muqit, and N.W. Wood. 2006. Expanding insights of mitochondrial dysfunction in Parkinson's disease. *Nat Rev Neurosci*. 7:207-219.

Anichtchik, O., H. Diekmann, A. Fleming, A. Roach, P. Goldsmith, and D.C. Rubinsztein. 2008. Loss of PINK1 function affects development and results in neurodegeneration in zebrafish. *J Neurosci*. 28:8199-8207.

Bach, D., S. Pich, F.X. Soriano, N. Vega, B. Baumgartner, J. Oriola, J.R. Daugaard, J. Lloberas, M. Camps, J.R. Zierath, R. Rabasa-Lhoret, H. Wallberg-Henriksson, M. Laville, M. Palacin, H. Vidal, F. Rivera, M. Brand, and A. Zorzano. 2003. Mitofusin-2 determines mitochondrial network architecture and mitochondrial metabolism. A novel regulatory mechanism altered in obesity. *J Biol Chem*. 278:17190-17197.

Barbeau, A., L. Dallaire, N.T. Buu, J. Poirier, and E. Rucinska. 1985. Comparative behavioral, biochemical and pigmentary effects of MPTP, MPP+ and paraquat in Rana pipiens. *Life Sci*. 37:1529-1538.

Betarbet, R., T.B. Sherer, G. MacKenzie, M. Garcia-Osuna, A.V. Panov, and J.T. Greenamyre. 2000. Chronic systemic pesticide exposure reproduces features of Parkinson's disease. *Nat Neurosci*. 3:1301-1306.

Bindoff, L.A., M.A. Birch-Machin, N.E. Cartlidge, W.D. Parker, Jr., and D.M. Turnbull. 1991. Respiratory chain abnormalities in skeletal muscle from patients with Parkinson's disease. *J Neurol Sci*. 104:203-208.

Caballol, N., M.J. Marti, and E. Tolosa. 2007. Cognitive dysfunction and dementia in Parkinson disease. *Mov Disord*. 22 Suppl 17:S358-366.

Chan, N.C., A.M. Salazar, A.H. Pham, M.J. Sweredoski, N.J. Kolawa, R.L. Graham, S. Hess, and D.C. Chan. 2011. Broad activation of the ubiquitin-proteasome system by Parkin is critical for mitophagy. *Hum Mol Genet*. 20:1726-1737.

Chiueh, C.C., S.P. Markey, R.S. Burns, J.N. Johannessen, D.M. Jacobowitz, and I.J. Kopin. 1984. Neurochemical and behavioral effects of 1-methyl-4-phenyl-1,2,3,6- tetrahydropyridine (MPTP) in rat, guinea pig, and monkey. *Psychopharmacol Bull*. 20:548-553.

Clark, I.E., M.W. Dodson, C. Jiang, J.H. Cao, J.R. Huh, J.H. Seol, S.J. Yoo, B.A. Hay, and M. Guo. 2006. Drosophila pink1 is required for mitochondrial function and interacts genetically with parkin. *Nature*. 441:1162-1166.

Corti, O., S. Lesage, and A. Brice. 2011. What genetics tells us about the causes and mechanisms of Parkinson's disease. *Physiol Rev*. 91:1161-1218.

Cui, M., X. Tang, W.V. Christian, Y. Yoon, and K. Tieu. 2010. Perturbations in mitochondrial dynamics induced by human mutant PINK1 can be rescued by the mitochondrial division inhibitor mdivi-1. *J Biol Chem*. 285:11740-11752.

Dagda, R.K., S.J. Cherra, 3rd, S.M. Kulich, A. Tandon, D. Park, and C.T. Chu. 2009. Loss of PINK1 function promotes mitophagy through effects on oxidative stress and mitochondrial fission. *J Biol Chem*. 284:13843-13855.

Darios, F., O. Corti, C.B. Lucking, C. Hampe, M.P. Muriel, N. Abbas, W.J. Gu, E.C. Hirsch, T. Rooney, M. Ruberg, and A. Brice. 2003. Parkin prevents mitochondrial swelling and cytochrome c release in mitochondria-dependent cell death. *Hum Mol Genet*. 12:517-526.

Dauer, W., and S. Przedborski. 2003. Parkinson's disease: mechanisms and models. *Neuron*. 39:889-909.

Deng, H., M.W. Dodson, H. Huang, and M. Guo. 2008. The Parkinson's disease genes pink1 and parkin promote mitochondrial fission and/or inhibit fusion in Drosophila. *Proc Natl Acad Sci U S A*. 105:14503-14508.

Detmer, S.A., and D.C. Chan. 2007. Functions and dysfunctions of mitochondrial dynamics. *Nat Rev Mol Cell Biol*. 8:870-879.

Dexter, D.T., and P. Jenner. 2013. Parkinson's disease: From pathology to molecular disease mechanisms. *Free Radic Biol Med*.

Ding, W.X., H.M. Ni, M. Li, Y. Liao, X. Chen, D.B. Stolz, G.W. Dorn, 2nd, and X.M. Yin. 2010. Nix is critical to two distinct phases of mitophagy, reactive oxygen species-mediated autophagy induction and Parkin-ubiquitin-p62-mediated mitochondrial priming. *J Biol Chem*. 285:27879-27890.

Exner, M., and P. Hartemann. 2009. Summary of the second meeting of the International Forum on Water Hygiene in Buildings (IFOWAHB) from 01 to 02.06.2007 in Stockholm. *Int J Hyg Environ Health*. 212:449-458.

Exner, N., A.K. Lutz, C. Haass, and K.F. Winklhofer. 2012. Mitochondrial dysfunction in Parkinson's disease: molecular mechanisms and pathophysiological consequences. *EMBO J*. 31:3038-3062.

Exner, N., B. Treske, D. Paquet, K. Holmstrom, C. Schiesling, S. Gispert, I. Carballo-Carbajal, D. Berg, H.H. Hoepken, T. Gasser, R. Kruger, K.F. Winklhofer, F. Vogel, A.S. Reichert, G. Auburger, P.J. Kahle, B. Schmid, and C. Haass. 2007. Loss-of-function of human PINK1 results in mitochondrial pathology and can be rescued by parkin. *J Neurosci*. 27:12413-12418.

Fernandes, C., and Y. Rao. 2011. Genome-wide screen for modifiers of Parkinson's disease genes in Drosophila. *Mol Brain*. 4:17.

Ferree, A., and O. Shirihai. 2012. Mitochondrial dynamics: the intersection of form and function. *Adv Exp Med Biol*. 748:13-40.

Flinn, L., H. Mortiboys, K. Volkmann, R.W. Koster, P.W. Ingham, and O. Bandmann. 2009. Complex I deficiency and dopaminergic neuronal cell loss in parkin-deficient zebrafish (Danio rerio). *Brain*. 132:1613-1623.

Frank, S., B. Gaume, E.S. Bergmann-Leitner, W.W. Leitner, E.G. Robert, F. Catez, C.L. Smith, and R.J. Youle. 2001. The role of dynamin-related protein 1, a mediator of mitochondrial fission, in apoptosis. *Dev Cell*. 1:515-525.

Gautier, C.A., T. Kitada, and J. Shen. 2008. Loss of PINK1 causes mitochondrial functional defects and increased sensitivity to oxidative stress. *Proc Natl Acad Sci U S A*. 105:11364-11369.

Gegg, M.E., J.M. Cooper, K.Y. Chau, M. Rojo, A.H. Schapira, and J.W. Taanman. 2010. Mitofusin 1 and mitofusin 2 are ubiquitinated in a PINK1/parkin-dependent manner upon induction of mitophagy. *Hum Mol Genet*. 19:4861-4870.

Gegg, M.E., and A.H. Schapira. 2011. PINK1-parkin-dependent mitophagy involves ubiquitination of mitofusins 1 and 2: Implications for Parkinson disease pathogenesis. *Autophagy*. 7:243-245.

Geisler, S., K.M. Holmstrom, D. Skujat, F.C. Fiesel, O.C. Rothfuss, P.J. Kahle, and W. Springer. 2010. PINK1/Parkin-mediated mitophagy is dependent on VDAC1 and p62/SQSTM1. *Nat Cell Biol*. 12:119-131.

Glater, E.E., L.J. Megeath, R.S. Stowers, and T.L. Schwarz. 2006. Axonal transport of mitochondria requires milton to recruit kinesin heavy chain and is light chain independent. *J Cell Biol*. 173:545-557.

Greene, J.C., A.J. Whitworth, I. Kuo, L.A. Andrews, M.B. Feany, and L.J. Pallanck. 2003. Mitochondrial pathology and apoptotic muscle degeneration in Drosophila parkin mutants. *Proc Natl Acad Sci U S A*. 100:4078-4083.

Guo, M. 2010. What have we learned from Drosophila models of Parkinson's disease? *Prog Brain Res*. 184:3-16.

Guo, M. 2012. Drosophila as a model to study mitochondrial dysfunction in Parkinson's disease. *Cold Spring Harb Perspect Med*. 2.

Guo, X., G.T. Macleod, A. Wellington, F. Hu, S. Panchumarthi, M. Schoenfield, L. Marin, M.P. Charlton, H.L. Atwood, and K.E. Zinsmaier. 2005. The GTPase dMiro is required for axonal transport of mitochondria to Drosophila synapses. *Neuron*. 47:379-393.

Haque, M.E., K.J. Thomas, C. D'Souza, S. Callaghan, T. Kitada, R.S. Slack, P. Fraser, M.R. Cookson, A. Tandon, and D.S. Park. 2008. Cytoplasmic Pink1 activity protects neurons from dopaminergic neurotoxin MPTP. *Proc Natl Acad Sci U S A*. 105:1716-1721.

Hattori, N., M. Tanaka, T. Ozawa, and Y. Mizuno. 1991. Immunohistochemical studies on complexes I, II, III, and IV of mitochondria in Parkinson's disease. *Ann Neurol*. 30:563-571.

Imai, Y., T. Kanao, T. Sawada, Y. Kobayashi, Y. Moriwaki, Y. Ishida, K. Takeda, H. Ichijo, B. Lu, and R. Takahashi. 2010. The loss of PGAM5 suppresses the mitochondrial degeneration caused by inactivation of PINK1 in Drosophila. *PLoS Genet*. 6:e1001229.

Jankovic, J. 2008. Parkinson's disease: clinical features and diagnosis. *J Neurol Neurosurg Psychiatry*. 79:368-376.

Keeney, P.M., J. Xie, R.A. Capaldi, and J.P. Bennett, Jr. 2006. Parkinson's disease brain mitochondrial complex I has oxidatively damaged subunits and is functionally impaired and misassembled. *J Neurosci*. 26:5256-5264.

Kissova, I., M. Deffieu, S. Manon, and N. Camougrand. 2004. Uth1p is involved in the autophagic degradation of mitochondria. *J Biol Chem*. 279:39068-39074.

Kitada, T., S. Asakawa, N. Hattori, H. Matsumine, Y. Yamamura, S. Minoshima, M. Yokochi, Y. Mizuno, and N. Shimizu. 1998. Mutations in the parkin gene cause autosomal recessive juvenile parkinsonism. *Nature*. 392:605-608.

Kitada, T., A. Pisani, D.R. Porter, H. Yamaguchi, A. Tscherter, G. Martella, P. Bonsi, C. Zhang, E.N. Pothos, and J. Shen. 2007. Impaired dopamine release and synaptic plasticity in the striatum of PINK1-deficient mice. *Proc Natl Acad Sci U S A*. 104:11441-11446.

Kolata, G. 1983. Monkey model of Parkinson's disease. *Science*. 220:705.

Langston, J.W., P. Ballard, J.W. Tetrud, and I. Irwin. 1983. Chronic Parkinsonism in humans due to a product of meperidine-analog synthesis. *Science*. 219:979-980.

Langston, J.W., I. Irwin, E.B. Langston, and L.S. Forno. 1984a. Pargyline prevents MPTP-induced parkinsonism in primates. *Science*. 225:1480-1482.

Langston, J.W., E.B. Langston, and I. Irwin. 1984b. MPTP-induced parkinsonism in human and non-human primates--clinical and experimental aspects. *Acta Neurol Scand Suppl*. 100:49-54.

Lee, Y.J., S.Y. Jeong, M. Karbowski, C.L. Smith, and R.J. Youle. 2004. Roles of the mammalian mitochondrial fission and fusion mediators Fis1, Drp1, and Opa1 in apoptosis. *Mol Biol Cell*. 15:5001-5011.

Liu, S., and B. Lu. 2010. Reduction of protein translation and activation of autophagy protect against PINK1 pathogenesis in Drosophila melanogaster. *PLoS Genet*. 6:e1001237.

Liu, S., T. Sawada, S. Lee, W. Yu, G. Silverio, P. Alapatt, I. Millan, A. Shen, W. Saxton, T. Kanao, R. Takahashi, N. Hattori, Y. Imai, and B. Lu. 2012. Parkinson's disease-associated kinase PINK1 regulates Miro protein level and axonal transport of mitochondria. *PLoS Genet*. 8:e1002537.

Lutz, A.K., N. Exner, M.E. Fett, J.S. Schlehe, K. Kloos, K. Lammermann, B. Brunner, A. Kurz-Drexler, F. Vogel, A.S. Reichert, L. Bouman, D. Vogt-Weisenhorn, W. Wurst, J. Tatzelt, C. Haass, and K.F. Winklhofer. 2009. Loss of parkin or PINK1 function increases Drp1-dependent mitochondrial fragmentation. *J Biol Chem*. 284:22938-22951.

Matsuda, N., S. Sato, K. Shiba, K. Okatsu, K. Saisho, C.A. Gautier, Y.S. Sou, S. Saiki, S. Kawajiri, F. Sato, M. Kimura, M. Komatsu, N. Hattori, and K. Tanaka. 2010. PINK1 stabilized by mitochondrial depolarization recruits Parkin to damaged mitochondria and activates latent Parkin for mitophagy. *J Cell Biol*. 189:211-221.

Misko, A., S. Jiang, I. Wegorzewska, J. Milbrandt, and R.H. Baloh. 2010. Mitofusin 2 is necessary for transport of axonal mitochondria and interacts with the Miro/Milton complex. *J Neurosci*. 30:4232-4240.

Narendra, D., L.A. Kane, D.N. Hauser, I.M. Fearnley, and R.J. Youle. 2010a. p62/SQSTM1 is required for Parkin-induced mitochondrial clustering but not mitophagy; VDAC1 is dispensable for both. *Autophagy*. 6:1090-1106.

Narendra, D., A. Tanaka, D.F. Suen, and R.J. Youle. 2008. Parkin is recruited selectively to impaired mitochondria and promotes their autophagy. *J Cell Biol*. 183:795-803.

Narendra, D.P., S.M. Jin, A. Tanaka, D.F. Suen, C.A. Gautier, J. Shen, M.R. Cookson, and R.J. Youle. 2010b. PINK1 is selectively stabilized on impaired mitochondria to activate Parkin. *PLoS Biol*. 8:e1000298.

Nicklas, W.J., I. Vyas, and R.E. Heikkila. 1985. Inhibition of NADH-linked oxidation in brain mitochondria by 1-methyl-4-phenyl-pyridine, a metabolite of the neurotoxin, 1-methyl-4-phenyl-1,2,5,6-tetrahydropyridine. *Life Sci*. 36:2503-2508.

Otsuga, D., B.R. Keegan, E. Brisch, J.W. Thatcher, G.J. Hermann, W. Bleazard, and J.M. Shaw. 1998. The dynamin-related GTPase, Dnm1p, controls mitochondrial morphology in yeast. *J Cell Biol*. 143:333-349.

Palacino, J.J., D. Sagi, M.S. Goldberg, S. Krauss, C. Motz, M. Wacker, J. Klose, and J. Shen. 2004. Mitochondrial dysfunction and oxidative damage in parkin-deficient mice. *J Biol Chem*. 279:18614-18622.

Palmer, C.S., L.D. Osellame, D. Stojanovski, and M.T. Ryan. 2011. The regulation of mitochondrial morphology: intricate mechanisms and dynamic machinery. *Cell Signal*. 23:1534-1545.

Park, J., S.B. Lee, S. Lee, Y. Kim, S. Song, S. Kim, E. Bae, J. Kim, M. Shong, J.M. Kim, and J. Chung. 2006. Mitochondrial dysfunction in Drosophila PINK1 mutants is complemented by parkin. *Nature*. 441:1157-1161.

Parker, W.D., Jr., S.J. Boyson, and J.K. Parks. 1989. Abnormalities of the electron transport chain in idiopathic Parkinson's disease. *Ann Neurol*. 26:719-723.

Petit, A., T. Kawarai, E. Paitel, N. Sanjo, M. Maj, M. Scheid, F. Chen, Y. Gu, H. Hasegawa, S. Salehi-Rad, L. Wang, E. Rogaeva, P. Fraser, B. Robinson, P. St George-Hyslop, and A. Tandon. 2005. Wild-type PINK1 prevents basal and induced neuronal apoptosis, a

protective effect abrogated by Parkinson disease-related mutations. *J Biol Chem*. 280:34025-34032.

Poole, A.C., R.E. Thomas, L.A. Andrews, H.M. McBride, A.J. Whitworth, and L.J. Pallanck. 2008. The PINK1/Parkin pathway regulates mitochondrial morphology. *Proc Natl Acad Sci U S A*. 105:1638-1643.

Pridgeon, J.W., J.A. Olzmann, L.S. Chin, and L. Li. 2007. PINK1 protects against oxidative stress by phosphorylating mitochondrial chaperone TRAP1. *PLoS Biol*. 5:e172.

Rakovic, A., A. Grunewald, J. Kottwitz, N. Bruggemann, P.P. Pramstaller, K. Lohmann, and C. Klein. 2011. Mutations in PINK1 and Parkin impair ubiquitination of Mitofusins in human fibroblasts. *PLoS One*. 6:e16746.

Rakovic, A., K. Shurkewitsch, P. Seibler, A. Grunewald, A. Zanon, J. Hagenah, D. Krainc, and C. Klein. 2013. Phosphatase and Tensin Homolog (PTEN)-induced Putative Kinase 1 (PINK1)-dependent Ubiquitination of Endogenous Parkin Attenuates Mitophagy: STUDY IN HUMAN PRIMARY FIBROBLASTS AND INDUCED PLURIPOTENT STEM CELL-DERIVED NEURONS. *J Biol Chem*. 288:2223-2237.

Ramsay, R.R., J.I. Salach, and T.P. Singer. 1986. Uptake of the neurotoxin 1-methyl-4-phenylpyridine (MPP+) by mitochondria and its relation to the inhibition of the mitochondrial oxidation of NAD+-linked substrates by MPP+. *Biochem Biophys Res Commun*. 134:743-748.

Rodriguez-Enriquez, S., I. Kim, R.T. Currin, and J.J. Lemasters. 2006. Tracker dyes to probe mitochondrial autophagy (mitophagy) in rat hepatocytes. *Autophagy*. 2:39-46.

Rubin, G.M. 2000. Biological annotation of the Drosophila genome sequence. *Novartis Found Symp*. 229:79-82; discussion 82-73.

Sandebring, A., K.J. Thomas, A. Beilina, M. van der Brug, M.M. Cleland, R. Ahmad, D.W. Miller, I. Zambrano, R.F. Cowburn, H. Behbahani, A. Cedazo-Minguez, and M.R. Cookson. 2009. Mitochondrial alterations in PINK1 deficient cells are influenced by calcineurin-dependent dephosphorylation of dynamin-related protein 1. *PLoS One*. 4:e5701.

Santel, A., and M.T. Fuller. 2001. Control of mitochondrial morphology by a human mitofusin. *J Cell Sci*. 114:867-874.

Schapira, A.H., J.M. Cooper, D. Dexter, P. Jenner, J.B. Clark, and C.D. Marsden. 1989. Mitochondrial complex I deficiency in Parkinson's disease. *Lancet*. 1:1269.

Sherer, T.B., R. Betarbet, C.M. Testa, B.B. Seo, J.R. Richardson, J.H. Kim, G.W. Miller, T. Yagi, A. Matsuno-Yagi, and J.T. Greenamyre. 2003. Mechanism of toxicity in rotenone models of Parkinson's disease. *J Neurosci*. 23:10756-10764.

Shimura, H., N. Hattori, S. Kubo, Y. Mizuno, S. Asakawa, S. Minoshima, N. Shimizu, K. Iwai, T. Chiba, K. Tanaka, and T. Suzuki. 2000. Familial Parkinson disease gene product, parkin, is a ubiquitin-protein ligase. *Nat Genet*. 25:302-305.

Shoffner, J.M., R.L. Watts, J.L. Juncos, A. Torroni, and D.C. Wallace. 1991. Mitochondrial oxidative phosphorylation defects in Parkinson's disease. *Ann Neurol*. 30:332-339.

Smirnova, E., D.L. Shurland, S.N. Ryazantsev, and A.M. van der Bliek. 1998. A human dynamin-related protein controls the distribution of mitochondria. *J Cell Biol*. 143:351-358.

Stowers, R.S., L.J. Megeath, J. Gorska-Andrzejak, I.A. Meinertzhagen, and T.L. Schwarz. 2002. Axonal transport of mitochondria to synapses depends on milton, a novel Drosophila protein. *Neuron*. 36:1063-1077.

Tain, L.S., H. Mortiboys, R.N. Tao, E. Ziviani, O. Bandmann, and A.J. Whitworth. 2009. Rapamycin activation of 4E-BP prevents parkinsonian dopaminergic neuron loss. *Nat Neurosci*. 12:1129-1135.

Tanaka, A., M.M. Cleland, S. Xu, D.P. Narendra, D.F. Suen, M. Karbowski, and R.J. Youle. 2010. Proteasome and p97 mediate mitophagy and degradation of mitofusins induced by Parkin. *J Cell Biol*. 191:1367-1380.

Valente, E.M., P.M. Abou-Sleiman, V. Caputo, M.M. Muqit, K. Harvey, S. Gispert, Z. Ali, D. Del Turco, A.R. Bentivoglio, D.G. Healy, A. Albanese, R. Nussbaum, R. Gonzalez-Maldonado, T. Deller, S. Salvi, P. Cortelli, W.P. Gilks, D.S. Latchman, R.J. Harvey, B. Dallapiccola, G. Auburger, and N.W. Wood. 2004. Hereditary early-onset Parkinson's disease caused by mutations in PINK1. *Science*. 304:1158-1160.

Varadi, A., L.I. Johnson-Cadwell, V. Cirulli, Y. Yoon, V.J. Allan, and G.A. Rutter. 2004. Cytoplasmic dynein regulates the subcellular distribution of mitochondria by controlling the recruitment of the fission factor dynamin-related protein-1. *J Cell Sci*. 117:4389-4400.

Ved, R., S. Saha, B. Westlund, C. Perier, L. Burnam, A. Sluder, M. Hoener, C.M. Rodrigues, A. Alfonso, C. Steer, L. Liu, S. Przedborski, and B. Wolozin. 2005. Similar patterns of mitochondrial vulnerability and rescue induced by genetic modification of alpha-synuclein, parkin, and DJ-1 in Caenorhabditis elegans. *J Biol Chem*. 280:42655-42668.

Vo, S.H., M. Butzlaff, S.K. Pru, R.A. Ni Charthaigh, P. Karsten, A. Lankes, S. Hamm, M. Simons, B. Adryan, J.B. Schulz, and A. Voigt. 2012. Large-scale screen for modifiers of ataxin-3-derived polyglutamine-induced toxicity in Drosophila. *PLoS One*. 7:e47452.

Wang, X., D. Winter, G. Ashrafi, J. Schlehe, Y.L. Wong, D. Selkoe, S. Rice, J. Steen, M.J. LaVoie, and T.L. Schwarz. 2011. PINK1 and Parkin target Miro for phosphorylation and degradation to arrest mitochondrial motility. *Cell*. 147:893-906.

Weihofen, A., K.J. Thomas, B.L. Ostaszewski, M.R. Cookson, and D.J. Selkoe. 2009. Pink1 forms a multiprotein complex with Miro and Milton, linking Pink1 function to mitochondrial trafficking. *Biochemistry*. 48:2045-2052.

Wood-Kaczmar, A., S. Gandhi, Z. Yao, A.Y. Abramov, E.A. Miljan, G. Keen, L. Stanyer, I. Hargreaves, K. Klupsch, E. Deas, J. Downward, L. Mansfield, P. Jat, J. Taylor, S. Heales, M.R. Duchen, D. Latchman, S.J. Tabrizi, and N.W. Wood. 2008. PINK1 is necessary for long term survival and mitochondrial function in human dopaminergic neurons. *PLoS One*. 3:e2455.

Yang, Y., S. Gehrke, Y. Imai, Z. Huang, Y. Ouyang, J.W. Wang, L. Yang, M.F. Beal, H. Vogel, and B. Lu. 2006. Mitochondrial pathology and muscle and dopaminergic neuron degeneration caused by inactivation of Drosophila Pink1 is rescued by Parkin. *Proc Natl Acad Sci U S A*. 103:10793-10798.

Yang, Y., Y. Ouyang, L. Yang, M.F. Beal, A. McQuibban, H. Vogel, and B. Lu. 2008. Pink1 regulates mitochondrial dynamics through interaction with the fission/fusion machinery. *Proc Natl Acad Sci U S A*. 105:7070-7075.

Yoshino, H., Y. Nakagawa-Hattori, T. Kondo, and Y. Mizuno. 1992. Mitochondrial complex I and II activities of lymphocytes and platelets in Parkinson's disease. *J Neural Transm Park Dis Dement Sect*. 4:27-34.

Zhang, Y., J. Gao, K.K. Chung, H. Huang, V.L. Dawson, and T.M. Dawson. 2000. Parkin functions as an E2-dependent ubiquitin- protein ligase and promotes the degradation of the synaptic vesicle-associated protein, CDCrel-1. *Proc Natl Acad Sci U S A*. 97:13354-13359.

Ziviani, E., R.N. Tao, and A.J. Whitworth. 2010. Drosophila parkin requires PINK1 for mitochondrial translocation and ubiquitinates mitofusin. *Proc Natl Acad Sci U S A*. 107:5018-5023.

CHAPTER 2

Loss-of-Function Analysis Suggests That *Omi/HtrA2* Is Not an Essential Component of the *pink1/parkin* Pathway *In Vivo*

Jina Yun,[1,2], Joseph H. Cao,[1] Mark W. Dodson,[1,4] Ira E. Clark,[1] Pankaj Kapahi,[5] Ruhena B. Chowdhury,[6] and Ming Guo[1,2,3,4]

Departments of [1]Neurology and [2]Molecular and Medical Pharmacology and [3]Brain Research Institute, The David Geffen School of Medicine, and [4]Molecular Biology Institute, University of California, Los Angeles, Los Angeles, California 90095, [5]Buck Institute for Age Research, Novato, California 94945, and [6]Cancer Research UK, London Research Institute, London WC2A 3PX, United Kingdom

Published in

Journal of Neuroscience

ABSTRACT

Recently, a mutation in the mitochondrial protease Omi/HtrA2, G399S, was found in sporadic Parkinson's disease (PD) patients, leading to the designation of *Omi/HtrA2* as PD locus 13 (*PARK13*). G399S reportedly results in reduced Omi protease activity. *In vitro* studies have suggested that *Omi/HtrA2* acts downstream of *PINK1*, mutations in which mediate recessive forms of PD. We, as well as other, have previously shown that the *Drosophila* homologs of the familial PD genes, *PINK1* (*PARK6*) and *PARKIN* (*PARK2*), function in a common genetic pathway to regulate mitochondrial integrity and dynamics. Whether *Omi/HtrA2* regulates mitochondrial integrity and whether it acts downstream of *PINK1 in vivo* remain to be explored. Here, we show that *Omi/HtrA2* null mutants in *Drosophila*, in contrast to *pink1* or *parkin* null mutants, do not show mitochondrial morphological defects. Extensive genetic interaction studies do not provide support for models in which *Omi/HtrA2* functions in the same genetic pathway as *pink1*, or carries out partially redundant functions with pink1, at least with respect to regulation of mitochondrial integrity and dynamics. Furthermore, Omi/HtrA2 G399S retains significant, if not full, function of Omi/HtrA2, compared with expression of protease-comprOmised versions of the protein. In light of recent findings showing that G399S can be found at comparable frequencies in PD patients and healthy controls, we do not favor a hypothesis in which *Omi/HtrA2* plays an essential role in PD pathogenesis, at least with respect to regulation of mitochondrial integrity in the *pink1/parkin* pathway.

INTRODUCTION

Parkinson disease (PD) is characterized by degeneration of nigrostriatal dopaminergic neurons in the midbrain (Dauer and Przedborski, 2003), and genetic forms of the disease have

provided insight into PD pathogenesis (Hardy et al., 2006). Mutations in *PINK1 (PARK6)*, a nuclear gene encoding a mitochondrial serine-threonine kinase, and *PARKIN (PARK2)*, cause recessively inherited forms of PD/Parkinsonism (Kitada et al., 1998; Valente et al., 2004b). *Drosophila* homologs of *PINK1* and *PARKIN* act in a common genetic pathway (Clark et al., 2006b; Park et al., 2006; Yang et al., 2006) to promote mitochondrial fission and/or inhibit mitochondrial fusion in multiple tissues including dopaminergic neurons (Deng et al., 2009; Poole et al., 2008b; Yang et al., 2008a). Consistent with findings in *Drosophila*, patients with *PINK1* or *PARKIN* mutations have indistinguishable clinical features, and also show mitochondrial defects (Dodson and Guo, 2007; Ibanez et al., 2006). Recent studies also suggest that *PINK1* and *PARKIN* regulate mitochondrial functions in mammals (Exner et al., 2007; Gautier et al., 2008; Piccoli et al., 2008; Wood-Kaczmar et al., 2008).

Omi/HtrA2 encodes a serine protease localized to mitochondrial intermembrane space. While overexpression of *Omi/HtrA2* leads to apoptosis, following its release into the cytosol (reviewed by (Walle et al., 2008), mice lacking *Omi/HtrA2* or mice harboring a mutation in *Omi/HtrA2* disrupting protease function (Jones et al., 1993; Jones et al., 2003) show loss of non-dopaminergic neurons in the striatum, but not loss of apoptosis (Martins et al., 2004; Rathke-Hartlieb et al., 2002). These studies underscore the importance of studying the in vivo functions of *Omi/HtrA2* using loss-of-function studies.

Recent reports have suggested links between *Omi/HtrA2* and PD (Bogaerts et al., 2008b; Strauss et al., 2005a). One mutation in Omi/HtrA2, G399S, was identified in sporadic PD patients and reportedly impairs activation of protease activity. In addition, Omi/HtrA2 can physically bind to PINK1 in vitro, and Omi/HtrA2 can be phosphorylated by a serine-threonine kinase, p38, with this phosphorylation being dependent on *PINK1*. Furthermore, substitution of a

putative *PINK1*-dependent phosphorylation site with a non-phosphorylatable moiety (S400A) markedly reduced protease activity (Plun-Favreau et al., 2007). Thus, it has been suggested that *Omi/HtrA2* functions downstream of *PINK1,* with PINK1 positively regulating Omi/HtrA2 (Plun-Favreau et al., 2007). Based on these intriguing links between *Omi/HtrA2* and PD, *Omi/HtrA2* was recently designated as *Parkinson disease-13* locus (*PARK13*).

However, two recent human genetic studies report no association of *Omi/HtrA2* with PD (Ross et al., 2008b; Simon-Sanchez et al., 2008), with the G399S allele detected in both PD patients and healthy controls at a similar frequency. Because of these conflicting results, it is unclear whether *Omi/HtrA2* acts as a true PD gene and whether it performs a major function downstream of *PINK1*. Resolution of these questions is crucial for understanding PD pathogenesis. Studies on the endogenous function of *Omi/HtrA2* as it relates to *PINK1* function are required to address these questions. Here, we report studies on loss-of-function and disease-associated mutants of *Drosophila Omi*, and the results of extensive genetic interaction studies between *pink1* and *Omi.*

MATERIALS & METHODS

Molecular Biology

To generate UAS-*Omi*, GMR-*Omi* and TMR-*Omi*, the *Omi* cDNA (EST clone from *Drosophila* Genome Research Center, AT14262) was subcloned into each vector (Brand and Perrimon, 1993; Hay et al., 1994; Huh et al., 2004). To generate *Drosophila* Omi mutants analogous to human Omi/HtrA2 mutations, S276C, S306A, G399S and S400A, site-specific mutagenesis of S236C, S266A, G363S and S364A of Omi was carried out, and the altered cDNAs were subcloned into pUASt and pTMR vector, respectively. A fly mutation corresponding to the human PINK1G309D mutation, Pink1G426D, was generated by site-

specific mutagenesis (made by I.E.C and Atsushi Yamaguchi). To silence *Omi*, the *Omi* transcript corresponding to the coding region was targeted using a microRNA-based technology (Chen et al., 2007) (Ganguly et al., 2008), PCR products of these microRNA precursors were cloned into pUASt. To generate CaSpeR-*pink1G426D*, site-specific mutagenesis in the backbone of CaSpeR-*pink1* was carried out and the product subcloned into pCaSpeR4 vector. To generate CaSpeR-*Omi*, a 2.5kb PCR product, generated using the following primers, was subcloned into pCaSpeR4 vector (a gift from Nic Tapon): 5' primer: CAACTCGAGGAAGTACATTGGG-CGGGTC; 3' primer: GGGACTAGTGGGTTTGTCAGCGATTTC, All cloned PCR products were confirmed by DNA sequencing.

Drosophila Genetics and Strains

EMS mutations were recovered using the *Drosophila* Tilling Service (Fred Hutchinson Cancer Research Center). These alleles were generated in a prior screen (Koundakjian et al., 2004). Omi^{NSO} is a nonsense allele resulting from a base substitution of C to T, leading to generation of a stop codon at Q196, and Omi^{V110E} is a missense allele due to substitution of T to A. We independently confirmed these alleles by sequencing. Prosα6T-GFP flies (Zhong and Belote, 2007) were obtained from J.M. Belote, UAS-mitoGFP and *Df(3R)ED5644* flies were obtained from the BloOmington *Drosophila* Stock Center. $pink1^{5}$, TMR-*pink1,* UAS-*pink1* and CaSpeR-*pink1-9myc* (Clark et al., 2006b), UAS-*parkin* (Greene et al., 2003) and Mef2-Gal4 (Deng et al., 2008a) flies were previously described. For experiments involving transgenic flies, multiple independent fly lines were generated (Rainbow Transgenic Flies) and tested for each transgene. *Drosophila* strains were maintained in an 18^{O}C, 25^{O}C or 29^{O}C humidified incubator, or at room temperature.

Male and Female Fertility Tests

Recently eclosed individual male flies were placed with four virgin females in vials. Single 0-3 day old females were placed in a vial supplemented with dry yeast along with five sibling males and maintained at 25°C. Males or females were scored as sterile if they failed to produce progeny by day 6.

Phase-contrast, Immunofluorescence and Confocal Microscopy.

For light microscopic analysis of the male germline, testes were dissected from recently eclosed males, squashed in PBS buffer, and imaged using an Olympus BX51 microscope equipped with phase contrast optics. For analysis of muscle, nota of adult flies were dissected, fixed in 4% paraformaldehyde, and indirect muscle fibers isolated and imaged by a Zeiss LSM5 confocal microscope. For analysis of dopaminergic neurons, anti-Tyrosine Hydroxylase (TH) (Immunostar) antibodies were used and imaged by a Zeiss LSM5 confocal microscope, and only clearly stained anti-TH-positive cells were counted. Wildtype, *pink1* or *Omi* mutant brains were counted blindly. The Immunofluorescent staining was performed as previously described (Guo et al., 1996). Phalloidin was used 1:1000 for testes staining (Invitrogen). Anti-Omi antibodies were a kind gift from M. Miura and were used 1: 300 for immunocytochemistry.

Transmission Electron Microscopy.

Testes and muscle were dissected, fixed in paraformaldehyde/glutaraldehyde, postfixed in osmium tetroxide, dehydrated and embedded in Epon. 1.5µm-thick tissue sections were stained with Toluidine Blue. 80nm thin sections were stained with uranyl acetate and lead citrate, and

examined using a JEOL 100C transmission electron microscope (UCLA Brain Research Institute EM Facility). At least three testes or thoraces of each genotype were examined by TEM.

Scanning Electron Microscopy

Freshly sacrificed flies were mounted on their sides, placed on a platform under vacuum and imaged at 180x magnification and 100 psi using a Hitachi 2460N scanning electron microscope. Analysis of eye phenotypes was performed as previously described (Gross et al., 2008; Guo et al., 2003).

Stress and longevity assays

0-3 day-old males were anaesthetized on ice, aged for 48 hours, starved for 6 hours and subjected to 5% sucrose plus each agent. Four vials of 30 flies were assayed simultaneously for each genotype. For longevity measurements, 120 males of each genotype were divided into six vials. Flies were maintained at 25^{O}C and transferred to fresh food every 2 days.

Lysate Preparation and Western Blotting

Heads or testes from age- and sex-matched adults were disrupted in lysis buffer containing complete protease inhibitor cocktail (Roche) using a sonicator-3000 from MISONIX. Samples were boiled, centrifuged, and total protein was analyzed by Western blotting. Antibodies used were anti-Myc (Upstate) and anti-Omi (Igaki et al., 2007).

Northern Blotting

Standard protocols were utilized using a full-length *pink1* probe as previously described (Clark et al., 2006b).

RESULTS

Overexpression-based genetic interactions of *pink1* and *Omi* in the eye

Omi/HtrA2 encodes a protein with a mitochondrial targeting sequence and a transmembrane domain, followed by a serine protease domain and a C-terminal PSD95/DlgA/Zo-1 (PDZ) domain (Vande Walle et al., 2008). *Drosophila melanogaster* contains a single homolog of *Omi/HtrA2* (CG8464, hereafter called *Omi*), with 50% amino acid sequence identity, and 68% similarity, and a domain structure similar to that of human Omi/HtrA2. To test the hypothesis that *Omi* and *pink1* function in the same pathway, we asked if genetic interactions between these two genes could be observed in the *Drosophila* eye. The fly eye is dispensable for viability and fertility, and has been widely used as a system to study human neurodegenerative diseases (reviewed by (Bonini and Fortini, 2003; Marsh and Thompson, 2006)). We generated transgenic flies to carry out tissue-specific overexpression using the UAS-Gal4 system (Brand and Perrimon, 1993). When *Omi* was overexpressed at high levels in the eye (25^{O}C), small and rough eyes were observed (Fig. 1K compared with A), similar to a previously report (Igaki et al., 2007). These small eyes likely result from the ability of Omi to activate cell death when overexpressed (Challa et al., 2007; Igaki et al., 2007; Khan et al., 2008). The eye phenotypes due to *Omi* overexpression were very sensitive to the level of *Omi* expression. Flies expressing lower levels of *Omi* (18^{O}C) exhibited wildtype-appearing eyes, providing a sensitized genetic background for interaction studies (Fig. 1B). Eye-specific *pink1* overexpression resulted in mild rough eyes (Fig. 1C)(Poole et al., 2008b). However, flies overexpressing both *pink1* and *Omi* at 18^{O}C exhibited smaller and rougher eyes than those associated with *pink1* overexpression alone (Fig. 1F). This suggests that there is an overexpression-based interaction between *pink1* and *Omi,* which is consistent with a recent report (Whitworth et al., 2008b) and has been interpreted, in

conjunction with other observations, as indicating that *Omi* acts downstream of *pink1* in a common genetic pathway (Whitworth et al., 2008b).

One possible explanation for the interaction observed when *pink1* and *Omi* are coexpressed is that overexpression of two mitochondrially-targeted proteins causes competition for limited amounts of mitochondrial import machinery. In such a model, increased import of Pink1 could lead to excess Omi in the cytosol, resulting in a rough eye. Overexpression of a mitochondrial matrix-targeted Green Fluorescent Protein (mitoGFP) with either *pink1* or *Omi,* however, did not lead to any enhancement of *Omi* or *pink1* overexpression phenotypes, suggesting that mitochondrial import is not limited (Supplementary Fig. S1). The *Omi/pink1* co-overexpression interaction was dependent on the protease activity of Omi, since flies overexpressing a protease-dead version of Omi, Omi-S266A (Fig. 1D, see below), failed to show enhanced eye phenotypes when in conjunction with *pink1* overexpression (Fig. 1G).

Further exploring the hypothesis that *Omi* acts downstream of *pink1*, we found that *pink1* overexpression-induced eye phenotypes could not be suppressed by loss of *Omi* function (Fig. 1I, J). Similarly, the eye phenotype due to *Omi* overexpression could not be modified by lack of *pink1* (Fig. 1K,L). Thus, these results do not provide support for *Omi* functioning downstream of *pink1*. We next explored the relationship between these interactions observed in the eye and the well characterized functions of *pink* in regulating mitochondrial morphology. We generated transgenic flies expressing Pink1G426D, a *Drosophila* mutation analogous to the PINK1 PD-associated mutation G309D. G309D alters a residue in the kinase domain (Valente et al., 2004b), and has a significant reduction of PINK1 kinase activity, as assayed by in vitro autophosphorylation (Beilina et al., 2005). *pink1* null mutant flies carrying G426D showed a

largely abolished ability to rescue male sterility (<2% fertile, n=60), muscle degeneration and mitochondrial morphological defects of *pink1* null mutants (Fig. 2), indicating that this mutant protein is strongly comprOmised with respect to normal *pink1* function. Surprisingly, however, expression of Pink1G426D still led to a small and rough eye phenotype when combined with *Omi* overexpression (Fig. 1H). These results suggest that *pink1* functions required to mediate *Omi* overexpression-based interactions in the eye are distinct from *pink1* functions required to provide normal mitochondrial function. Taken together, although *Omi* and *pink1* displayed genetic interactions in overexpression-based assays, these results do not provide evidence to support models in which *Omi* plays a major role in transducing *pink1*-dependent signals to regulate mitochondrial function.

Omi null mutants are male sterile, but show phenotypes distinct from those seen in *pink1* or *parkin* null mutants.

To further explore the roles of *Omi* as it relates to *pink1,* we carried out loss-of-function studies of *Omi* mutants. The endogenous functions of *Omi* in *Drosophila* have not been fully studied due to the absence of loss-of-function mutants. This analysis is more relevant to the role of *Omi* as it relates to PD, since mutations in *Omi* observed in PD patients are postulated to be loss-of-function or dOminant-negative mutations, not resulting in increased activity. To obtain loss-of-function mutations in *Omi*, we used TILLING (Till et al., 2003), a method for detecting ethyl methanesulfonate (EMS)-induced point mutations in a gene of interest following chemical mutagenesis. We obtained one nonsense mutation in *Omi*, Omi^{NSO}, and one missense mutation, V110E (see below). The truncated protein encoded by Omi^{NSO} is predicted to lack the active site of the protease domain and the PDZ domain (Fig. 3A), and thus represents a null allele. Flies

homozygous for *Omi*^{NSO} were semi-lethal. However, flies carrying *Omi*^{NSO} in trans to a deficiency in the region, *Df(3R)ED5644*, were fully viable, suggesting that the lethality associated with *Omi*^{NSO} is due to a background mutation. Flies with ubiquitous expression of RNAi-*Omi* using a tubulin-Gal4 driver were also viable. The silencing effect of RNAi-*Omi* was confirmed by its ability to completely suppress *Omi* overexpression induced eye phenotypes (Supplementary Fig. S2). As expected, Western blotting using an anti-Omi antibody revealed no detectable Omi-positive bands in *Omi*^{NSO}*/Df(3R)ED5644* flies (Supplementary Fig. S3).

Omi^{NSO}*/Df(3R)ED5644* flies, hereafter called *Omi* mutants, did not show any gross external defects. *Omi* mutant females were fertile (96%, n=50), but *Omi* mutant males were sterile (100%, n=110). In these males, seminal vesicles, which store mature sperm, were empty (Fig. 3D,D'), and no motile sperm were observed, suggesting defects in either production or transport to the seminal vesicles. To ensure that these phenotypes were due to lack of *Omi*, we generated multiple transgenic fly lines expressing *Omi* specifically in the male germline (TMR-*Omi*). Overexpression of *Omi* was confirmed using anti-Omi antibodies (Supplementary Fig. S3). Many of these lines were male sterile. However, three of ten lines were fertile. Those fertile lines show weaker overexpression of *Omi* compared with the sterile lines (Supplementary Fig. S3). This suggests that the sterility is due to high level of overexpression, likely resulting in prOmiscuous activity of the Omi protease. Introduction of any of the fertile *Omi* overexpression lines into the *Omi* mutant background resulted in the presence of motile sperm in the seminal vesicles (Fig.3E,E') and restoration of fertility (95%, n=100). A single copy of a genOmic rescue transgene containing *Omi*, but not surrounding genes, also fully rescued the male sterility of *Omi* mutants (100%, n=50). Together, these results demonstrate that *Omi* is essential for spermatogenesis.

We also analyzed the second *Omi* EMS allele. V110 corresponds to V154 in human Omi/HtrA2, which is located in a highly conserved region (Fig. 3A, B) predicted by structural studies to mediate homo-trimerization of Omi/HtrA2, which is required to activate its protease activity (Li et al., 2002). $Omi^{V110E}/Df(3R)ED5644$ and Omi^{V110E}/Omi^{NSO} mutant flies were also male sterile (0%, n=45; 0%, n=65), displayed empty seminal vesicles, and had no motile sperm, indicating that Omi^{V110} is likely a null or strong hypomorphic allele. These results provide in vivo support for an important role for the trimerization motif for Omi function, and suggest that the protease activity of Omi is crucially important for its role in regulating spermatogenesis.

Since *pink1* mutants also show male sterility, we asked if *Omi* mutant testes show defects in mitochondrial morphology, a prOminent feature of *pink1* mutants (Clark et al., 2006b; Deng et al., 2008a). During *Drosophila* spermatogenesis, mitochondria undergo significant morphological changes {Fuller, 1993 #26}. Stem cell differentiation is followed by mitosis and meiosis with incomplete cytokinesis, creating syncytial cysts of 64 spermatids. Early spermatids undergo mitochondrial aggregation and fusion, creating two giant mitochondria that form a spherical structure known as the nebenkern {Fuller, 1993 #26}. Under phase-contrast microscopy, such 'onion stage' spermatids can be identified as having two adjacent spherical structures: the nucleus and the nebenkern (Fig. 3I,J). During subsequent spermatid elongation, the nebenkern begins to unfurl, creating two mitochondria at this "leaf-blade" stage (Fig. 3I,M). Following elongation, spermatids undergo a process known as individualization, in which the cytoplasmic bridges that link the 64 spermatids within a cyst are broken and excess cytoplasm is extruded {Fuller, 1993 #26}. This individualization process requires synchronized movement of an actin-based structure known as the investment cone. After individualization, each spermatid tail consists largely of the axoneme, a microtubule-based structure required for motility, and

mitochondrial derivatives (Fig. 3P,Q).

As expected for a protein with a mitochondrial targeting sequence, Omi localizes to nebenkerns (Fig. 6A-C). In onion-stage spermatids, the nebenkerns of *pink1* mutants show significant vacuolation (Fig. 3L), and during the subsequent leaf blade stage *pink1* and *parkin* mutants contain only one mitochondrial derivative (Fig. 3O) rather than the two seen in wildtype (Fig. 3M) (Clark et al., 2006b; Deng et al., 2008a; Riparbelli and Callaini, 2007). Surprisingly, mitochondria in *Omi* mutants were indistinguishable from those in wildtype. During the onion stage, the border of the neberkern was smooth and no vacuolation was observed (Fig. 3K). At the leaf blade stage, *Omi* mutant spermatids contained two mitochondrial derivatives instead of one observed in *pink1* or *parkin* mutants (Fig. 3N). *pink1* and *parkin* mutants also show dramatic defects in mitochondrial morphology during post-individualization stages, as visualized with transmission electron microscopy (EM) (Fig. 3S) (Clark et al., 2006b; Deng et al., 2008a; Greene et al., 2003; Riparbelli and Callaini, 2007). In contrast, mitochondria appeared normal in stage-matched *Omi* mutants, though individual spermatids were somewhat disorganized within the cyst (Fig. 3R). In addition, investment cones in *Omi* mutants were scattered (Fig. 3G compared with F), suggesting that movement of these structures is asynchronous. Such a phenotype is associated with individualization defects (Huh et al., 2004). While the individualization defects were suppressed by testes-specific *Omi* overexpression (Fig. 3H), we cannot rule out the possibility that defects in other post-individualization steps of spermatogenesis also contribute to sterility associated with *Omi* mutants. This possibility seems particularly likely since the individualization defects observed in *Omi* mutants appear relatively mild. In summary, *Omi* mutant phenotypes in testes are distinct from those of *pink1* or *parkin* mutants, in which defects in mitochondrial morphology are observed. In contrast to *pink1* mutants, *Omi* mutants do not

show dopaminergic neuronal loss, muscle degeneration or defects in mitochondrial integrity.

Next, we asked if *Omi* mutants show phenotypes similar to those of *pink1* mutants in other tissues and contexts. *Omi* mutants were sensitive to treatments with multiple stress-inducing agents including paraquat, a free radical inducer, rotenone, which impairs complex I activity in the mitochondrial respiratory chain (Przedborski and Ischiropoulos, 2005), protein folding inhibitors and high concentrations of salt (Supplementary Fig. S4). Thus, rather than being specifically sensitive to oxidative stress, *Omi* mutant flies are generally stress sensitive. These results may suggest a general sickness of *Omi* mutants, particularly since *Omi* mutants had a shortened life span (Supplementary Fig. S5).

An age-dependent decrease in the number of dopaminergic neurons has been reported in *pink1* or *parkin* mutants (Meulener et al., 2005; Park et al., 2006; Yang et al., 2006) (Fig. 4A,B,D,E). In contrast, *Omi* mutants did not show any dopaminergic neuronal loss in the brains of flies aged for 40 days (Fig. 4C,F). *pink1* or *parkin* mutants also show striking indirect flight muscle degeneration, and severely disrupted mitochondrial morphology with broken cristae, which are prOminent in 1-2 day old flies (Fig. 4I,J compared with G,H)(Clark et al., 2006b; Greene et al., 2003; Park et al., 2006; Pesah et al., 2004; Yang et al., 2006). In contrast, though Omi is expressed in muscle and localized to mitochondria (data not shown), *Omi* mutants did not exhibit any muscle degeneration, even when they were aged for 30 days (Fig. 4K). EM analysis of *Omi* mutant muscle also failed to show any defects in mitochondrial integrity (Fig. 4L). Taken together, our data demonstrate that *Omi* mutants, in contrast to *pink1* mutants, do not display mitochondrial morphological defects in multiple tissues, including spermatids and muscle. *Omi* mutants also fail to show dopaminergic neuronal loss seen in *pink1* mutants.

Loss-of-function studies fail to detect any genetic interactions between *pink1* and *Omi*

To further explore the hypothesis that *Omi* and *pink1* work together to regulate mitochondrial integrity, we searched for genetic interactions based on loss-of-function of these genes. Genetic interactions between *pink1* and *parkin* provide an important reference for testing whether *Omi* and *pink1* act in a common pathway (Clark et al., 2006b; Park et al., 2006). We, as well as others, have previously shown that *Drosophila pink1* and *parkin* act in a common genetic pathway, with *pink1* functioning upstream of *parkin* (Clark et al., 2006b; Park et al., 2006; Yang et al., 2006). This conclusion is based on several observations. Loss-of-function mutations in *pink1* and *parkin* result in highly similar, if not identical, defects in mitochondrial integrity (Clark et al., 2006b; Deng et al., 2008a; Park et al., 2006; Poole et al., 2008b; Yang et al., 2006). While overexpression of *parkin* rescues *pink1* null mutant phenotypes, overexpression of *pink1* fails to rescue *parkin* null mutant phenotypes (Clark et al., 2006b; Park et al., 2006). In addition, double mutants removing both *pink1* and *parkin* show phenotypes identical to those of single mutants alone (Clark et al., 2006b; Park et al., 2006).

In contrast to *pink1* (Fig. 5C,H) or *parkin* overexpression (Clark et al., 2006b), testes-specific *Omi* overexpression did not rescue the male sterility or the mitochondrial phenotype of *pink1* mutants (0% fertile, n=65) (Fig. 5D,I). Expression of mutant versions of Omi analogous to S306A, S276C, G399S or S400A (see below), also did not rescue male sterility of *pink1* mutants (0% fertile, n>30). Similarly, *Omi* overexpression, which leads to massive loss of muscle integrity, also failed to rescue the muscle degeneration phenotypes seen in *pink1* mutants. In addition, expression of a protease dead version of Omi, S266A, which does not result in loss of muscle integrity, also failed to rescue muscle phenotypes seen in *pink1* mutants (data not shown).

Consistent with the hypothesis that *pink1* and *Omi* function independently, neither the expression levels nor the mitochondrial localization of Omi was altered in *pink1* mutants (Fig. 6D-F).

To investigate if *pink1* functions downstream of *Omi,* we carried out reverse rescue experiments. However, *pink1* overexpression failed to rescue male sterility seen in *Omi* mutants (0% fertile, n=70). In addition, neither the protein levels nor cleavage patterns of Pink1 were altered in *Omi* mutants (Fig. 6). Thus, we failed to find any positive evidence that *Omi* functions either upstream or downstream of *pink1* in a common pathway.

To test the hypothesis that *Omi* might function in a parallel pathway with *pink1* in a partially redundant manner, we generated double mutants that remove both *pink1* and *Omi*. These double mutant flies were viable, and showed survival rates comparable to those of *pink1* mutants alone. These animals were male sterile and exhibited mitochondrial morphological defects in spermatids and muscle that were indistinguishable from those of *pink1* mutants alone, indicating that loss of *Omi* function does not enhance *pink1* mutant phenotypes (Fig. 5E,J,N; compare with B, G, L). Together, our loss-of-function in vivo studies do not provide support for the hypothesis that *Omi* functions either upstream or downstream of *pink1,* or in parallel with *pink1*, at least with respect to the regulation of mitochondrial integrity.

<u>PD-associated mutations in Omi, and a mutation abolishing a putative Pink1-dependent phosphorylation site, show distinct phenotypes from mutations impairing Omi protease function.</u>

Since we failed to detect any loss-of-function based genetic interactions between *pink1* and *Omi*, we decided to examine the function of the PD disease-related *Omi* mutations. The PD associated polymorphism in Omi/HtrA2, A141S (detected in more than 1% of the normal population), and the mutation, G399S, have been reported to function as dOminant negative

mutations, leading to a reduction of protease function of Omi/HtrA2 (Strauss et al., 2005a). G399, which is located in the PDZ domain, is conserved in *Drosophila,* while A141, which is located in the IAP binding domain of Omi/HtrA2, is not. Interestingly, S400, a residue next to G399, has been identified as a PINK1-dependent putative phosphorylation site for p38 (Plun-Favreau et al., 2007). This phosphorylation is reported to be important for Omi/HtrA2 activity, since S400A, a phosphorylation-incompetent mutation, markedly reduces protease activity (Plun-Favreau et al., 2007). To investigate whether these mutations affect Omi/HtrA2 function *in vivo*, we generated transgenic flies expressing *Omi* G363S or S364A, which are analogous to G399S or S400A in human Omi/HtrA2.

Both G399S and S400A reportedly comprOmise Omi protease activity *in vitro* (Plun-Favreau et al., 2007; Strauss et al., 2005a). If this were true *in vivo*, G399S or S400A mutant forms of Omi would be expected to show similar phenotypes to protease comprOmised Omi mutants. To test this hypothesis, we also generated two protease-impaired versions of *Drosophila* Omi, S266A and S236C. S266A is analogous to S306A in human Omi/HtrA2, which alters the active site serine in the protease domain and abolishes protease activity (Li et al., 2002), and S236C is analogous to the S276C mutation present in the *mnd2* mice, which significantly reduces the protease function of Omi/HtrA2 (Jones et al., 2003) (Table 1). These mutants were expressed and assayed in multiple somatic tissues using the UAS-GAL4 system (Brand and Perrimon, 1993), and in the male germline using the TMR promoter (Clark et al., 2006b; Huh et al., 2004). The actions of G363S and S364A were compared with that of wildtype Omi (Omi WT), as well as the protease-deficient S266A and S236C mutant forms.

In contrast to overexpression of Omi WT, which resulted in male sterility in most transgenic lines, all transgenic lines expressing S266A or S236C were male fertile (n>13 transgenic lines tested for each mutant). Expression of S266A also failed to rescue the male sterility (0% fertile, n>60) and empty seminal vesicle phenotypes due to lack of *Omi* (Fig. 7B, Table 1). These data suggest that protease comprOmised mutations result in loss of Omi function. Further supporting this hypothesis, eye-specific overexpression of S266A or S236C, in contrast to overexpression of Omi WT, resulted in wildtype appearing eyes (Fig. 7E-G, Table 1). Similarly, muscle specific overexpression of S266A or S236C, in contrast to Omi WT, did not affect muscle integrity, (Table 1, data not shown). Expression of S266A and S236C were confirmed using an anti-Omi antibody (Fig. 7D). These results, together with those described earlier with the missense mutation, Omi^{V110E}, in the region responsible for activation of protease activity, suggest that Omi protease activity is important for its function *in vivo*.

In contrast, testes-specific expression of either OmiG363S or S364A resulted in significant male sterility, with only 3-4 lines out of the 10-13 lines tested per construct giving fertile males, similar to what is seen with overexpression of Omi WT. These fertile lines likely represent those with lower expression levels. Using these fertile lines, we found that expression of G363S rescued the sterility and individualization phenotypes due to *Omi* loss-of-function, as did those expressing Omi WT (Fig. 7C, Table 1). These results suggest that mutations analogous to G399S and S400A retain a significant amount of Omi activity. Further supporting this hypothesis, eye-specific overexpression of G363S or S364A resulted in small and rough eyes similar to those seen following overexpression of Omi WT (Fig. 7H-J, Table 1). Similarly, muscle specific overexpression of G363S or S364A, or Omi WT, resulted in a massive loss of muscle integrity (Table 1, data not shown). Together, these observations (summarized in Table 1) suggest that

Omi mutant proteins analogous to G399S and S400A behave similarly to Omi WT, but differently from those with comprOmised protease activity *in vivo*.

DISCUSSION

The in vivo function of *Omi*

Omi/HtrA2 has been studied extensively for its role in apoptosis (reviewed in (Vande Walle et al., 2008). However, while overexpression of *Omi/HtrA2* induces apoptosis robustly in mammalian cells, mice lacking *Omi/HtrA2* fails to show decreased apoptosis, but instead show non-dopaminergic neuronal loss in the striatum (Martins et al., 2004). *Omi/HtrA2* function is also implicated in regulating stress resistance (Vande Walle et al., 2008). Thus, determining the endogenous function of *Omi/HtrA2* is crucially important to understanding its roles in both health and disease. Using *Drosophila* as a model, we have dissected the in vivo function of Omi. We find that *Omi* is essential for spermatogenesis, stress resistance and maintaining a normal life span. Furthermore, the protease activity of Omi is crucial for its function.

We have identified an essential role of *Omi* during spermatogenesis. However, although Omi is localized to mitochondria in both testes and muscle, no mitochondrial morphology defects are observed in *Omi* null mutants in either of these tissues. It is possible that Omi is responsible for some aspects of mitochondrial function, such as chaperone activity or modulation of respiratory chain function, which do not affect mitochondrial morphology, and thus are not detected in our assays. It is also possible that *Omi* is required only in certain contexts, such as during exposure to oxidative stress, and that mitochondrial defects may be revealed in *Omi* mutants under these conditions. Alternatively, Omi may function in the cytosol rather than in the

mitochondria, with mitochondria serving to regulate the release of Omi into the cytosol. Future studies are required to distinguish these possibilities.

Interaction of Omi and Pink1

The genetic interactions observed between *pink1* and *parkin* serve as an important reference for tests of the hypothesis that *Omi* and *pink1* act in a common pathway. In contrast to *pink1* mutants, which show striking defects in mitochondrial integrity in muscle and testes, and a decrease in the number of dopaminergic neurons, *Omi* mutants show normal mitochondrial morphology in both muscle and testes, and a normal number of dopaminergic neurons. Furthermore, in contrast to *parkin* overexpression, *Omi* overexpression does not rescue *pink1* mutant phenotypes. Overexpression of *pink1* also fails to rescue male sterility due to *Omi* loss-of-function. Lack of *pink1* does not affect the levels or the subcellular localization of Omi, and Pink1 levels and processing are not altered in *Omi* mutants. In addition, double mutants removing both *pink1* and *Omi* show identical phenotypes to *pink1* mutants alone, suggesting that *pink1* does not negatively regulate *Omi*, and that *Omi* does not carry out partially redundant functions with *pink1*. Together, these data do not provide any in vivo evidence supporting the hypothesis that *Omi* functions in the same pathway either upstream or downstream of *pink1*, or that it acts in a parallel fashion to regulate mitochondrial morphology. These loss-of-function based analyses are more relevant to PD than are *Omi* overexpression based analyses, because reported *Omi/HtrA2* mutations associated with PD are proposed to represent loss-of-function or dOminant negative mutations (Strauss et al., 2005a).

Genetic interactions between *pink1* and *Omi* have been observed by ourselves and others (Whitworth et al., 2008b) in eye-based overexpression studies: co-overexpression of *pink1* with

Omi results in small eye phenotypes not associated with expression of either protein alone. While in isolation, these results could be explained by a model in which *Omi* and *pink1* function in a common pathway (Whitworth et al., 2008a), this model is difficult to reconcile with our loss-of-function data. The cellular basis of the *pink1* overexpression-induced eye phenotype, and its relationship to the normal endogenous roles of *pink1* in regulating mitochondrial function, is unclear. While null mutants of *pink1* and *parkin* show highly similar, if not identical, phenotypes in almost all assays tested, overexpression of *pink1* results in a rough eye phenotype, whereas overexpresison of *parkin* does not (data not shown) (Poole et al., 2008a; Whitworth et al., 2008a). Furthermore, a PD-causing, kinase-deficient mutant form of *pink1,* which fails to rescue *pink1* null mutant phenotypes in multiple tissues, still interacts with *Omi* in the eye-based overexpression assay, suggesting that Pink1 kinase activity is required for its mitochondrial functions but not for the genetic interaction with *Omi* in this assay. Based on our findings, one is led to conclude that the functions of *pink1* that mediate its co-overexpression interaction with *Omi* are distinct from the functions of *pink1* and *parkin* in regulating mitochondrial morphology. Such a mitochondrial integrity-independent role of *pink* may be important, but has yet to be identified in vivo. Alternatively, it is possible that the *pink1-Omi* interaction observed in the eye is not physiologically relevant. Overexpression studies, as well as in vitro studies, can identify interactions that are forced to happen, but that do not normally occur. For example, either protein, when overexpressed, may act on inappropriate targets or act in inappropriate subcellular compartments, thus generating cellular toxicity. In combination, this toxicity may be augmented. This possibility is further suggested by the results of overexpression-based observations that place Rhomboid 7 as an upstream positive regulator of Pink1 (Whitworth et al., 2008a). This conclusion is difficult to reconcile with more physiological loss-of-function based observations

showing that *Drosophila rhomboid 7* functions to promote mitochondrial fusion (McQuibban et al., 2006), while both *pink1* and *parkin* function to promote mitochondrial fission (Deng et al., 2008b; Poole et al., 2008a; Yang et al., 2008b). In any case, our loss-of-function studies demonstrate that *Omi* does not play an essential role in regulating mitochondrial integrity in the *pink1/parkin* pathway. They leave open the possibility that interactions between *pink1* and *Omi* are modulatory, or important in other contexts. However, these in vivo contexts remain to be identified.

Implications for *Omi/HtrA2* as a PD gene

Omi/HtrA2 was recently designated as *PARK13*, based on a report identifying G399S mutations in sporadic PD patients (Strauss et al., 2005a). Mammalian cell culture studies suggest that G399S results in a significant reduction in Omi/HtrA2 protease activity, providing a possible functional basis for disease association (Strauss et al., 2005a). In contrast to previous in vitro observations (Plun-Favreau et al., 2007; Strauss et al., 2005a), we find that both G399S and S400A retain significant, if not full, Omi function in vivo, leading to the conclusion that mutations previously thought to be associated with disease are functional in at least some contexts in vivo. Importantly, our conclusion is consistent with two recent reports showing that Omi G399S is found at similar frequencies in normal controls and PD patients (Ross et al., 2008a; Simon-Sanchez and Singleton, 2008),

We cannot exclude the possibility that human *Omi/HtrA2* has a dopaminergic neuron- specific function that is revealed under certain circumstances, nor can we exclude the possibility that *Drosophila Omi* acts differently from human *Omi/HtrA2*. However, the extensive homology and conservation of key domain structures between fly and human Omi/HtrA2 suggests that it is

likely that studies in *Drosophila* Omi are relevant to the function of Omi/HtrA2 in humans. Taken together with the observations that *Omi* mutant phenotypes are distinct from those associated with loss of *pink1* and *parkin* function, and that *pink1* and *Omi* fail to interact in loss-of-function based assays, we favor a hypothesis in which *Omi/HtrA2* does not play an essential role in PD pathogenesis.

FIGURES AND FIGURE LEGENDS

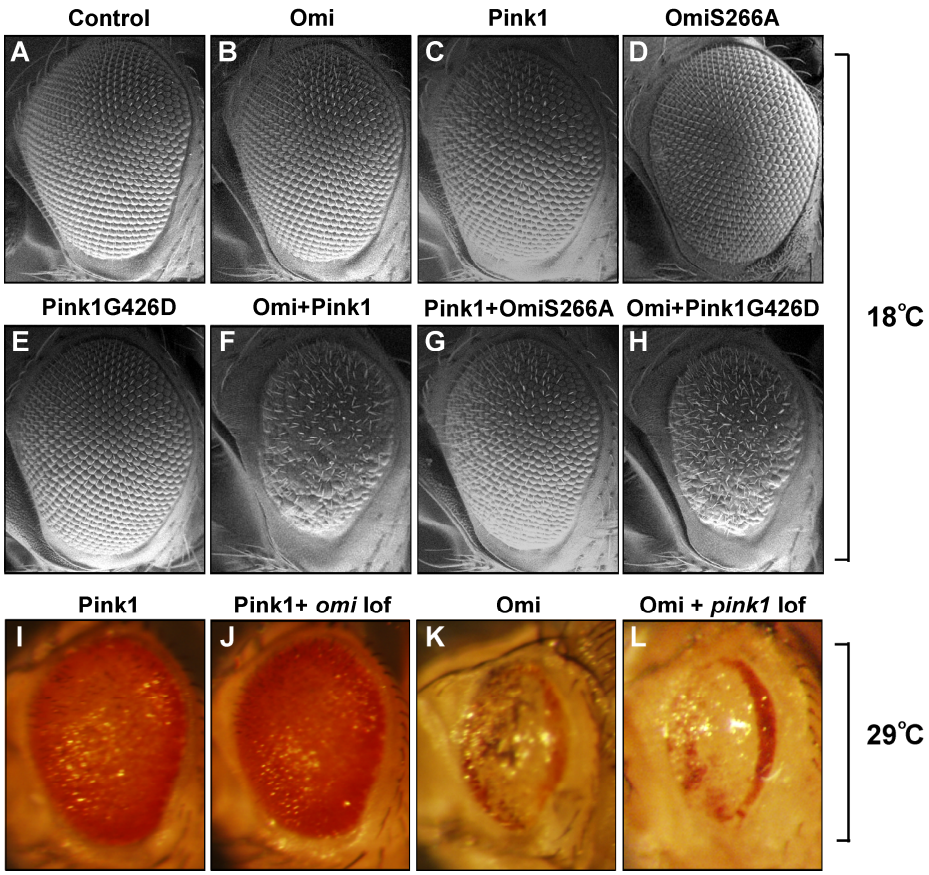

Figure 2-1. Overexpression based genetic interactions between *pink* and *Omi*.

Scanning EM and light micrographs of *Drosophila* eyes. At 18^{O}C, *Omi* overexpression (B) results in wildtype-appearing eyes, whereas overexpression of *pink1* (C) leads to mild rough eyes. Overexpression of both *Omi* and *pink1* results in a small and rough eye (F). This *pink1-Omi* overexpression interaction is abolished with expression of a protease inactive version of Omi, S266A (G). Expression of OmiS266A by itself does not result in any eye phenotypes (D). Expression of a mutation analogous to the Pink1 disease mutant, G426D, has no phenotype (E), however, it still shows an interaction with *Omi* overexpression (H). The phenotype of *pink1* overexpression cannot be suppressed by loss of *Omi* function induced by RNAi-*Omi*, even when

raised at 29^{O}C (I, J). Silencing of *Omi* function by RNAi-*Omi* is strong since it completely suppresses the *Omi* overexpression induced eye phenotype (Supplementary Fig. S2). Similarly, the eye phenotype due to *Omi* overexpression cannot be modified by lack of *pink1* (K,L). Panels A-H are from flies raised at 18^{O}C, whereas panels I-L are from flies raised at 29^{O}C. Genotypes: Control: *w*; GMR-Gal4/+. Omi: *w*; GMR-Gal4, UAS-*Omi*/+. Pink1: *w*; GMR-Gal4, UAS-*pink1*/+. Pink1G426D: *w*; GMR-Gal4/UAS-Pink1G426D. Omi+Pink1: *w*; UAS-*Omi*/+; GMR-Gal4, UAS-*pink1*/+. Omi+Pink1G426D: *w*; GMR-Gal4, UAS-*Omi*/UAS-Pink1G426D. Pink1+OmiS266A: *w;* UAS-OmiS266A/+; GMR-Gal4, UAS-*pink1*/+. Pink1+*Omi* lof: *w;* GMR-Gal4, UAS-*pink1*/UAS-RNAi-*Omi.* Omi+*pink1* lof: *w pink1*^{5}; GMR-Gal4, UAS-*Omi*/+.

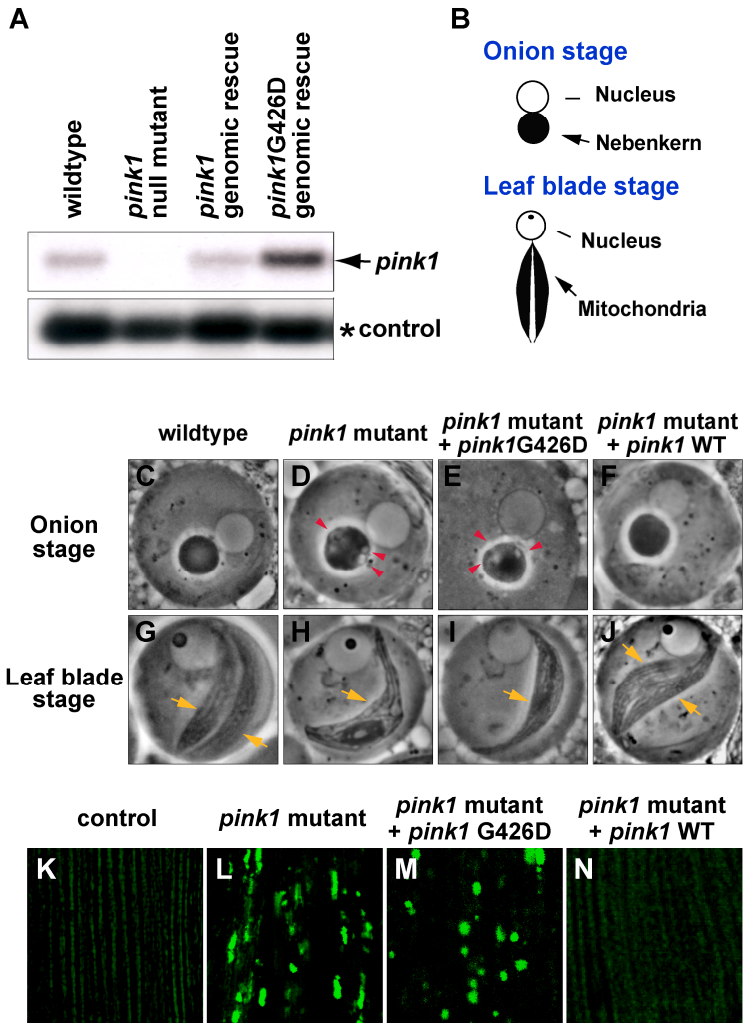

Figure 2-2. mRNA expression and phenotypic analysis of Pink1G426D, a mutation analogous to PD associated mutation PINK1G309D.

(A) Northern blot of whole flies using full-length *pink1* as a probe. Compared with wildtype, *pink1* null mutant (*pink1*^{5}) flies do not show full length mRNA. Transgenic flies expressing *pink1*G426D mutants show comparable or higher expression of *pink1* than is seen in flies expressing wildtype *pink1*. Arrow points to *pink1* expression and *rp49* (*) serves as an RNA loading control. (B-J) Schematic and phase contrast micrographs of spermatid mitochondria during the "onion stage" (C-F) and "the leaf blade stage" (G-J). Compared with wildtype, *pink1*

mutants show vacuolation (red arrowhead) in the nebenkern during the onion stage (D), and one instead of two mitochondrial derivatives (yellow arrow) seen in wildtype at the leaf blade stage (H). A genOmic rescue transgene carrying wildtype *pink1* (CaSpeR-*pink1*) completely rescues the male sterility due to lack of *pink1* (100% fertile, n>120) (Clark et al., 2006a), and spermatid phenotypes in both the onion stage and the leaf-blade stage (F,J). In contrast, *pink1*G426D (CaSpeR-*pink1*G426D) fails to rescue the sterility of *pink1* males (<2% fertile, n=60), or the spermatid phenotypes (E,I). Red arrowheads point to vacuolation of the nebenkern and orange arrows mark each mitochondrial derivative. (K-N) Mitochondria of indirect flight muscle are labeled by mito-GFP. Compared with control (K), *pink1* mutants display overall reduced levels of mitoGFP signal, and large clumps of intense GFP signal (L), which can be completely rescued by overexpression of Pink1WT (N), but not Pink1G426D (M).

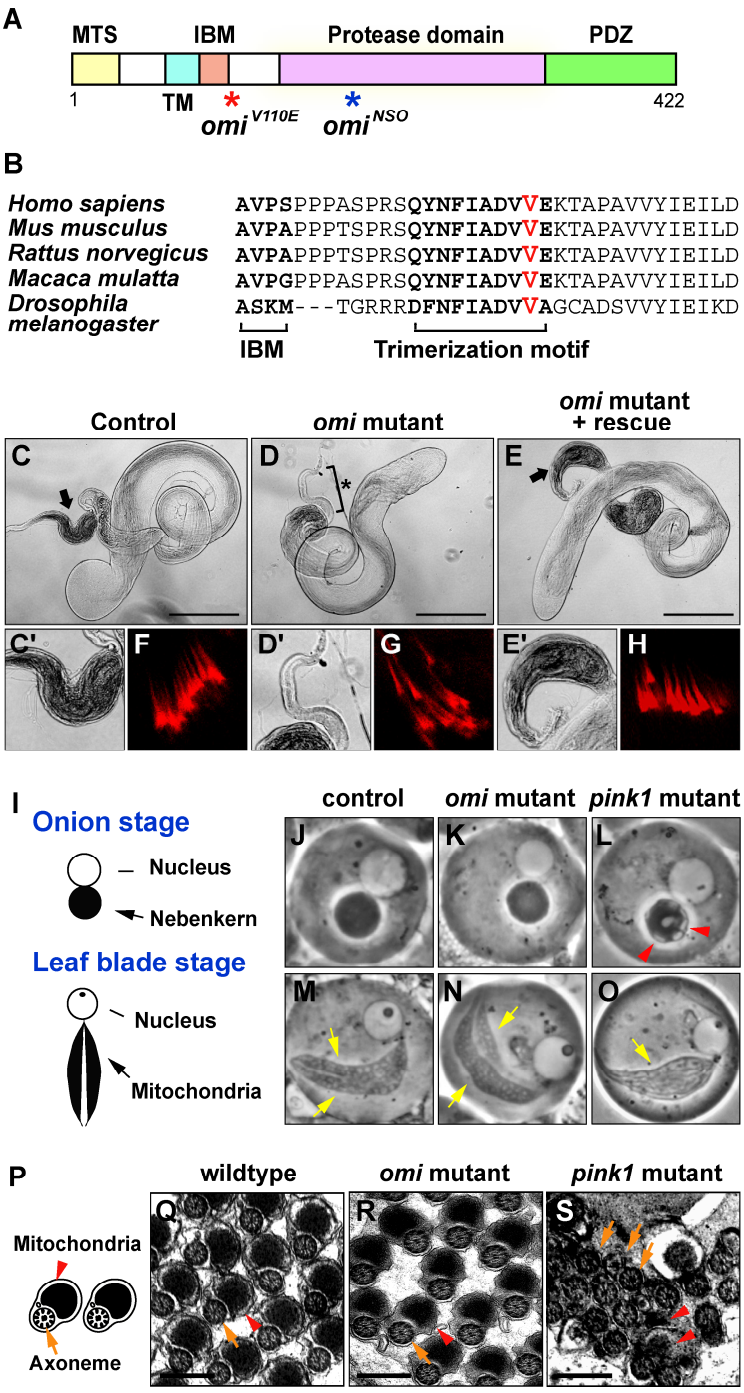

Figure 2-3. *Omi* null mutants show defects in spermatogenesis, but have normal mitochondrial morphology in testes. (A) Schematic depicting domains of Omi. MTS: mitochondrial targeting sequence. TM: transmembrane domain. IBM: IAP binding motif. The exact locations of Omi^{NSO} and Omi^{V110E} are depicted as a blue and a red asterisk, respectively.

(B) Sequence alignment of Omi/HtrA2 in various species in a highly conserved region, in which the conserved Valine, mutated in *Omi*^{V110E}, is marked in red. (C-E, C'-E') Phase contrast micrographs of testes. In contrast to a control fly (C, C') in which the seminal vesicles (arrow) is full of sperm (phase dark), *Omi* mutants (D, D') show empty seminal vesicle (bracket with an asterisk), which can be rescued by *Omi* overexpression (E, E') (arrow pointing to the seminal vesicle). C'-E' are higher magnification views of the seminal vesicle from C-E. (F-H) Phalloidin staining of investment cones within one syncytial cyst. In contrast to controls in which investment cones are well aligned indicating synchronized movement (F), *Omi* mutants show scattered investment cones in some of the cysts, indicative of a mild defect in individualization (G), which can be rescued by *Omi* overexpression (H). (I-P) Schematics and phase contrast micrographs of spermatid mitochondria during the "onion stage" (I-L) and "the leaf blade stage" (I, M-O). Compared with wildtype (J,M), *Omi* mutants do not show any defects in either stage (K,N), whereas *pink1* mutants show vacuolation (red arrowhead) in the nebenkern during the onion stage (L), and one instead of two mitochondrial derivatives (yellow arrow) seen in wildtype at the leaf blade stage (O). (P-S) Schematic and transmission EM images of a portion of a post-individualization cyst. Each spermatid contains an axoneme (orange arrow) and mitochondrial derivative (red arrowhead) within an individual plasma membrane. The *Omi* mutant cyst (R) shows disorganization of spermatids and occasional individualization defects (data not shown). However, compared with *pink1* mutants, which show severe impairment in the size and morphology of mitochondria (S), *Omi* mutant cysts show normal appearing mitochondria (R). Genotypes: wildtype: *w*/Y; control: *w*/Y; *Omi*^{NSO}/+; *Omi* mutant: *w*/Y; *Omi*^{NSO}*/Df(3R)ED5644*; *Omi* mutant + rescue: *w*/Y; TMR-*Omi*/+; *Omi*^{NSO}*/Df(3R)ED5644*. Scale bars: 500µm in C-E; 500nm in Q-S.

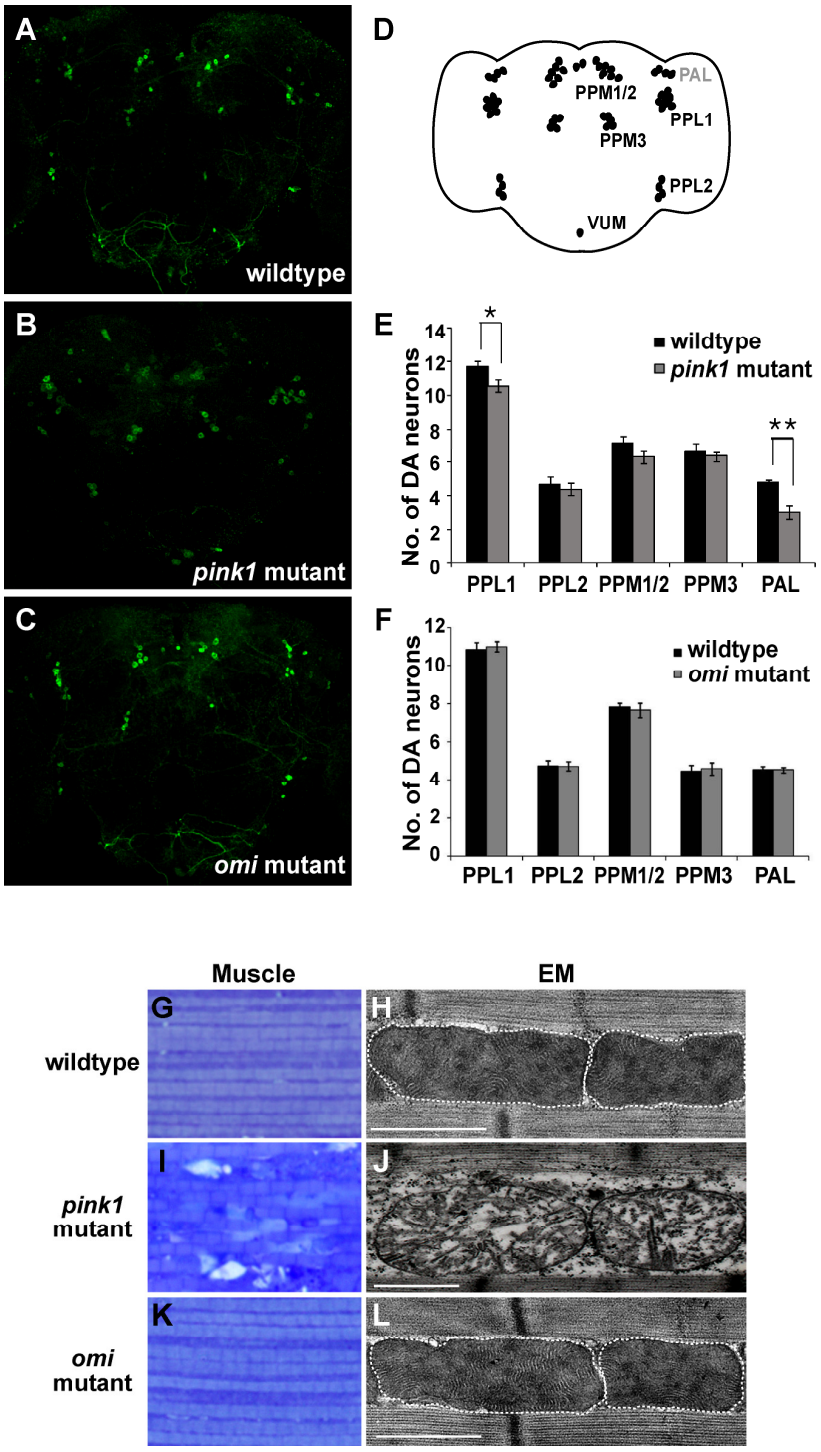

Figure 2-4. *Omi* null mutants do not show dopaminergic neuronal loss, muscle degeneration, or mitochondrial morphological defects. (A-C) Anti-Tyrosine Hydroxylase immunostaining of whole-mount brains from 40-day old wildtype (A), *pink1* mutant (B) and *Omi*

mutant flies (C). 17-27 individual flies (both hemispheres) were counted for each genotype. (D) Schematic depicting locations of the major dopaminergic neuron clusters in the adult brain as designated by abbreviations (Nassel and Elekes, 1992). The major dopaminergic neuron clusters are located near the posterior surface of the brain, with the exception of the PAL, which is located near the anterior surface (labeled in gray). (E,F) Quantification of dopaminergic neurons in each cluster in *pink1* mutant flies and wildtype flies (E), *Omi* mutant flies and wildtype flies (F) aged for 40 days at 25^{O}C. Error bars represent standard deviations, and student T-test is used for statistical analysis. Toluidine Blue staining of indirect flight muscle fibers (G,I,K) and EM studies of these muscles (H,J,L). The borders of mitochondria are marked with white dashed lines. In contrast to *pink1* mutants (I,J), *Omi* mutants do not show muscle degeneration or mitochondrial morphological defects (K,L), even when aged for 30 days. Genotypes: wildtype: *w*/Y. *Omi* mutant: *w*/Y; *Omi*^{NSO}*/Df(3R)ED5644*. *pink1* mutant: *w pink1*^{5}/Y. Scale bars: 1μm in F,H,J.

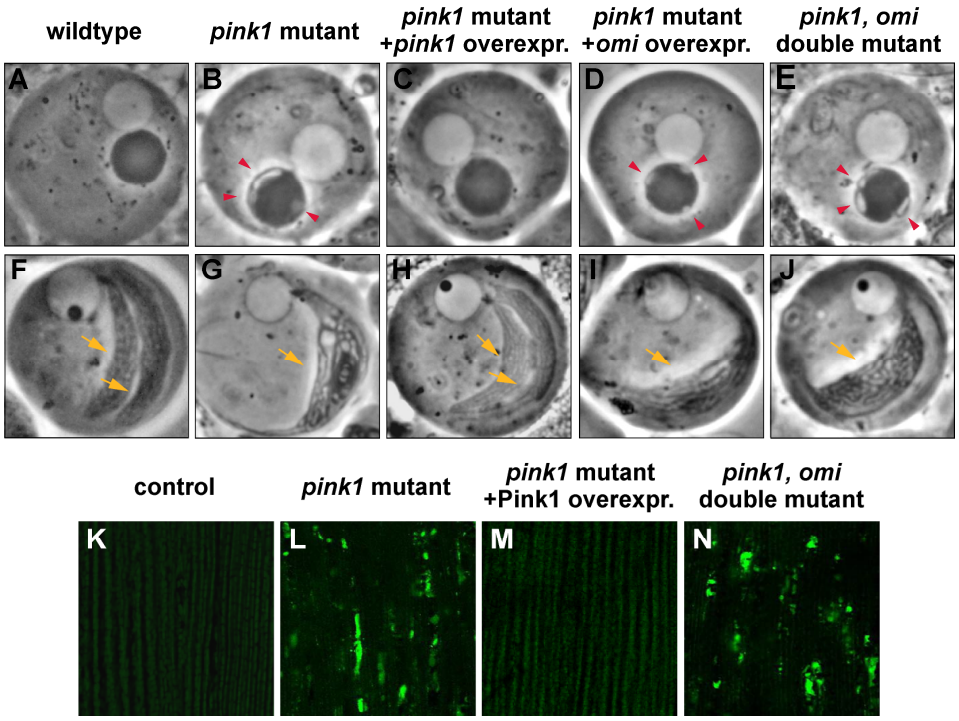

Figure 2-5. Lack of genetic interactions between *pink1* and *Omi* in loss-of-function studies of mitochondrial morphology.

(A-H) Phase contrast micrographs of spermatid mitochondria during the "onion stage" (A-E) and "the leaf blade stage" (F-J). *pink1* null mutants show vacuolation of nebenkerns (B) and one single mitochondrial derivative (G). This phenotype can be completely suppressed by *pink1* overexpression (C,H), but not by *Omi* overexpression (D,I). Double mutants removing both *pink1* and *Omi* function result in *pink1* mutant-like phenotypes without any enhancement (E,J). Red arrowheads point to vacuolation of the nebenkern and orange arrows mark each mitochondrial derivative. (K-N) Mitochondria of indirect flight muscle are labeled by mito-GFP. Compared with control (K), *pink1* mutants display overall reduced levels of mitoGFP signal, and large clumps of intense GFP signal (L), which can be completely rescued by *pink1* overexpression (M). Double mutants of *pink1* and *Omi* show *pink1* mutant-like phenotypes (N).

Genotypes: (A,F) *w*. (B,G) *w pink1*^{5}/Y. (C,H) *w pink1*^{5}/Y; TMR-*pink1*/+. (D,I) *w pink1*^{5}/Y; TMR-*Omi*/+. (E,J) *w pink1*^{5}/Y; *Omi*^{NSO}*/Df(3R)ED5644*. (K) *FM6/*Y; Mef2-Gal4, UAS-mitoGFP/+. (L) *w pink1*^{5}/Y; Mef2-Gal4, UAS-mitoGFP/+. (M) *w pink1*^{5}/Y; Mef2-Gal4, UAS-mitoGFP/UAS-*pink1*. (N) *w pink1*^{5}/Y; Mef2-Gal4, UAS-mitoGFP/UAS-RNAi-*Omi.*

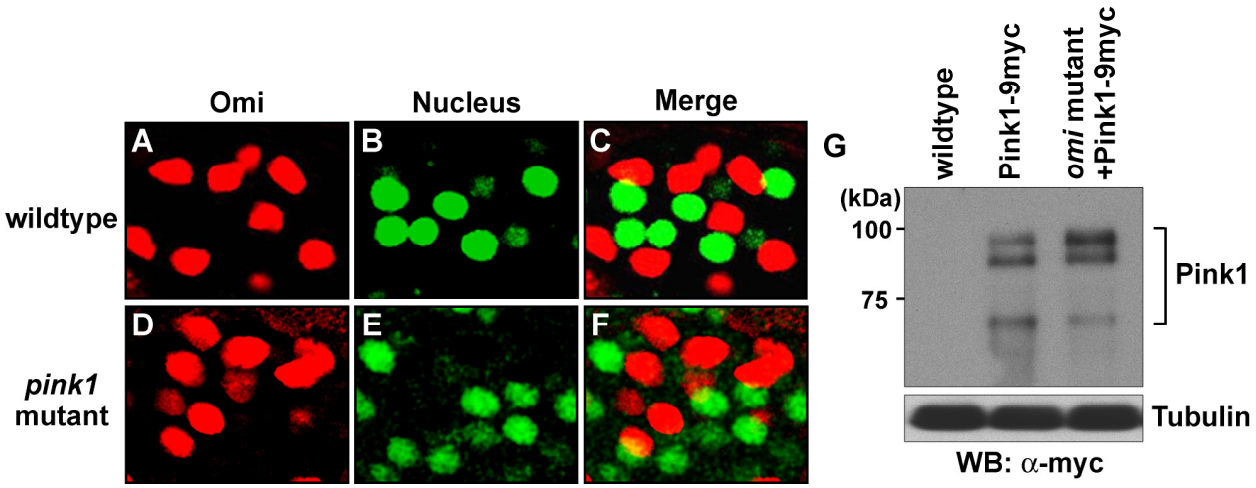

Figure 2-6. Omi is localized to mitochondria, and its expression is not altered in *pink1* null mutants; Pink1 expression is not altered in *Omi* mutants either.

(A-F) Double labeling of onion-staged spermatids in wildtype (A-C) and *pink1* mutants (D-F) using Prosα6T-GFP (green), which labels the nucleus, and an anti-Omi antibody (red), which labels the Nebenkern. In *pink1* null mutants, Omi is still localized to the nebenkerns of spermatids. (G) Western blotting of endogenous Pink1-9Myc expression using a genOmic rescue transgene. Loss of *Omi* function does not alter the cleavage pattern of Pink1.

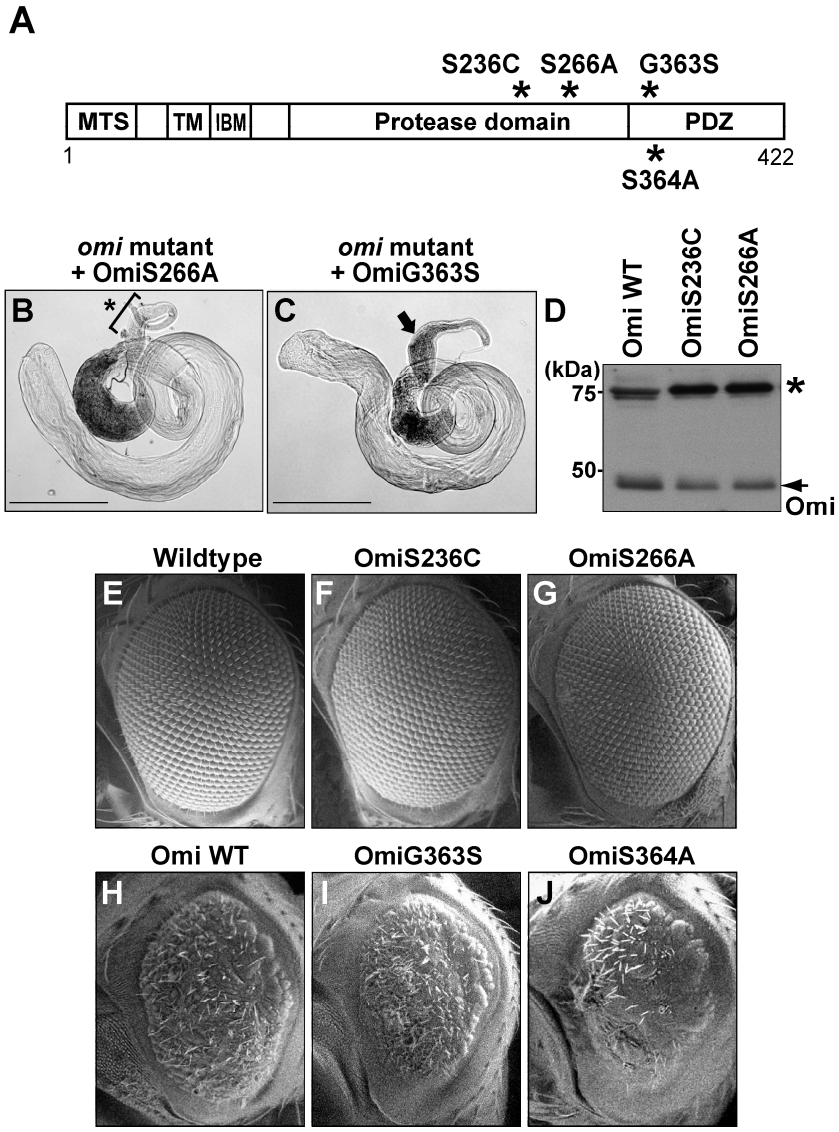

Figure 2-7. Functional analysis of Omi mutants.

(A) Schematic depicting positions of 4 mutations (*) with respect to domains in Omi. (B-C) Phase contrast micrographs. As with overexpression of Omi WT (Fig. 3E,E'), expression of G363S (C), but not S266A (B), restores the production of motile sperm in the seminal vesicle of *Omi* mutants. An arrow in C indicates the presence of sperm (phase dark), whereas a bracket and an asterisk in B point to the absence of sperm. (D) Both OmiS236C and OmiS266A are expressed at a comparable levels compared with Omi WT, as detected by an anti-Omi antibody.

Western blots of head lysates from flies overexpressing OmiWT, Omi236C or S266A using anti-Omi antibodies. Overexpression is accomplished using the eye-specific driver (GMR-Gal4), and flies are raised at 18^{O}C to avoid cell death comprOmising recovery of proteins. A non-specific band (*) serves as protein loading control. (E-J) Scanning EM micrographs of *Drosophila* eyes. Compared with overexpression of Omi WT, which results in small and rough eyes at 25^{O}C (H), overexpression of Omi G363S or S364A leads to similar rough eye phenotypes (I,J), while overexpression of Omi S236C or S266A results in wildtype-appearing eyes (F,G). GMR-Gal4 is used as an eye-specific driver. Scale bars: 500μm in B,C.

Genotype Fly (Human)	Molecular function from literature	Protease activity from literature	Tissue-specific overexpression			Ability to rescue *omi* mutant sterility
			Testes	Eye	Muscle	
Omi WT	-	-	sterile	small and rough	disrupted	rescue
S236C (S276C)	*mnd2* mice	reduced	fertile	wildtype appearing	wildtype appearing	-
S266A (S306A)	protease active site	protease dead	fertile	wildtype appearing	wildtype appearing	fail to rescue
G363S (G399S)	PD-associated mutation	reduced	sterile	small and rough	disrupted	rescue
S364A (S400A)	*pink1*-dependent phosphorylation site	reduced	sterile	small and rough	disrupted	-

Table 2-1. Summary of phenotypic effects of various Omi mutants reported in this study and by others.

SUPPLEMENTARY FIGURES AND FIGURE LEGENDS

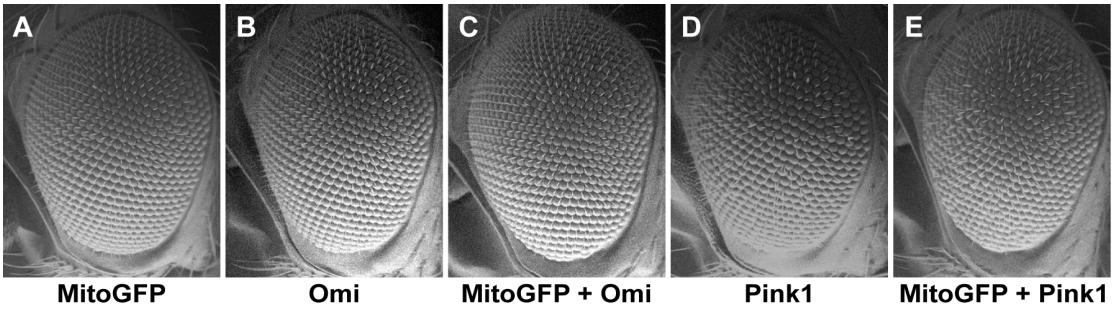

Supplementary Figure S2-1. Coexpression of mitoGFP does not modify the eye phenotypes of either *pink1* overexpression or *Omi* overexpression.

Scanning EM micrographs of Drosophila eyes. Overexpression is accomplished using the eyespecific driver (GMR-Gal4), and flies are raised at 18^{O}C. Panel B and D are the same images shown in Fig. 1B and 1C, respectively.

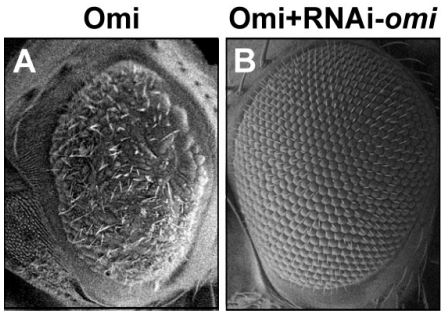

Supplementary Figure S2-2. Silencing of Omi function *in vivo*.

Silencing of Omi function is strong since it completely suppressed the *Omi* overexpression induced eye phenotype at 25 ^{O}C. Note the panel A is the same image shown in Fig. 7H.

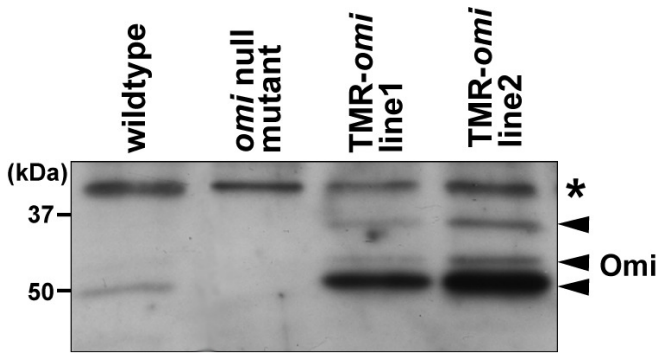

Supplementary Figure S2-3. Expression analysis of the *Omi* null mutant and *Omi* overexpression.

Western blots of testes lysates using anti-Omi antibodies. Compared with wildtype, *Omi* null mutant flies (Omi^{NSO}/Df(3R)ED5644) do not show any Omi expression, while elevated levels of Omi are observed from two independent Omi overexpression lines. *Omi* overexpression results in three anti-Omi positive bands (arrowheads), consistent with a previous report (Igaki et al., 2007). A non-specific band (*) serves as an internal loading control.

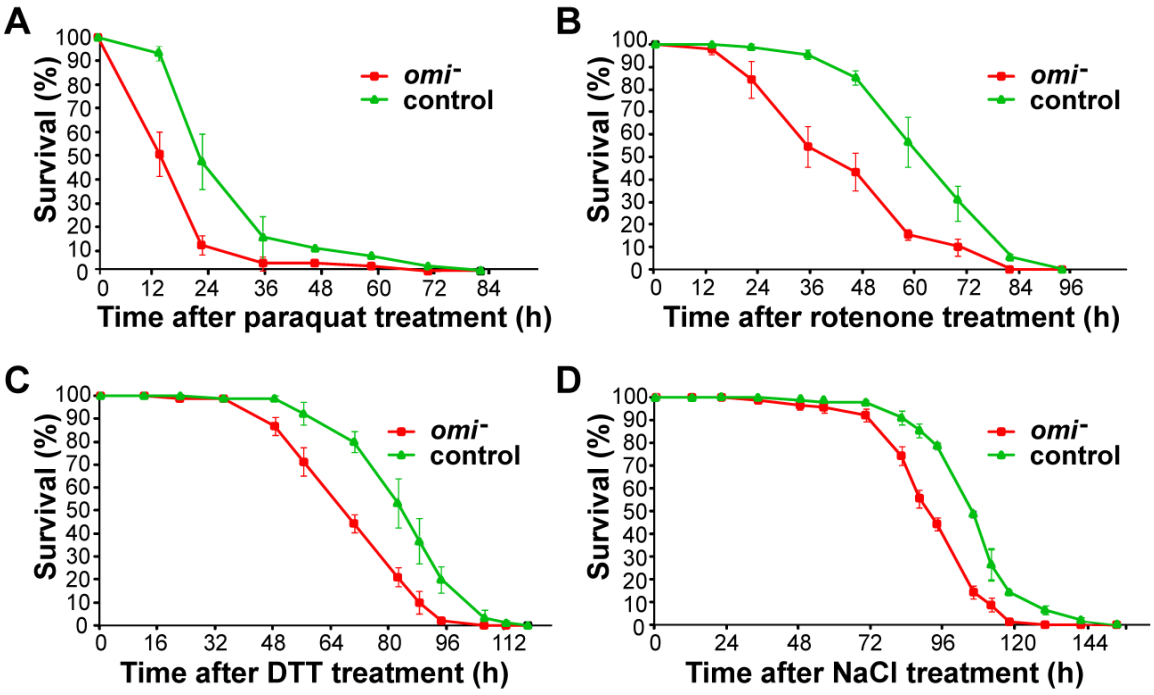

Supplementary Figure S2-4. *Omi* mutants are sensitive to multiple stresses.

Survival of *Omi* mutants (red), and *Omi* mutants carrying one copy of an Omi genOmic rescue transgene (green) as controls after exposure to 20mM paraquat (A), 10mM rotenone (B), 100mM DTT (C) and 500mM NaCl (D). Mean survival times (in hours) for *Omi* mutants, and Omi mutants carrying a single copy of an Omi genOmic rescue transgene, respectively, are: paraquat 14.9±2.1 and 26.5±3.9; rotenone 39.8±2.8 and 59.8±2.3; DTT 66.6±0.9, and 82.9±3.5; NaCl 89.9±2.1 and 100.9±2.0. Error bars indicate standard deviations. Genotypes: *Omi* mutants: w/Y; Omi^{NSO} /Df(3R)ED5644. Control: w/Y; CaSpeR-*Omi*/+; Omi^{NSO}/Df(3R)ED5644. Student's t-test was used.

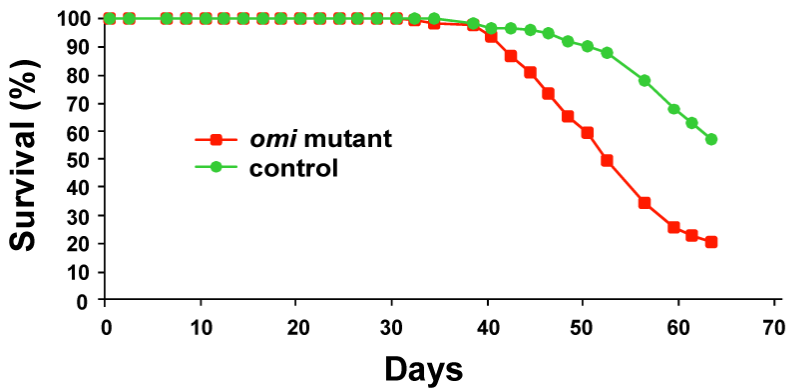

Supplementary Figure S2-5. *Omi* null mutants are short lived.

Survival of Omi mutants (red), and Omi mutants carrying a single copy of Omi genOmic rescue transgene (green) as controls over time. Genotypes: *Omi* mutants: w/Y; Omi^{NSO} /Df(3R)ED5644. Control: w/Y; CaSpeR-*Omi*/+; Omi^{NSO} /Df(3R)ED5644.

REFERENCES

Beilina, A., M. Van Der Brug, R. Ahmad, S. Kesavapany, D.W. Miller, G.A. Petsko, and M.R. Cookson. 2005. Mutations in PTEN-induced putative kinase 1 associated with recessive parkinsonism have differential effects on protein stability. *Proc Natl Acad Sci U S A*. 102:5703-5708.

Bogaerts, V., K. Nuytemans, J. Reumers, P. Pals, S. Engelborghs, B. Pickut, E. Corsmit, K. Peeters, J. Schymkowitz, P.P. De Deyn, P. Cras, F. Rousseau, J. Theuns, and C. Van Broeckhoven. 2008. Genetic variability in the mitochondrial serine protease HTRA2 contributes to risk for Parkinson disease. *Hum Mutat*. 29:832-840.

Bonini, N.M., and M.E. Fortini. 2003. Human neurodegenerative disease modeling using Drosophila. *Annu Rev Neurosci*. 26:627-656.

Brand, A.H., and N. Perrimon. 1993. Targeted gene expression as a means of altering cell fates and generating dOminant phenotypes. *Development*. 118:401-415.

Challa, M., S. Malladi, B.J. Pellock, D. Dresnek, S. Varadarajan, Y.W. Yin, K. White, and S.B. Bratton. 2007. Drosophila Omi, a mitochondrial-localized IAP antagonist and proapoptotic serine protease. *EMBO J*. 26:3144-3156.

Chen, C.H., H. Huang, C.M. Ward, J.T. Su, L.V. Schaeffer, M. Guo, and B.A. Hay. 2007. A synthetic maternal-effect selfish genetic element drives population replacement in Drosophila. *Science*. 316:597-600.

Clark, I.E., M.W. Dodson, C. Jiang, J.H. Cao, J.R. Huh, J.H. Seol, S.J. Yoo, B.A. Hay, and M. Guo. 2006. Drosophila pink1 is required for mitochondrial function and interacts genetically with parkin. *Nature*. 441:1162-1166.

Dauer, W., and S. Przedborski. 2003. Parkinson's disease: mechanisms and models. *Neuron*. 39:889-909.

Deng, B.L., Y. Zhao, T.L. Hartman, K. Watson, R.W. Buckheit, Jr., C. Pannecouque, E. De Clercq, and M. Cushman. 2009. Synthesis of alkenyldiarylmethanes (ADAMs) containing benzo[d]isoxazole and oxazolidin-2-one rings, a new series of potent non-nucleoside HIV-1 reverse transcriptase inhibitors. *Eur J Med Chem*. 44:1210-1214.

Deng, H., M.W. Dodson, H. Huang, and M. Guo. 2008a. The Parkinson's disease genes pink1 and parkin promote mitochondrial fission and/or inhibit fusion in Drosophila. *Proc Natl Acad Sci U S A*. 105:14503-14508.

Deng, H., M.W. Dodson, H. Huang, and M. Guo. 2008b. The Parkinson's disease genes pink1 and parkin promotes mitochondrial fission and/or inhibits mitochodnrial fusion. *PNAS*. 105:14503-14508.

Dodson, M.W., and M. Guo. 2007. Pink1, Parkin, DJ-1 and mitochondrial dysfunction in Parkinson's disease. *Curr Opin Neurobiol*. 17:331-337.

Exner, N., B. Treske, D. Paquet, K. Holmstrom, C. Schiesling, S. Gispert, I. Carballo-Carbajal, D. Berg, H.H. Hoepken, T. Gasser, R. Kruger, K.F. Winklhofer, F. Vogel, A.S. Reichert, G. Auburger, P.J. Kahle, B. Schmid, and C. Haass. 2007. Loss-of-function of human PINK1 results in mitochondrial pathology and can be rescued by parkin. *J Neurosci*. 27:12413-12418.

Ganguly, A., R.M. Feldman, and M. Guo. 2008. ubiquilin antagonizes presenilin and promotes neurodegeneration in Drosophila. *Hum Mol Genet*. 17:293-302.

Gautier, C.A., T. Kitada, and J. Shen. 2008. Loss of PINK1 causes mitochondrial functional defects and increased sensitivity to oxidative stress. *Proc Natl Acad Sci U S A*. 105:11364-11369.

Greene, J.C., A.J. Whitworth, I. Kuo, L.A. Andrews, M.B. Feany, and L.J. Pallanck. 2003. Mitochondrial pathology and apoptotic muscle degeneration in Drosophila parkin mutants. *Proc Natl Acad Sci U S A*. 100:4078-4083.

Gross, G.G., R.M. Feldman, A. Ganguly, J. Wang, H. Yu, and M. Guo. 2008. Role of X11 and ubiquilin as in vivo regulators of the amyloid precursor protein in Drosophila. *PLoS One*. 3:e2495.

Guo, M., E.J. Hong, J. Fernandes, S.L. Zipursky, and B.A. Hay. 2003. A reporter for amyloid precursor protein gamma-secretase activity in Drosophila. *Hum Mol Genet*. 12:2669-2678.

Guo, M., L.Y. Jan, and Y.N. Jan. 1996. Control of daughter cell fates during asymmetric division: interaction of Numb and Notch. *Neuron*. 17:27-41.

Hardy, J., H. Cai, M.R. Cookson, K. Gwinn-Hardy, and A. Singleton. 2006. Genetics of Parkinson's disease and parkinsonism. *Ann Neurol*. 60:389-398.

Hay, B.A., T. Wolff, and G.M. Rubin. 1994. Expression of baculovirus P35 prevents cell death in Drosophila. *Development*. 120:2121-2129.

Huh, J.R., S.Y. Vernooy, H. Yu, N. Yan, Y. Shi, M. Guo, and B.A. Hay. 2004. Multiple apoptotic caspase cascades are required in nonapoptotic roles for Drosophila spermatid individualization. *PLoS Biol*. 2:E15.

Ibanez, P., S. Lesage, E. Lohmann, S. Thobois, G. De Michele, M. Borg, Y. Agid, A. Durr, and A. Brice. 2006. Mutational analysis of the PINK1 gene in early-onset parkinsonism in Europe and North Africa. *Brain*. 129:686-694.

Igaki, T., Y. Suzuki, N. Tokushige, H. Aonuma, R. Takahashi, and M. Miura. 2007. Evolution of mitochondrial cell death pathway: Proapoptotic role of HtrA2/Omi in Drosophila. *Biochem Biophys Res Commun*. 356:993-997.

Jones, J.M., R.L. Albin, E.L. Feldman, K. Simin, T.G. Schuster, W.A. Dunnick, J.T. Collins, C.E. Chrisp, B.A. Taylor, and M.H. Meisler. 1993. mnd2: a new mouse model of inherited motor neuron disease. *GenOmics*. 16:669-677.

Jones, J.M., P. Datta, S.M. Srinivasula, W. Ji, S. Gupta, Z. Zhang, E. Davies, G. Hajnoczky, T.L. Saunders, M.L. Van Keuren, T. Fernandes-Alnemri, M.H. Meisler, and E.S. Alnemri. 2003. Loss of Omi mitochondrial protease activity causes the neuromuscular disorder of mnd2 mutant mice. *Nature*. 425:721-727.

Khan, F.S., M. Fujioka, P. Datta, T. Fernandes-Alnemri, J.B. Jaynes, and E.S. Alnemri. 2008. The interaction of DIAP1 with dOmi/HtrA2 regulates cell death in Drosophila. *Cell Death Differ*. 15:1073-1083.

Kitada, T., S. Asakawa, N. Hattori, H. Matsumine, Y. Yamamura, S. Minoshima, M. Yokochi, Y. Mizuno, and N. Shimizu. 1998. Mutations in the parkin gene cause autosomal recessive juvenile parkinsonism. *Nature*. 392:605-608.

Koundakjian, E.J., D.M. Cowan, R.W. Hardy, and A.H. Becker. 2004. The Zuker collection: a resource for the analysis of autosomal gene function in Drosophila melanogaster. *Genetics*. 167:203-206.

Li, W., S.M. Srinivasula, J. Chai, P. Li, J.W. Wu, Z. Zhang, E.S. Alnemri, and Y. Shi. 2002. Structural insights into the pro-apoptotic function of mitochondrial serine protease HtrA2/Omi. *Nat Struct Biol*. 9:436-441.

Marsh, J.L., and L.M. Thompson. 2006. Drosophila in the study of neurodegenerative disease. *Neuron*. 52:169-178.

Martins, L.M., A. Morrison, K. Klupsch, V. Fedele, N. Moisoi, P. Teismann, A. Abuin, E. Grau, M. Geppert, G.P. Livi, C.L. Creasy, A. Martin, I. Hargreaves, S.J. Heales, H. Okada, S. Brandner, J.B. Schulz, T. Mak, and J. Downward. 2004. Neuroprotective role of the Reaper-related serine protease HtrA2/Omi revealed by targeted deletion in mice. *Mol Cell Biol*. 24:9848-9862.

McQuibban, G.A., J.R. Lee, L. Zheng, M. Juusola, and M. Freeman. 2006. Normal mitochondrial dynamics requires rhomboid-7 and affects Drosophila lifespan and neuronal function. *Curr Biol*. 16:982-989.

Meulener, M., A.J. Whitworth, C.E. Armstrong-Gold, P. Rizzu, P. Heutink, P.D. Wes, L.J. Pallanck, and N.M. Bonini. 2005. Drosophila DJ-1 mutants are selectively sensitive to environmental toxins associated with Parkinson's disease. *Curr Biol*. 15:1572-1577.

Park, J., S.B. Lee, S. Lee, Y. Kim, S. Song, S. Kim, E. Bae, J. Kim, M. Shong, J.M. Kim, and J. Chung. 2006. Mitochondrial dysfunction in Drosophila PINK1 mutants is complemented by parkin. *Nature*. 441:1157-1161.

Pesah, Y., T. Pham, H. Burgess, B. Middlebrooks, P. Verstreken, Y. Zhou, M. Harding, H. Bellen, and G. Mardon. 2004. Drosophila parkin mutants have decreased mass and cell size and increased sensitivity to oxygen radical stress. *Development*. 131:2183-2194.

Piccoli, C., A. Sardanelli, R. Scrima, M. Ripoli, G. Quarato, A. D'Aprile, F. Bellomo, S. Scacco, G. De Michele, A. Filla, A. Iuso, D. Boffoli, N. Capitanio, and S. Papa. 2008. Mitochondrial respiratory dysfunction in familiar parkinsonism associated with PINK1 mutation. *Neurochem Res*. 33:2565-2574.

Plun-Favreau, H., K. Klupsch, N. Moisoi, S. Gandhi, S. Kjaer, D. Frith, K. Harvey, E. Deas, R.J. Harvey, N. McDonald, N.W. Wood, L.M. Martins, and J. Downward. 2007. The mitochondrial protease HtrA2 is regulated by Parkinson's disease-associated kinase PINK1. *Nat Cell Biol*. 9:1243-1252.

Poole, A.C., R.E. Thomas, L.A. Andrews, H.M. McBride, A.J. Whitworth, and L.J. Pallanck. 2008a. The PINK1/Parkin pathway regulates mitochondrial morphology. *Proc Natl Acad Sci U S A*. 105:1638-1643.

Poole, A.C., R.E. Thomas, L.A. Andrews, H.M. McBride, A.J. Whitworth, and L.J. Pallanck. 2008b. The PINK1/Parkin pathway regulates mitochondrial morphology. *Proceedings of the National Academy of Sciences of the United States of America*. 105:1638-1643.

Przedborski, S., and H. Ischiropoulos. 2005. Reactive oxygen and nitrogen species: weapons of neuronal destruction in models of Parkinson's disease. *Antioxid. Redox. Signal*. 7:685-693.

Rathke-Hartlieb, S., U. Schlomann, P. Heimann, M.H. Meisler, H. Jockusch, and J.W. Bartsch. 2002. Progressive loss of striatal neurons causes motor dysfunction in MND2 mutant mice and is not prevented by Bcl-2. *Exp Neurol*. 175:87-97.

Riparbelli, M.G., and G. Callaini. 2007. The Drosophila parkin homologue is required for normal mitochondrial dynamics during spermiogenesis. *Dev Biol*. 303:108-120.

Ross, O.A., A.I. Soto, C. Vilarino-Guell, M.G. Heckman, N.N. Diehl, M.M. Hulihan, J.O. Aasly, S. Sando, J.M. Gibson, T. Lynch, A. Krygowska-Wajs, G. Opala, M. Barcikowska, K. Czyzewski, R.J. Uitti, Z.K. Wszolek, and M.J. Farrer. 2008a. Genetic variation of Omi/HtrA2 and Parkinson's disease. *Parkinsonism Relat Disord*. 14:539-543.

Ross, O.A., A.I. Soto, C. Vilarino-Guell, M.G. Heckman, N.N. Diehl, M.M. Hulihan, J.O. Aasly, S. Sando, J.M. Gibson, T. Lynch, A. Krygowska-Wajs, G. Opala, M. Barcikowska, K.

Czyzewski, R.J. Uitti, Z.K. Wszolek, and M.J. Farrer. 2008b. Genetic variation of Omi/HtrA2 and Parkinson's disease. *Parkinsonism & related disorders*.

Simon-Sanchez, J., S. Scholz, M. Matarin Mdel, H.C. Fung, D. Hernandez, J.R. Gibbs, A. Britton, J. Hardy, and A. Singleton. 2008. Genomewide SNP assay reveals mutations underlying Parkinson disease. *Hum Mutat*. 29:315-322.

Simon-Sanchez, J., and A.B. Singleton. 2008. Sequencing analysis of OMI/HTRA2 shows previously reported pathogenic mutations in neurologically normal controls. *Hum Mol Genet*.

Strauss, K.M., L.M. Martins, H. Plun-Favreau, F.P. Marx, S. Kautzmann, D. Berg, T. Gasser, Z. Wszolek, T. Muller, A. Bornemann, H. Wolburg, J. Downward, O. Riess, J.B. Schulz, and R. Kruger. 2005. Loss of function mutations in the gene encoding Omi/HtrA2 in Parkinson's disease. *Hum Mol Genet*. 14:2099-2111.

Till, B.J., S.H. Reynolds, E.A. Greene, C.A. Codomo, L.C. Enns, J.E. Johnson, C. Burtner, A.R. Odden, K. Young, N.E. Taylor, J.G. Henikoff, L. Comai, and S. Henikoff. 2003. Large-scale discovery of induced point mutations with high-throughput TILLING. *Genome Res*. 13:524-530.

Valente, E.M., S. Salvi, T. Ialongo, R. Marongiu, A.E. Elia, V. Caputo, L. ROmito, A. Albanese, B. Dallapiccola, and A.R. Bentivoglio. 2004. PINK1 mutations are associated with sporadic early-onset parkinsonism. *Ann Neurol*. 56:336-341.

Vande Walle, L., M. Lamkanfi, and P. Vandenabeele. 2008. The mitochondrial serine protease HtrA2/Omi: an overview. *Cell Death Differ*. 15:453-460.

Walle, L.V., M. Lamkanfi, and P. Vandenabeele. 2008. The mitochondrial serine protease HtrA2/Omi: an overview. *Cell Death Differ*. 15:453-460.

Whitworth, A.J., J.R. Lee, V.M. Ho, R. Flick, R. Chowdhury, and G.A. McQuibban. 2008a. Rhombiod-7 and HtrA2/Omi act in a common pathway with the Parkinson's disease factors Pink1 and Parkin. *Disease Models & Mechanisms*. 1:168-174.

Whitworth, A.J., J.R. Lee, V.M. Ho, R. Flick, R. Chowdhury, and G.A. McQuibban. 2008b. Rhomboid-7 and HtrA2/Omi act in a common pathway with the Parkinson's disease factors Pink1 and Parkin. *Dis Model Mech*. 1:168-174; discussion 173.

Wood-Kaczmar, A., S. Gandhi, Z. Yao, A.Y. Abramov, E.A. Miljan, G. Keen, L. Stanyer, I. Hargreaves, K. Klupsch, E. Deas, J. Downward, L. Mansfield, P. Jat, J. Taylor, S. Heales, M.R. Duchen, D. Latchman, S.J. Tabrizi, and N.W. Wood. 2008. PINK1 is necessary for long term survival and mitochondrial function in human dopaminergic neurons. *PLoS One*. 3:e2455.

Yang, Y., S. Gehrke, Y. Imai, Z. Huang, Y. Ouyang, J.W. Wang, L. Yang, M.F. Beal, H. Vogel, and B. Lu. 2006. Mitochondrial pathology and muscle and dopaminergic neuron degeneration caused by inactivation of Drosophila Pink1 is rescued by Parkin. *Proc Natl Acad Sci U S A*. 103:10793-10798.

Yang, Y., Y. Ouyang, L. Yang, M.F. Beal, A. McQuibban, H. Vogel, and B. Lu. 2008a. Pink1 regulates mitochondrial dynamics through interaction with the fission/fusion machinery. *Proc Natl Acad Sci U S A*. 105:7070-7075.

Yang, Y., Y. Ouyang, L. Yang, M.F. Beal, A. McQuibban, H. Vogel, and B. Lu. 2008b. Pink1 regulates mitochondrial dynamics through interaction with the fission/fusion machinery. *Proceedings of the National Academy of Sciences of the United States of America*. 105:7070-7075.

Zhong, L., and J.M. Belote. 2007. The testis-specific proteasome subunit Prosalpha6T of D. melanogaster is required for individualization and nuclear maturation during spermatogenesis. *Development*. 134:3517-3525.

CHAPTER 3

MUL1, a novel suppressor of *PINK1*, acts in parallel to the PINK1/parkin pathway to regulate mitochondrial integrity and body fat.

Jina Yun,[1,2], Huan Yang*,[1,3] ,Rajat Puri*,[6], Chunlai Wu[7], Michael Lizzio[1], Zuhang Sheng[6], and Ming Guo[1,2,3,4,5]

*co-second authors

Departments of [1]Neurology and [2]Molecular and Medical Pharmacology and [3]Molecular, Cellular and Integrative Physiology, [4]Brain Research Institute, and [5]The David Geffen School of Medicine, University of California, Los Angeles, Los Angeles, CA 90095, [6]National Institute of Neurological Disorders and Stroke, National Institutes of Health, Bethesda, MD 20892, and [7]Neuroscience Center of Excellence, Louisiana State University Health Sciences Center, New Orleans, Louisiana

In preparation

ABSTRACT

Mutations in *PINK1* or *parkin* cause early onset hereditary PD. Genetic studies indicate that *PINK1* and *parkin* function in the same pathway to regulate mitochondrial dynamics through MFN. In mammalian cell culture studies, PINK1 recruits Parkin to mitochondria upon mitochondrial damage, which results in selective removal of damaged mitochondria, a process called mitophagy. Here, we identify *MUL1*, a mitochondrially targeted ubiquitin E3 ligase, as a novel suppressor of *PINK1* and *parkin* mutants. We show that *MUL1* suppresses *PINK1* and *parkin* phenotypes including mitochondrial morphology, muscle degeneration, and dopaminergic neuronal phenotypes. We also demonstrate that *MFN* overexpression phenocopies *PINK1* and *parkin* mutant phenotypes, suggesting increased level of MFN as a potential cause of pathogenesis. We further show that the *MUL1* suppresses *PINK1* and *parkin* phenotypes by reduction of MFN levels through ubiquitination. Interestingly, *MUL1* does not affect Parkin-mediated mitophagy upon mitochondrial damage in HeLa and primary cortical neurons, suggesting that *MUL1* acts on a different pathway. Consistently, genetic epistasis studies in flies indicate that *MUL1* acts in parallel to the PINK1/parkin pathway. Out work suggests that reduction of MFN by *MUL1* is sufficient to reverse *PINK1* and *parkin* deficiency phenotypes. It proposes *MUL1* as a potential therapeutic target to modulate PD pathology.

INTRODUCTION

Parkinson's Disease (PD) is the second most common neurodegenerative disease. Mutation(s) in PD genes *PINK1* and *parkin* cause(s) autosomal recessive forms of PD. In *Drosophila*, genetic studies have shown that *PINK1* and *parkin* act in the same genetic pathway regulating mitochondrial integrity (Clark et al., 2006; Park et al., 2006; Yang et al., 2006). Mitochondrial morphology is maintained through a balance between mitochondrial fusion and

mitochondrial fission. Mitochondrial fusion is regulated by Mitofusin 1 and 2 (MFN1 and MFN2) in mammalian cells while mitochondrial fission is mediated by Drp1. Genetic studies in *Drosophila* have shown that modulation of mitochondrial dynamics; inhibition of fusion and/or promotion of fission suppresses *PINK1* or *parkin* loss of function phenotypes (Deng et al., 2008; Poole et al., 2008; Yang et al., 2008), indicating the PINK1/Parkin pathway regulation of mitochondrial dynamics. The direct evidence of the PINK1/Parkin pathway in regulating mitochondrial dynamics came from studies showing that MFN is ubiquitinated by Parkin (Poole et al., 2010; Ziviani et al., 2010). The same regulation has been shown in other systems (Gegg et al., 2010; Gegg and Schapira, 2011; Rakovic et al., 2011).

In mammalian cell culture system, the PINK1/Parkin pathway has been shown to mediate mitophagy- the selective autophagic degradation of mitochondria (Narendra et al., 2008a; Narendra et al., 2010b). When mitochondria lose membrane potential due to mitochondrial damages, PINK1 is stabilized on the mitochondria, which results in recruitment of Parkin to the mitochondria (Matsuda et al., 2010; Narendra et al., 2010b). Recruited Parkin ubiquitinates mitochondrial outermembrane proteins including MFN. This ubiquitination and proteasomal degradation signal recruitment of p62 and autophagosome leading autophagic degradation of mitochondria (Chan et al., 2011a; Geisler et al., 2010; Narendra et al., 2010a; Ziviani et al., 2010).

Further understanding of the PINK1/Parkin pathway and prevention the pathology of *PINK1* and *parkin* deficiency are of great interest. Thus, we pursued to look for suppressors of *PINK1* mutant phenotypes and indentified *MUL1* as a novel suppressor of *PINK1*. *Drosophila MUL1* gene (CG1134) is predicted to encode a protein with two transmembrane domains and one highly conserved RING finger (RNF) domain. There is no loss of function study of *MUL1* in

any system. However, cell-based overexpression studies revealed that human *MUL1* mainly localizes to mitochondria (Li et al., 2008; Neuspiel, 2008; Zhang et al., 2008) onto which two transmembrane domains anchor the protein exposing RNF domain to the cytosol (Li et al., 2008). The RNF domain has both SUMO and ubiquitin E3 ligase activity. The SUMO E3 ligase activity is important in promotion of mitochondrial fission through sumoylation of Drp1 (Braschi et al., 2009). On the other hand, E3 ligase activity is important in degradation of Akt and p53 (Bae et al., 2012; Jung et al., 2011). The targets of *MUL1* suggest *MUL1*'s broader roles in cell growth, survival, and death as well as mitochondrial dynamics. To better understand *MUL1*, loss of function studies would be valuable.

In this study, we identify *MUL1* as a novel suppressor of *PINK1* and *parkin* mutants. *MUL1* suppresses *PINK1* and *parkin* pathology by reduction of MFN levels through ubiquitination. *MUL1* acts in parallel to the PINK1/parkin pathway providing a new way to modulate *PINK1* and *parkin* deficiency pathology.

MATERIALS & METHODS

Molecular biology.

To generate UAS-*MUL1*, the *MUL1* cDNA (EST clone from *Drosophila* Genome Research Center, AT15655) was subcloned into UASt vector using EcoRI and XhoI sites. *Drosophila MUL1* ligase dead mutant (*MUL1* LD) was generated by mutating H307 to A via site-specific mutagenesis (Stragene QuikChangeII XL Kit). To generate UAS-*MFN*, the *MFN* cDNA (EST clone from *Drosophila* Genome Research Center, RE04414) was subcloned into UASt vector. For UAS-*MUL1*-GFP, UAS-*MFN*-myc, and UAS-HA-*parkin*, each gene's conding region was fused to different tags by gateway cloning system (Invitrogen). For RNAi to silence

MUL1 and *drp1*, the *MUL1* and *drp1* transcripts to the coding region were targeted using a microRNA-based technology, and PCR products of these microRNA precursors were cloned into pUASt. All constructs made were confirmed by DNA sequencing. UAS-SUMO RNAi was obtained from Vienna *Drosophila* RNAi center. pAC-*MFN*-Flag was a gift from Alexander J. Whitworth (University of Sheffield). Human *MUL1* cDNA (BC010101) was purchased from ATCC and cloned into pEGFP vector (Clontech). Human *MUL1 LD* was generated by mutating H319 to A, which corresponds to *Drosophila MUL1* H307A, via site-specific mutagenesis (Stragene QuikChangeII XL Kit). Human sh*MUL1* constructs were purchased from OriGene.

Drosophila genetics and strains.

CaSpeR-HA-*drp1* flies were gifts from Hugo J. Bellen (Baylor College of Medicine). UASp-SUMO was gift from Albert J. Courey. *MUL1*^{EY12156}, UAS-mitoGFP, Mef2-GAL4, OK6-GAL4 and TH-GAL4 flies were obtained from the BloOmington *Drosophila* Stock Center. *PINK1*^{5}, *parkin25*, and UAS-Drp1 flies have been previously described (Clark et al., 2006b; Deng et al., 2008a). For experiments involving transgenic flies, constructs were injected to w^{1118} and multiple independent fly lines were generated (Rainbow Transgenic Flies, Inc.). *Drosophila* strains were maintained in a 25°C humidified incubator.

Immunofluorescence and confocal microscopy.

For analysis of muscles, thoraces of 1-2 day-old-adult flies were dissected and fixed in 4% paraformaldehyde in phosphate buffered saline (PBS). After thoraces were washed 3 times in PBS, muscle fibers were isolated from thoraces and stained with Rhodamine Phalloidin (Invitrogen, 1:1000) in PBS+1% Triton X-100. For antibody staining, muscle fibers were permeabilized in PBS+0.1% Triton X-100, blocked in 5% normal goat serum in PBS, and incubated in primary and secondary antibodies diluted in 5% normal goat serum in PBS. For

analysis of dopaminergic neurons, brains of 3-day-old male flies were dissected and fixed in 4% paraformaldehyde in PBS. Blocking, primary and secondary antibody staining were performed as described previously (Yun et al., 2008). The following primary antibodies were used for immunocytochemistry: mouse anti-ATPase synthase (Mitosciences), chicken anti-HA (Millipore), mouse anti-tyrosine hydroxylase (Immunostar), and rabbit anti-SUMO (a gift from Albert J. Courey). All images were taken by a Zeiss LSM5 confocal microscope.

TUNEL assay

Adult male flies were aged for 5 days at 25°C. Thoraces of the flies were dissected and fixed in 4% paraformaldehyde in PBS. Muscle fibers were dissected and permeabilized/blocked in T-TBS-3% BSA (T-TBS: 0.1% Triton X-100, 50mM Tris-Cl (pH 7.4), 188mM NaCl). After blocking, TUNEL staining was carried out using *in situ* cell death detection kit according to the manufacturer's instructions (Roche).

Toluidine blue staining and transmission electron microscopy.

Thoraces from 3-day-old male flies were dissected, fixed in paraformaldehyde/glutaraldehyde, postfixed in osmium tetraoxide, dehydrated in ethanol, and embedded in Epon. Toluidine blue was used to stain 1.5-μm-thick tissue sections. Thin sections (80 nm thick) were stained with uranyl acetate and lead citrate, and examined using a JEOL 100C transmission electron microscope (University of California, Los Angeles Brain Research Institute Electron Microscopy Facility).

Immunofluorescence and quantification of mitochondrial number, size, and total area in salivary glands.

To analyze mitochondria in salivary glands, salivary glands of 3rd instar larvae were dissected, fixed in 4% paraformaldehyde in PBS, and stained with Rhodamine Phalloidin.

Images were taken by a Zeiss LSM5 confocal microscope. Each cell in images was outlined, and the outlined area was analyzed for mitochondrial number, average size and total area using the Analyze Particles function in ImageJ software (NIH).

TLC assay.

TLC assays were performed as described (Al-Anzi et al., 2009). Briefly, male flies of each genotype were aged for 10 days and crushed in chloroform: methanol (2:1) solution. The supernatant was blotted on a silica TLC plate. Hexane: ethyl ether (4:1) solution was used for mobile phase, and then the plate was stained in ceric ammonium molybdate (CAM) solution. After staining, the plate was baked at 80°C incubator for 20-25 mins. Each genotype was repeated 4 times.

Drosophila lysate preparation and western blot.

Thoraces from adult flies or whole animals were collected and disrupted in RIPA buffer containing protease inhibitors (Roche) using pestles. Total protein concentration was measured using Bradford assay kit (Bio-Rad), and the same amount of proteins was loaded into SDS-polyacryamide gels. Following primary antibodies were used for western blot: mouse anti-myc (Millipore), mouse anti-HA (Millipore), mouse anti-Tubulin (Sigma), rabbit anti-Actin (Sigma), mouse anti-Porin (mitosciences), and rabbit anti-MFN (a generous gift from Alexander J. Whitworth).

S2 cell culture and transfection.

S2 cells were cultured in Schneider's *Drosophila* Medium (Gibco) with 10% fetal bovine serum (Invitrogen) and 1% penicillin/streptomycin (Invitrogen). Cells were seeded a day before transfection, and transfections were performed using the Qiagen Effectene kit according to the manufacturer's recommendations. pAC-GAL4 was transfected along with UAS-*MFN*-myc,

UAS-HA-*parkin*, and UAS-*MUL1*-GFP for protein expression. UAS vector was used as empty vector. Cells were harvested 2 days after transfection.

RNAi treatment in S2 cells

Double-stranded RNA (dsRNA) against coding regions of *GFP, PINK1, parkin, MUL1*, and *MFN* were generated using the T7 RiboMax express RNAi system (Promega). Primers that were used to generate dsRNAs are described in supplementary information. S2 cells were seeded and treated with dsRNAs in serum-free medium for 40 minutes. After dsRNA treatment, complete medium was added into the culture, and the culture was incubated for 2-3 days.

Co-immunoprecipitation.

S2 cells were lysed in RIPA buffer containing protease inhibitors (Roche), and western blots were performed with 2% of lysates to check protein expression. Immunoprecipitations were performed with the rest of lysates using Dynabeads (Invitrogen) according to the manufacturer's instructions. Proteins bound to beads were eluted in SDS sample buffer, and western blots were performed. Following primary antibodies were used for immunoprecipitations and western blots: mouse anti-Myc (Millipore), rabbit anti-GFP (Invitrogen), rabbit anti-HA (Sigma), and rabbit anti-Actin (Sigma).

Ubiquitination assay.

After treatment of dsRNA for 2 days, S2 cells were transfected with *MFN*-Flag and incubated for a day. Before harvest, cells were treated with proteasome inhibitor MG132 (Milliopore) for 4 hours. Cells were lysed and boiled in SDS lysis buffer (1% SDS, 150 mM NaCl, 10 mM Tris-HCl, pH 8.0) with protease inhibitors (Roche) for 10 minutes. Dilution buffer (10 mM Tris-HCl, pH 8.0, 150 mM NaCl, 2 mM EDTA, 1% Triton) was added, and

immunoprecipitations were performed using mouse anti-Flag antibody (Sigma). After immunoprecipitations, western blots were probed with mouse anti-ubiquitin (Covance).

Protein purification and in vitro ubiquitination assay

For in vitro ubiquitination assay, the glutathione *S*-transferase (GST)-tagged expression vectors pGex-*MUL1* and pGEX-*MUL1* LD were generated. GST fusion proteins (GST-*MUL1* and GST-*MUL1* LD) were expressed in *E. coli*. and purified as inclusion body. MFN-myc was expressed in S2 cells and purified with myc antibody bound magnetic beads. The in vitro ubiquitination assay included 25 mM Tris (pH 7.5), 5 mM MgCl2, 100 mM NaCl, 1 mM DTT, and 2 mM ATP in addition to the following (as indicated): E1 (Rabbit), E2 (UbcH5C), GST-*MUL1*, GST-*MUL1* LD, MFN-myc, and/or Ubiquitin, in the presence of 0.05 mM of MG1115. Reaction mixtures were incubated at 30°C for 2 hours, and reactions were terminated by boiling in SDS loading buffer.

Mammalian cell culture, transfection, and western blot.

HeLa and HeLa overexpressing Parkin were obtained from David C. Chan. Cells were cultured in Dulbeco's modified Eagle's medium (DMEM, Gibco) containing 10% fetal bovine serum (Invitrogen) and 1% penicillin/streptomycin (Invitrogen). Cells were plated a day before transfections, and transfections were performed using the Effectene kit (Qiagen) or X-tremeGENE 9 DNA Transfection Reagent (Roche) according to the manufacturer's recommendations. After transfections, Z-VAD-FMK (Santa Cruz Biotechnology) was added to cultures every 24 hours to inhibit apoptosis. Cells were harvested 48 hours later and lysed in RIPA buffer containing protease inhibitors (Roche). Western blots were performed with following primary antibodies: rabbit anti-*MUL1* (Sigma), mouse anti-MFN1mouse (Abcam), mouse anti-MFN2 (Abcam), rabbit anti-Actin (Sigma), and mouse anti-Porin (mitosciences).

Mitophagy assay.

HeLa cells or HeLa cells stably expressing sh*MUL1* were seeded in chamber slides and transfected with YFP-Parkin one day later. 24 hours after transfection, cells were treated with DMSO or 40 μg/ml Antimycin A (Sigma) for 1.5, 3, 24, or 48 hours as indicated to dissipate mitochondrial membrane potential. For *MUL1* overexpression, HeLa cells stably expressing YFP-Parkin and mitoRFP (a gift from Mark R. Cookson) were seeded and transfected with Myc-*MUL1* one day later. Cells were treated with DMSO or 80 μg/ml Antimycin A for 1.5 or 3 hours. After treatment of Antimycin A, cells were fixed in 10% Formalin solution (Sigma), permeabilized with 0.1% Triton X-100 in PBS, and blocked in PBS containing 5% fetal bovine serum. Primary and secondary antibody staining were performed in 5% fetal bovine serum + PBS. The following primary antibodies were used: mouse anti-Tom20 (BD), mouse anti-Flag (Sigma), rabbit anti-GFP (Invitrogen), and rabbit anti-Parkin (Abcam). More than 100 cells for each experiment were counted for quantification, and the experiments were repeated twice.

Protein turnover.

HeLa and HeLa expressing sh*MUL1* were treated with cycloheximide for 0, 2, 4, 6 hours. After cycloheximide treatment, cells were harvested and lysed. Protein concentration of each lysate was determined by Bradford assay (Bio-Rad), and equal amount of total proteins was subjected to western blot. Blots were probed with anti-MFN2 and Actin antibodies. Levels of MFN2 and Actin were quantified using Image J.

RESULTS

Overexpression of *MUL1*, but not ligase dead form, suppresses *PINK1* and *parkin* mutant phenotypes.

To find additional components in the PINK1/Parkin pathway, we sought to look for suppressors of *PINK1* mutants using *Drosophila*. *Drosophila* has clusters of dopaminergic (DA) neurons, which can be marked with anti-Tyrosine hydroxylase (TH) antibody staining. In *PINK1* mutant flies, DA neurons present abnormal mitochondrial clumps (Park et al., 2006), and this mitochondrial phenotype is rescued by several *PINK1* suppressors including Drp1 (Imai et al., 2010; Koh et al., 2012; Liu and Lu, 2010; Liu et al., 2012; Yang et al., 2008). Based on a previous study showing that *MUL1* positively regulates Drp1 (Braschi et al., 2009), we postulated *MUL1* as a potential *PINK1* suppressor. *Drosohila MUL1* encodes a protein that contains two transmembrane (TM) domains and a conserved RNF domain at its C-terminus (Fig. 1A and B). *MUL1* is highly conserved among species. Human *MUL1* sequence shows about 52% similarity to *Drosophila MUL1* sequence and has the same domain sturcture. From DA specific overexpression of *MUL1* using UAS/GAL4 system, we investigated if *MUL1* suppresses mitochondrial clumps in *PINK1* mutant DA neurons. In wildtype flies, mitochondria visualized by mitoGFP are dispersed in the cytosol of DA nerons (Fig. 1C). In *PINK1* mutants, abnormal mitochondrial clumps are observed (Fig. 1C', arrow heads), and the clumps are suppressed by *MUL1* overexpression (Fig. 1Q).

To observe mitochondrial morphology and other *PINK1* mutant phenotypes with better resolution, we exploited indirect flight muscles of *Drosophila*. As previously observed in several studies (Clark et al., 2006; Park et al., 2006; Yang et al., 2006), *PINK1* mutant flies show thoracic indentation due to muscle degeneration (Supplementary Fig. 1) as well as severe defects in mitochondrial morphology, including overall reduced mitoGFP signal and large mitoGFP clumps in the conforcal images (Fig. 1D and D') and swollen mitochondria with broken cristae as shown in the EM images (Fig. 1G and G'). In addition to mitochondrial defects, TUNEL

staining detecting apoptotic cell death indicates muscle cell death in *PINK1* mutants (Fig. 1E and E'). Furthermore, toluidine blue staining that shows tissue integrity reveals abnormal vacuolation in *PINK1* mutant muscles, indicating muscle degeneration (Fig. 1F and F'). Interestingly, *MUL1* overexpression rescues all the *PINK1* mutant phenotypes; thoracic indentation (Supplementary Fig. 1), mitochondrial morphology defects (Fig. 1D''), mitochondria with broken cristae (Fig. 1G''), cell death (Fig. 1E''), and abnormal vacuolation (Fig. 1F''). The suppression of *PINK1* mutant phenotypes in DA neurons and muscles identifies *MUL1* as a novel *PINK1* suppressor.

As described above, *MUL1* has a well-conserved RNF domain (Fig. 1B). To investigate if the E3 ligase activity is required for the *PINK1* suppression, we generated a ligase dead form of *MUL1* (*MUL1* LD) in which Histidine 307 residue within the conserved RNF domain was mutated to Alanine (Fig. 1A and B). The expression levels of *MUL1* and *MUL1* LD in muscles are comparable (Supplementary Fig. 1), and no mitochondrial clumps or muscle cell death are observed (Fig. 1H, H', I, and I'). However, unlike *MUL1 MUL1 LD* overexpression fails to suppress *PINK1* mutant thoracic indentation (Supplementary Fig 1), mitochondrial phenotypes (Fig. 1H''), and muscle cell death (Fig. 1I''), suggesting that *MUL1*'s E3 ligase activity is crucial to suppress *PINK1* mutant phenotypes.

Similarly, *MUL1* overexpression rescues the mitochondrial morphology defects (Fig. 1J and J') and cell death (Fig. 1K and K') in *parkin* mutant muscles whereas *MUL1 LD* overexpression fails to suppress these phenotypes (Fig. 1J'' and K'').

MUL1's role in regulation of mitochondrial morphology and body fat levels in _Drosophila_.

To study loss of function *MUL1* in *Drosophila*, we obtained $MUL1^{EY12156}$ ($MUL1^{EY}$) allele that has p-element inserted in 20 bp upstream of *MUL1* start codon (Fig. 2A). $MUL1^{EY}$

shows roughly 60% reduction of *MUL1* transcript (Supplementary Fig. 2A and B). Utilizing the $MUL1^{EY}$, we generated a deletion allele $MUL1^{A6}$ (*MUL1* mutant) that deletes approximately 1kb in *MUL1*, and the allele produces no detectable transcript (Fig. 2A and Supplementary Fig. 2A and B). Both *MUL1* mutant and $MUL1^{EY}$ flies are viable. We also generated RNAi constructs that target two different *MUL1*coding regions. These two RNAi lines show same phenotypes and reverse the suppression of *PINK1* mutant phenotypes by *MUL1* (Supplementary Fig. 2C).

Previous links of *MUL1* to Drp1 led us to study mitochondrial morphology. Close examination of *MUL1* null mutants or knockdown muscles show elongated mitochondria (Fig. 2B-D). *MUL1* overexpression results in small and fragmented mitochondria (Fig. 3E). To ask if different cell types show the similar phenotypes as muscles, we exploited larval salivary glands, which have large cells with an extensive tubular mitochondrial reticulum (Fig. 2F). Compared to wildtype, *MUL1* knockdown shows larger mitochondria and a stronger mitoGFP signal (Fig. 2G) whereas *MUL1* overexpression displays smaller and fragmented mitochondria (Fig. 2H). These mitochondrial morphology changes in *MUL* knockdown and overexpression are consistent with those in muscle. Quantification of number, average size, and total area of mitochondria suggests that the average number of mitochondria is reduced in *MUL1* knockdown and increased in *MUL1* overexpression (Fig. 2I). In contrast to mitochondrial number, the average size of mitochondria is slightly increased in *MUL1* RNAi and decreased in *MUL1* overexpression (Fig. 2J). Total mitochondrial areas are relatively similar between wildtype and *MUL1* RNAi but decreased in *MUL1* overexpression (Fig. 2K).

Interestingly, we observed that *MUL1* mutant larvae appear more transparent than wildtype, suggesting reduced body fat. This led us closely observe body fat levels of *MUL1* mutant and knockdown flies. Body fat levels of $MUL1^{EY}$ and two *MUL1* RNAi lines were

measured following the protocol using Thin Layer Chromatography (TLC) (Al-Anzi et al., 2009). Compared to controls, *MUL1*^{EY} and two different *MUL1* RNAi flies have 40-50% less body fat (Fig. 2L) while overexpression of *MUL1* increases body fat levels (Fig. 2M). These results provide evidence that *MUL1* has a role in regulation of body fat.

MFN overexpression displays similar phenotypes to _PINK1_ or _parkin_ mutants, and the phenotypes are suppressed by _MUL1_ overexpression.

Parkin regulates mitochondrial dynamics through ubiquitination of MFN (Chan et al., 2011a; Gegg and Schapira, 2011; Glauser et al., 2011; Poole et al., 2010; Ziviani et al., 2010). Consistent to this, increased MFN levels are observed in *PINK1* or *parkin* mutants (Poole et al., 2010; Ziviani et al., 2010). However, it is unclear if increased MFN levels would be sufficient to cause mitochondrial and muscle degeneration phenotypes observed in *PINK1* or *parkin* mutants. To address this question by *MFN* overexpression, we cloned *MFN* (also called *marf*, CG3869) transcript into UAS vector. Overexpression of *MFN* in muscles shows the same phenotype as *PINK1* or *parkin* mutants, large mitochondrial clumps and muscle degeneration phenotypes (Fig. 3A-C and F-H). This indicates that *MFN* overexpression is sufficient to cause the defects observed in *PINK1* or *parkin* mutants. Furthermore, *MUL1* overexpression suppresses these *MFN* overexpression phenotypes (Fig. 3D and I). To understand if similar phenotypes can be caused by inhibition of mitochondrial fission, we decided to observe loss of function *drp1* muscle. Since *drp1* null mutants are largely lethal (Verstreken et al., 2005), we generated *drp1* RNAi constructs that targets two different regions of *drp1* transcript. In contrast to *MFN* overexpression, *drp1* knockdown does not phenocopy *PINK1* or *parkin* mutants (Fig. 3E and J).

These findings suggest that mitochondrial defects and muscle cell death phenotypes in *PINK1* and *parkin* are due to increased MFN levels but not due to decreased Drp1 levels.

MUL1 binds to MFN and negatively regulates its levels through ubiquitination.

Based on our observations that *MUL1* regulates mitochondrial morphologies in several tissues and the previous study that *MUL1* positively regulates Drp1 through sumoylation (Braschi et al., 2009), we hypothesized that *MUL1* suppresses *PINK1* mutant phenotypes through the sumoylation and stabilization of Drp1. Sumoylation is a post-translational modification that involves conjugation of Small ubiquitin-like modifier (SUMO) moiety to target molecules by sequential enzymatic reactions of E1, E2 and E3 proteins. Sumoylation is involved in various processes including stress responses, transcriptional regulations, and protein stabilization (Gareau and Lima, 2010). As the sumoylation stabilizes Drp1, which results in increased protein levels and promotion of mitochondrial fission (Braschi et al., 2009; Harder et al., 2004), we first checked the regulation of Drp1 levels by *MUL1*. GenOmic rescue construct of HA-drp1 were expressed together with or without *MUL1* in muscles, and Drp1 levels were assessed using HA antibody. Surprisingly, *MUL1* overexpression failed to affect Drp1 levels (Fig. 4A upper panel). Since Drp1 level changes through stabilization of the protein may be too subtle to be observed in our system, we focused on the effect of SUMO in mitochondrial morphology. *Drosophila* genome contains one *SUMO* gene (*smt3*, CG4494). Immunostaining with SUMO antibody validates *SUMO* overexpression and knockdown in muscles (Supplementary Fig. 3A-C). Observation of mitochondrial phenotypes in *SUMO* overexpression or knockdown muscles reveals no clear morphological changes in mitochondria (Supplementary Fig. 3D-F). Next, we directly asked if *SUMO* knockdown inhibits the suppression of *PINK1* mutant phenotypes by either *MUL1* or *drp1* overexpression. However, knockdown of *SUMO* did not affect the

suppression of *PINK1* mutant mitochondrial phenotypes by *MUL1* or Drp1 (Supplementary Fig. 3G-J), suggesting that SUMO is not essential for the *PINK1* suppression. Taken all together, we failed to find evidence that sumoylation of Drp1 is important in suppression of *PINK1* mutant phenotypes by *MUL1* in *Drosophila*.

Instead, we found that *MUL1* regulates MFN levels. When myc-*MFN* and *MUL1* were expressed simultaneously, the levels of MFN were reduced compared to that of *MFN* overexpression only (Fig. 4A lower panel). Consistent to this, MFN levels are increased in *MUL1* null mutants as well as in *PINK1* and *parkin* mutants that are used as positive controls (Supplementary Fig. 4A). We observed the similar results in *Drosophila* S2 cells targeting *PINK1, parkin, MUL1*, or *MFN* using RNAi (Fig. 4B). We further investigated if *MUL1* could reduce MFN levels even in the absence of PINK1. Indeed, western blot data indicates that the increased MFN in *PINK1* mutants was reduced by *MUL1* overexpression in *PINK1* mutants (Fig. 4C), suggesting that *MUL1* suppresses *PINK1* mutant phenotypes through reduction of MFN -levels. Next, we explored if there is any physical interaction between *MUL1* and MFN. MFN, *MUL1*, and Parkin were expressed in S2 cells (shown in Fig. 4D INPUT panels), and immunoprecipitations were performed in both directions. *MUL1* co-immunoprecipitates with MFN, and vice versa (Fig. 4D). Parkin was used as a positive control and co-immunoprecipitated with MFN as expected.

Given that *MUL1* physically binds to MFN, we next investigated if the regulation of MFN levels by *MUL1* are through ubiquitination of MFN. In S2 cells treated with RNAi against either *MUL1*, *parkin*, or both, Flag-tagged MFN was overexpressed followed by treatment of proteasome inhibitor MG132. After immunoprecipitation with Flag antibodies, samples were subjected to western blot with Flag and Ubiquitin antibodies. In S2 cells, MFN is highly

ubiquitinated. Compared to control, cells treated with two different dsRNAs against *MUL1* show reduced ubiquitineted MFN levels similar to *parkin* RNAi treated cells, which serves as a positive control (Fig. 4E). To demonstrate that *MUL1* directly ubiquitinates MFN, we performed *in vitro* ubiquitination assay using purified *Drosophila MUL1*, *MUL1* LD, and MFN. Western blot probed with anti-GST antibody detects both *MUL1* and *MUL1* LD (Fig. 4F lower panel, arrowhead). However, only *MUL1* is self-ubiquitinated, but not *MUL1* LD (Fig. 4F lower panel, bracket), confirming that mutation in *MUL1* LD completely abolished its ligase activity. When the blot was probed with antibodies against poly-ubiquitinylated protein, it shows ubiquitinated *MUL1* (Fig. 4F upper panel, bracket). When *MUL1* is incubated with MFN, the ubiquitinated *MUL1* bands become weaker, and even higher molecular weight bands show up (Fig. 4F upper panel, bracket), suggesting that Ubiquitin on *MUL1* is transferred to MFN, resulting in ubiquitinated MFN. Take together, our work provides evidence that *MUL1* binds to and ubiquitinates MFN.

***MUL1*'s function in regulation of MFN is conserved in mammalian cells.**

To address if *MUL1* regulation on MFN is conserved in mammalian system, we expressed human *MUL1* and *MUL1 LD* in HeLa cells. Compared to untransfected cells, cells expressing GFP-*MUL1* or *MUL1 LD* are marked as asterisks (Fig. 5A-F). Cells expressing GFP-*MUL1* display mitochondrial clusters in peri-nuclear regions (Fig. 5A-C, asterisks). Mitochondria in the cells appear small and globular compared to controls (Fig. 5B, B' and B''). Even though *MUL1* LD expression levels are higher than *MUL1* (Fig 5G), *MUL1* LD neither causes mitochondrial clustering (Fig. 5D-F, asterisks) nor alters mitochondrial morphologies (Fig. 5E, E', and E'').

To study *MUL1* loss of function, we generated a HeLa cell line that stably expresses sh*MUL1*. This stable cell line shows roughly 60% knockdown of *MUL1* (Fig. 5H). *MUL1* overexpression or knockdown affects steady state levels of MFN. Overexpression of *MUL1* slightly decreases MFN2 levels while *MUL1* knockdown increases MFN2 levels (Fig. 5I). To carefully exam *MUL1*'s role in MFN 1 and 2 degradation, we monitored degradation of MFN1 and 2 in control and the stable cell line expressing sh*MUL1*. After treated with protein synthesis inhibitor cycloheximide for 0, 2, 4, or 6 hours, remaining MFN1 and 2 levels between control and sh*MUL1* were compared. The results clearly show that *MUL1* knockdown delays degradation of MFN1 and MFN2 (Fig. 5J-L), suggesting that *MUL1*'s function in MFN regulation is conserved in mammalian cells and *Drosophila*.

MUL1 does not affect Parkin translocation and Parkin-mediated mitophagy in HeLa.

The PINK1/Parkin pathway mediates mitophagy in mammalian cell culture (Narendra et al., 2008a; Narendra et al., 2010b). Based on that *MUL1* suppresses *PINK1* mutant phenotypes in *Drosophila* and that *MUL1*'s role is conserved in mammalian system, we hypothesized that *MUL1* could modulate Parkin-mediated mitophagy. Previously, the mitochondrial uncoupler CCCP was used to damage mitochondria by dissipating mitochondrial membrane potential. However, due to unspecificity of CCCP, we instead used antimycin A that specifically binds to ubiquinol, causing inhibition of electron transport chain. HeLa cells or HeLa cells stably expressing sh*MUL1* were transfected with YFP-Parkin and treated with DMSO or antimycin A for 1.5, 3, 24, or 48 hours. After antimycin A treatment for 1.5 or 3 hours, we observed that most Parkin is translocated to mitochondria in both HeLa and HeLa expressing sh*MUL1* (Fig. 6A upper panels). After 24 or 48 hour antimycin A treatment, Parkin is dispersed in cytosol and

mitochondria are not detected with Tom20 staining, indicating mitophagy (Fig 6A lower panels). Statistics show that there is no significant difference in Parkin recruitment to mitochondria and mitochondrial disappearance between HeLa cells and HeLa cells expressing sh*MUL1* (Fig 6B and C). Even experiments repeated with CCCP instead of antimycin A presented the same results (Supplementary Fig. 5). We next tested effect of *MUL1* overexpression on Parkin translocation. HeLa cells stably expressing Parkin with or without Flag-*MUL1* were treated with DMSO or Antimycin A for 1.5 or 3 hours. *MUL1* overexpression does not perturb Parkin recruitment to mitochondria in 1.5 or 3 hour treatment of Antimycin A (Fig 6D and E). In addition, *MUL1* overexpression did not block Parkin-induced mitophagy. Observation of cells expressing *MUL1* and Parkin together reveals that mitochondria normally disappeared after 24 hours of antimycin A treatment (data not shown). Taken together, these observations suggest that *MUL1* is not involved in Parkin-mediated mitophagy.

MUL1 acts in parallel to the PINK1/Parkin pathway to regulates mitochondrial morphology, MFN levels, and fat levels.

That *MUL1* does not affect Parkin-mediated mitophagy both in HeLa and primary neuronal cultures suggests the possibility that *MUL1* acts in a different pathway from the PINK1/Parkin pathway. However, our observation that *MUL1* overexpression suppresses *PINK1* or *parkin* mutant phenotypes proposes two possibilities. One is *MUL1* acting downstream of the PINK1/Parkin pathway, and the other is *MUL1* acting in a parallel pathway to the PINK1/Parkin pathway. Differences between the same pathway and parallel pathways are phenotypes of double null mutants of the genes. In case of the same pathway, when two genes in the pathway are affected, the outcome is as same as when either gene in the pathway is affected. An example of

this is that *PINK1 parkin* double null mutants show the same mitochondrial phenotypes as *PINK1* or *parkin* single null mutants (Clark et al., 2006; Park et al., 2006; Yang et al., 2006). On the other hand, when two genes in parallel pathways are affected, the phenotypes of double null mutants are stronger than when either gene is affected. To distinguish these two cases, several phenotypes of *PINK1 MUL1* and *parkin MUL1 parkin* double null mutants were observed.

First, *PINK1 MUL1* and *parkin MUL1* double null mutants show dramatically increased lethality at the pupal stage whereas single null mutants of *MUL1*, *PINK1, or parkin* are viable. However, double null mutants of *PINK1 parkin* that served as a control are viable as *PINK1* and *parkin* are in the same pathway. Moreover, *PINK1 MUL1* and *parkin MUL1* double null mutants show a more severe thoracic indentation compared to either *PINK1* or *parkin* mutants as well as *PINK1 parkin* double null mutants (Fig. 7A). Second, at the cellular level, *PINK1 MUL1* and *parkin MUL1* double null mutants have highly elongated and interconnected mitochondria. These mitochondrial phenotypes are very different from those of *PINK1, parkin*, or *MUL1* mutants (Fig. 7B). Third, *PINK1 MUL1* and *parkin MUL1* double null mutants have higher MFN levels compared to single null mutants of *MUL1, PINK1*, or *parkin* mutants (Fig. 7C). This suggests that *MUL1* functions in parallel to the PINK1/Parkin pathway to regulate MFN. Fourth, TLC assay shows that *MUL1*, *PINK1* or *parkin* mutant flies have reduced body fat levels. However, *parkin MUL1* and *PINK1 MUL1* double null mutant flies show further reduction of fat levels compared to single null mutants (Fig. 7D). We next investigated if changes in fat levels are achieved by regulation of MFN levels. Flies overexpressing *MFN* and *MFN* RNAi in muscles were aged for 10 days and subjected for TLC assay. Quantification of TLC assay indicates that *MFN* overexpression decreases fat levels while *MFN* RNAi increases fat levels (Fig. 7E).

Similar to thoracic indentation, mitochondrial morphology, and MFN levels, fat levels are also regulated by *MUL1* parallel to the PINK1/Parkin pathway. Taken together, our findings strongly suggest that *MUL1* acts in parallel to the PINK1/Parkin pathway to regulate mitochondrial dynamics and fat levels.

DISCUSSION

Mitochondrial dynamics and MUL1

We show that *MUL1* localizes to mitochondria and causes small and fragmented mitochondria in *Drosophila* similar to the studies from mammalian culture system. Changes in mitochondrial morphology by *MUL1* suggest a potential role in the regulation of mitochondrial dynamics. *MUL1* has been shown to promote mitochondrial fission by regulating Drp1 (Braschi et al., 2009). It was speculated that *MUL1* dependent sumolyation of Drp1 positively regulates mitochondrial fission by stabilizing Drp1 on the mitochondrial outer membrane (Scorrano and Liu, 2009). Based on the finding, we hypothesized that *MUL1* suppresses *PINK1* mutant phenotypes through the regulation of Drp1. However, we failed to find evidence that *MUL1* regulates Drp1 in *Drosophila*. *MUL1* does not affect Drp1 levels. It is possible that regulation of Drp1 by *MUL1* is not conserved or signal is below our detection levels.

Instead, we find that *MUL1* negatively regulates MFN levels. This regulation is through direct interaction and ubiquitination of MFN. During preparation of this manuscript, it is reported that *MUL1* ubiquitinates MFN under muscle wasting stimuli, confirming the role of *MUL1* in regulation of MFN (Lokireddy et al., 2012). In the report, muscle wasting triggers upregulation of *MUL1* and thus down regulation of MFN through ubiquitination. It is interesting to notice that *MUL1* promotes muscle wasting whereas in our finding *MUL1* improves muscle

health in muscle degeneration condition due to increased levels of MFN. We could speculate that MUL is responsible for the regulation of MFN levels and it depends on specific stimuli and background.

Deregulated PINK1/Parkin pathway and increased MFN

In several independent systems, Parkin has been shown to bind to MFN and negatively regulate MFN levels through ubiquitination (Gegg et al., 2010; Glauser et al., 2011; Poole et al., 2010; Tanaka et al., 2010; Ziviani et al., 2010). Loss of *PINK1* or *parkin* in *Drosophila* increases MFN levels. Consistently, fibroblasts from PD patients show defects in ubiquitination of MFN (Rakovic et al., 2011). Although increased MFN levels have been reported in *PINK1* or *parkin* mutants, it was not sure if increased levels of MFN cause phenotypes in *PINK1* or *parkin* muscles. We observe that *MFN* overexpression is sufficient to recapitulate mitochondrial and muscle degeneration phenotypes similar to *PINK1* or *parkin* mutants but not *drp1* knockdown. This observation suggests that the phenotypes of *PINK1* or *parkin* mutants are mainly due to increased levels of MFN rather than reduced levels of Drp1. In addition, the increased MFN levels in *PINK1* mutants are suppressed by the overexpression of *MUL1*. Taken all together, we conclude that *MUL1* overexpression suppresses the mitochondrial phenotypes of *PINK1* mutants through negative regulation of MFN levels.

MUL1 acts in parallel to the PINK1/Parkin pathway

Our finding that *MUL1* overexpression suppresses *PINK1* mutant phenotypes through the negative regulation of MFN levels and previous finding that Parkin negatively regulates MFN levels evoke an interesting question - does *MUL1* regulation of MFN depend on the PINK1/Parkin pathway? Our study shows that *MUL1* regulates MFN independent of the

PINK1/Parkin pathway, suggesting a parallel pathway to regulate MFN. Evidence for a parallel pathway are 1) *MUL1* overexpression suppresses *PINK1* or *parkin* null mutant phenotypes and 2) increased MFN levels in *PINK1* mutant were suppressed by *MUL1*. These two pieces of evidence show that the absence of PINK1 or Parkin does not disrupt the regulation of MFN by *MUL1*. 3) Double null mutants of *PINK1 MUL1* or *parkin MUL1* show stronger phenotypes than *PINK1*, *parkin*, or *MUL1* single null mutants on thoracic indentation, mitochondrial morphologies, and MFN levels. The enhancement of phenotypes in double null mutants suggests that *MUL1* constitutes a parallel pathway to the PINK1/Parkin pathway. The parallel pathways regulating MFN levels may explain why *PINK1* or *parkin* knockout mice do not show robust mitochondrial and dopaminergic neuronal phenotypes as *PINK1* or *parkin* mutant flies. In *PINK1* or *parkin* knockout mice, *MUL1* might have larger role in regulation of MFN and provide compensatory mechanism when the PINK1/Parkin pathway is deregulated. Thus, it will be interesting to determine whether loss of *MUL1* together with loss of *PINK1* or *parkin* causes stronger mitochondrial and dopaminergic neuronal phenotypes in double knockout mice. It is possible that *MUL1* dysfunction aggravates dysfunction of the PINK1/Parkin pathway in PD. Our finding shows that *MUL1* provides another way of regulating MFN.

Mitophagy and MUL1

Besides the regulation of mitochondrial dynamics, another important role of the PINK1/Parkin pathway is to mediate mitophagy. Ubiquitination of mitochondrial outer membrane proteins by Parkin and proteasomal degradation have been shown to be crucial for the mitophagy process (Chan et al., 2011; Tanaka et al., 2010). As *MUL1* shares MFN as a target molecule with Parkin, it was worth investigating if *MUL1* could affect Parkin-mediated

mitophagy. However, our data show that *MUL1* does not affect Parkin-mediated mitophagy. This supports the observation made previously that Parkin-mediated mitophagy in MFN1/2-null MEFs was blocked by proteasome inhibitor, showing that degradation of MFN1 and 2 is not enough to induce mitophagy. As both *MUL1* and Parkin are E3 ubiquitin ligases that regulate MFN, we tested if *MUL1* could affect Parkin-mediated mitophagy. However, our data show that *MUL1* does not affect Parkin-mediated mitophagy upon Antimycin A treatment. This supports the previous observation that Parkin-mediated mitophagy in MFN1/2-null MEFs was blocked by proteasome inhibitors, showing that degradation of MFN1/2 is not enough to induce mitophagy. This suggests that even though *MUL1* shares MFN as a target molecules with Parkin, the function of *MUL1* is distinct to Parkin. We observed that even though *MUL1* negatively regulates MFN like Parkin, the regulation happens under different conditions. HeLa cells have no detectable levels of Parkin and we observed that HeLa cells stably expressing sh*MUL1* have increased MFN1/2 levels without any mitochondrial damage. On the other hand, Parkin has been reported to ubiquitinate MFN upon mitochondrial damage such as CCCP treatment, but not without mitochondrial damage. From these observations, we speculate that *MUL1* is involved in the homeostasis of MFN levels while Parkin regulates MFN in a stress induced manner. Further work will be needed to understand why Parkin is constitutively active in flies whereas Parkin requires activation in mammalian cells and whether Parkin's stress-induced MFN regulation would give a greater role for *MUL1* in MFN homeostasis in mammals.

MUL1 and FAT

Here, we first reported a positive correlation between *MUL1* and total body fat levels. *MUL1* loss of function dramatically decreases total body fat while *MUL1* overexpression

increases total body fat levels. Interestingly, Parkin has been reported to localize to lipid rafts in brain (Fallon et al., 2002) and to involve in regulation of fat uptake in mice and human cells (Kim et al., 2011). Whether PINK1 also involves in fat regulation is to be further elucidated. However, our data suggest that the PINK1/parkin pathway regulates total body fat levels in *Drosophila*. Although the phenotypes are weak in single mutants, changes of fat levels in single mutants were enhanced with *MUL1* mutants. We further showed that modulation of MFN levels is sufficient enough to cause total body fat levels as consistent to previous finding(Kita et al., 2009). Our data suggest that these total body fat level changes are at least partially through regulation of MFN levels.

PD and MUL1 (MUL1's potential connection to PD)

As life expectancy gets longer, the number of PD patients will increase, and a better understanding of this disease and developing a cure will become more important. Causes of PD still need to be further elucidated, but there are growing evidence that deregulation of mitochondrial dynamics is one of the causes. *PINK1* and *parkin* are known to act in the same pathway to regulate mitochondrial integrity. Mutations in *PINK1* and *parkin* are found in early onset PD patients. Thus, understanding how the PINK1/Parkin pathway regulates mitochondrial dynamics and knowing what other players are involved in the pathway would help us understand the disease better and develop therapeutic targets. Our results show that *MUL1* acts in parallel to the PINK1/Parkin pathway and modulates deregulated PINK1/Parkin pathway. This provides a new approach to PD. Instead of directly fixing the pathway, which can be challenging in case of loss of gene function, we may be able to modulate the downstream though the regulation of the parallel pathways. This will expand options to develop therapeutic targets for PD.

So far, links between *MUL1* and PD have not been studied. However, it is interesting to point out that *MUL1* has been reported to bind to VPS35 (Braschi et al., 2010), which is identified as a new PD gene. Several studies reported that mutations in VPS35 cause PD (Kumar et al., 2012; Lesage et al., 2012; Vilarino-Guell et al., 2011; Zimprich et al., 2011). It is possible that polymorphisms in *MUL1* could affect interaction between *MUL1* and VPS35, potentially leading to PD. In addition, we noticed that *MUL1*'s level is tightly regulated (data not shown). Mutations that affect *MUL1* levels which results in changes in MFN levels might contribute to PD. Studying *MUL1* polymorphisms in sporadic forms of PD might provide more clear connection between *MUL1* and PD.

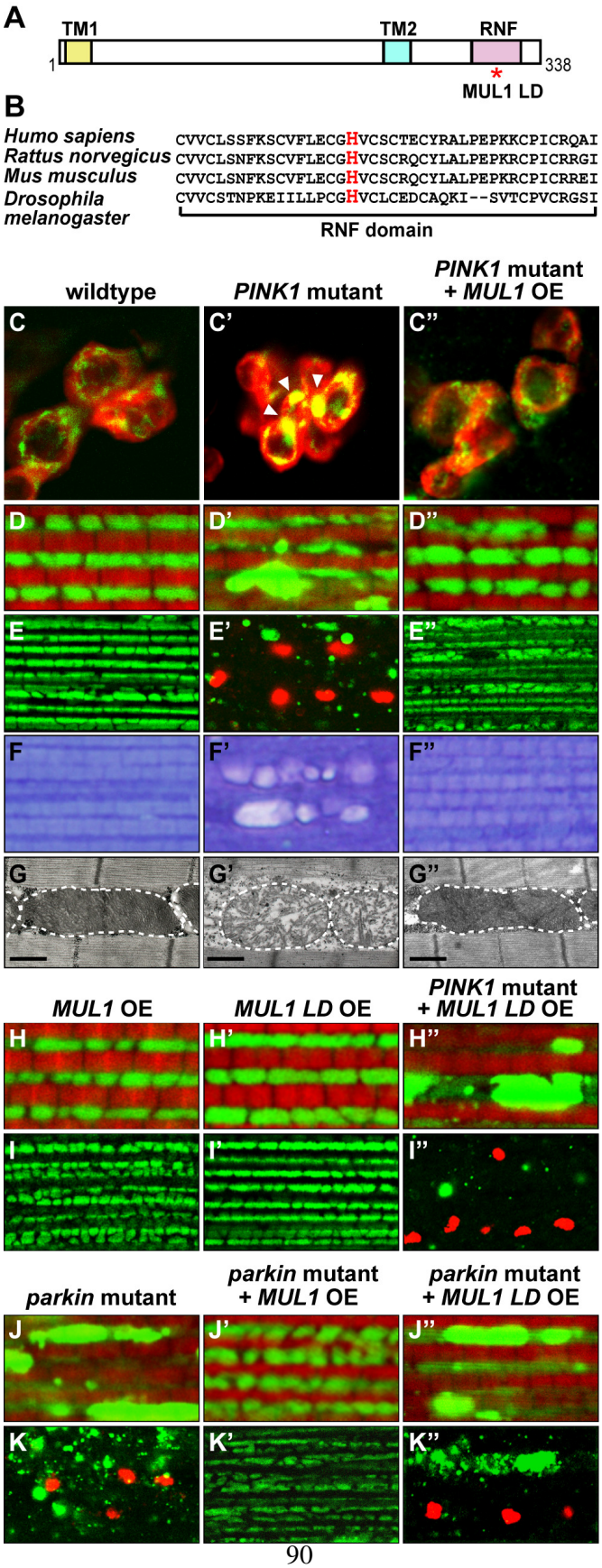
A
TM1
TM2
RNF
1
338
*
MUL1 LD
B
Humo sapiens CVVCLSSFKSCVFLECGHVCSCTECYRALPEPKKCPICRQAI
Rattus norvegicus CVVCLSNFKSCVFLECGHVCSCRQCYLALPEPKRCPICRRGI
Mus musculus CVVCLSNFKSCVFLECGHVCSCRQCYLALPEPKRCPICRREI
Drosophila melanogaster CVVCSTNPKEIILLPCGHVCLCEDCAQKI--SVTCPVCRGSI
RNF domain
wildtype
PINK1 mutant
PINK1 mutant + MUL1 OE
C
C'
C''
D
D'
D''
E
E'
E''
F
F'
F''
G
G'
G''
MUL1 OE
MUL1 LD OE
PINK1 mutant + MUL1 LD OE
H
H'
H''
I
I'
I''
parkin mutant
parkin mutant + MUL1 OE
parkin mutant + MUL1 LD OE
J
J'
J''
K
K'
K''

Figure 3-1. Overexpression of *MUL1*, but not ligase dead form, suppresses *PINK1* and *parkin* mutant phenotypes in *Drosophila*. (A) Protein domain organization of *Drosophila MUL1*. TM1, TM2, and RNF represent transmembrane domain 1 and 2, and RING FINGER domain correspondingly. The location of ligase dead (LD) mutation is marked as red asterisk. (B) Sequence alignment of *MUL1* in various species in a highly conserved RNF domain. In the RNF domain, highly conserved residue Histidine is marked as red, and the residue was mutated to Alanine in *MUL1* LD, ablating ligase activity. (C-C'') Dopaminergic neurons labeled with anti-TH antibody in red and mitoGFP in green. While dopaminergic neurons from wild type flies show dispersed mitochondria (C), mitochondria in *PINK1* mutant dopaminergic neurons show strong mitoGFP positive clumps (C', white arrow heads). *MUL1* overexpression suppresses the mitoGFP clumps in *PINK1* mutant dopaminergic neurons (C''). (D-D'') Confocal images of muscle fibers from fly thoraces. Mitochondria and myofibrils were labeled with mitoGFP in green and phalloidin in red accordingly. In wild type (D), muscle fiber has a well organized structure, where mitochondria have regular sizes and shapes and span between myofibrils. In *PINK1* mutants (D'), mitochondrial size becomes irregular, where GFP signal is small and reduced, but large mitochondrial clumps appear at the same time. *MUL1* overexpression suppresses the mitochondrial phenotypes of *PINK1* mutants (D''). (E-E'') TUNEL staining of muscle fibers. TUNEL positive cells are shown in red, indicating cell death, and mitoGFP labels mitochondria in green. Unlike wild type fibers (E), which are negative for TUNEL staining, *PINK1* mutants show TUNEL positive staining (E'). Muscle fibers overexpressing *MUL1* in *PINK1* mutants no longer have TUNEL positive staining (E''). (F-F'') Touidine blue staining of muscles. Compared with wild type (F), touidine blue staining of *PINK1* mutant muscles shows vacuolations, indicting muscle degeneration (F'). *MUL1* overexpression suppresses the

vacuolation phenotypes in *PINK1* mutant muscles (F''). (G-G'') EM images of mitochondria in muscles. Mitochondria are outlined with dashed white lines. Scale bars represent 0.5 μm. In wild type (G), mitochondrion has compact and organized cristae whereas mitochondria from *PINK1* mutant muscles (G') have swollen and fragmented cristae. The *PINK1* mutant broken cristae structure was rescued by *MUL1* overexpression (G''). (H-H'') Confocal images of muscle fibers. Muscle fibers of Overexpressing *MUL1* or *MUL1 LD* are shown (H and H'). *MUL1 LD* overexpression in *PINK1* mutants does not suppress *PINK1* mutant mitochondrial clumps in muscle (H''). (I-I'') TUNEL staining of muscle fibers. Muscle fibers overexpressing *MUL1* or *MUL1 LD* are TUNEL-negative (I and I'). Contrast to wildtype *MUL1* overexpression in *PINK1* mutant muscle fibers, *MUL1 LD* overexpression failed to suppress *PINK1* mutant apoptotic cell death (I''). (J-J'') Confocal images of muscle fibers labeled with mitoGFP in green and Actin in red. *parkin* mutant muscle fibers (J) show overall reduced mitoGFP signal and large mitochondrial clumps. (J') When *MUL1* is overexpressed, reduced mitoGFP signal and large mitochondrial clumps are suppressed. However, *MUL1 LD* overexpression failed to suppress the phenotypes (J''), showing similar phenotypes to *parkin* mutants. (K-K'') TUNEL assay of muscle fibers. Red indicates TUNEL positive cells, and mitGFP labels mitochondria in green. *parkin* mutant muscle fibers show TUNEL staining, which indicates cell death (K). *MUL1* overexpression suppresses *parkin* mutant TUNEL positive cells (K') whereas *MUL1 LD* overexpression fail to suppress cells death of *parkin* mutants (K'').

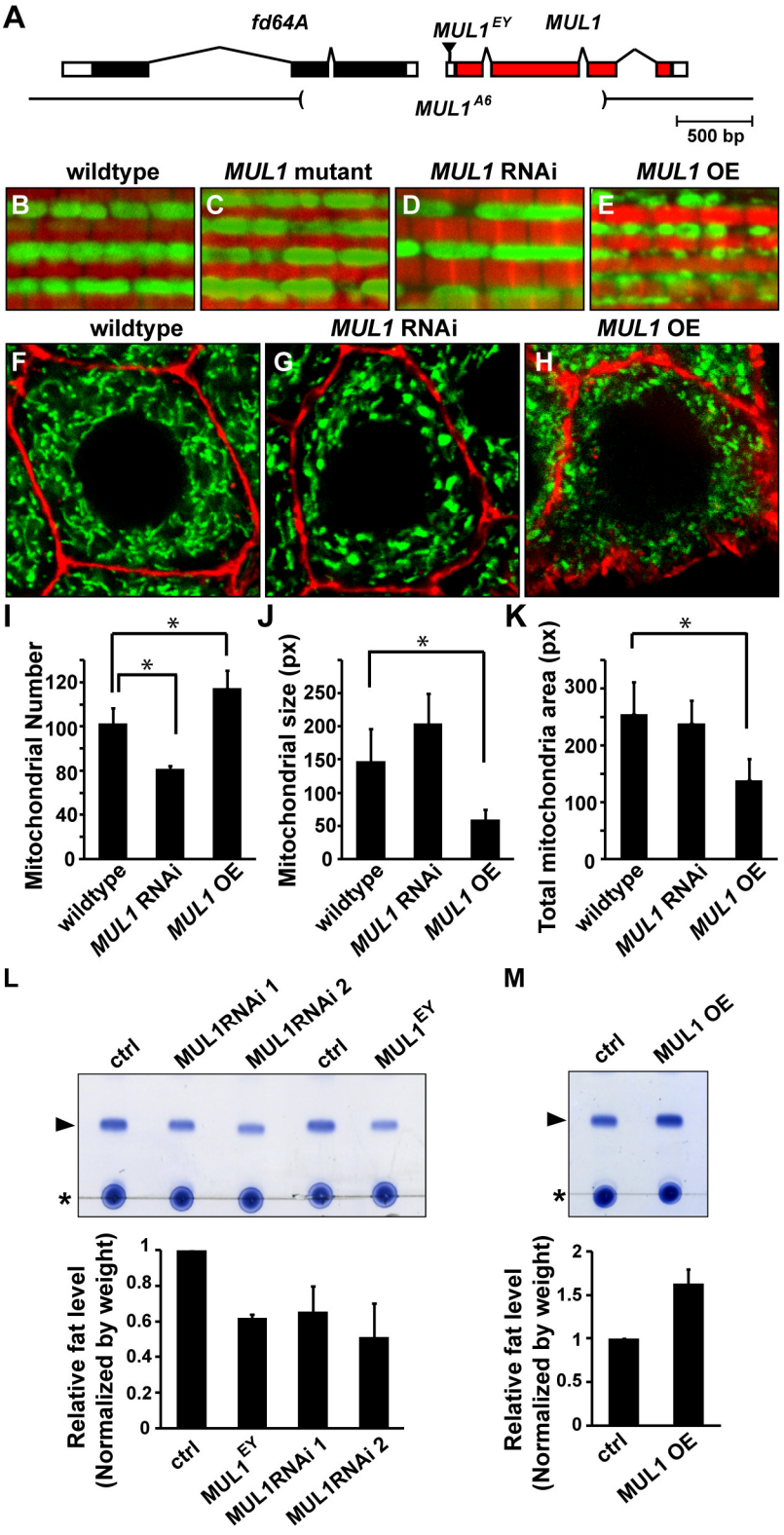
A
fd64A
MUL1^EY
MUL1
MUL1^A6
500 bp
wildtype
MUL1 mutant
MUL1 RNAi
MUL1 OE
B
C
D
E
wildtype
MUL1 RNAi
MUL1 OE
F
G
H
I
Mitochondrial Number
J
Mitochondrial size (px)
K
Total mitochondria area (px)
wildtype
MUL1 RNAi
MUL1 OE
L
ctrl
MUL1RNAi 1
MUL1RNAi 2
ctrl
MUL1^EY
Relative fat level (Normalized by weight)
M
ctrl
MUL1 OE

Figure 3-2. *MUL1* regulates mitochondrial morphology and fat levels. (A) Schematic depicting genOmic regions of *Drosophila MUL1* and upstream gene *fd64A*. GenOmic structure of *MUL1* is depicted above, and p-element insertion in 5' UTR is shown as inverted triangle ($MUL1^{EY}$). Deleted region of *MUL1* in deletion mutant $MUL1^{A6}$ is shown as parentheses. (B-E) Muscle fibers stained with mitoGFP in green and Actin in red. Compared with wild type (B), *MUL1* mutants (C) and *MUL1* RNAi (D) show slightly elongated mitochondria. In contrast, *MUL1* overexpression (E) causes small and fragmented mitochondria. (F-H) Salivary glands stained with Actin in red and mitoGFP in green. Boundaries of each cell in salivary glands were marked by Actin staining. In wild type (F) salivary glands, well distributed and tubular mitochondria are observed. *MUL1* RNAi salivary gland cell has less number of mitochondria compared to wildtype (G and I) and shows large mitochondrial clumps as well as tubular mitochondria (G and J). *MUL1* overexpression in salivary glands causes irregular cell boundaries (H), and mitochondria are smaller and fragmented while the number of mitochondria is increased (H and I). (I-K) Graphs showing quantification of mitochondrial number (I), average mitochondrial size (J), and total area of mitochondria (K). (L-M) Thin Layer Chromatography (TLC) plates (upper panel) and quantification of fat levels normalized by weight (lower panel). While *MUL1* loss of function decreases fat levels, *MUL1* overexpression in muscles increases overall fat levels approximately 1.5 fold.

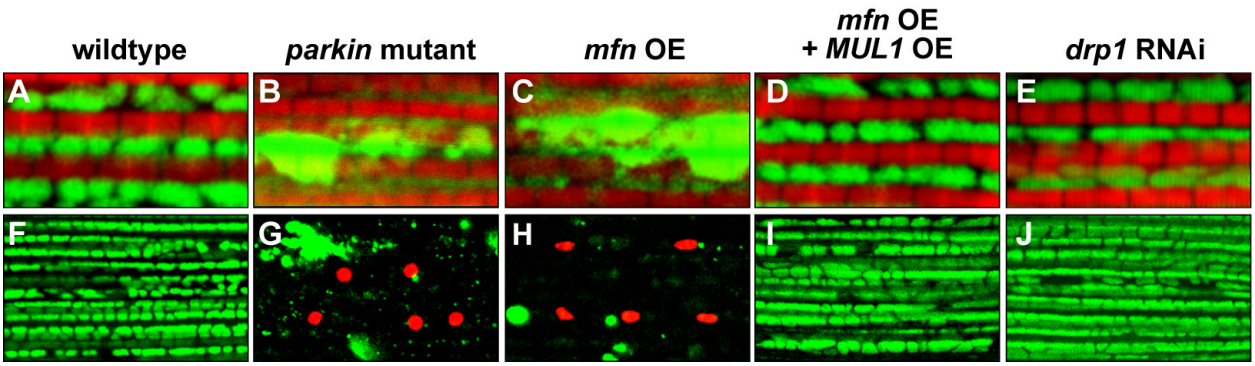

Figure 3-3. *MFN* overexpression phenocopies *PINK1/parkin* mutants and the phenotypes are suppressed by *MUL1* overexpression. (A-E) Confocal images of muscle fibers labeled with mitoGFP (green) and Actin (red). Compared with wild type (A), *parkin* mutants (B) display overall reduced levels of mitoGFP signal and large mitochondrial clumps. The similar mitochondrial phenotypes were observed in *MFN* overexpression (C). *MUL1* overexpression suppresses *MFN* overexpression phenotypes (D). However, knock down of *drp1* does not show any mitochondrial clumps unlike *parkin* mutants or *MFN* overexpression (E). (F-J) TUNEL assay of muscle fibers. TUNEL positive cells are stained in red and mitochondria are labeled with mitoGFP. In wild type (F) muscle fibers, there is no TUNEL positive signal, indicating no cell death. Both *parkin* mutants (G) and *MFN* overexpression (H) are TUNEL positive, but *MFN* and *MUL1* overexpression does not have TUNEL positive signal (I). *drp1* RNAi muscles are TUNEL negative (J).

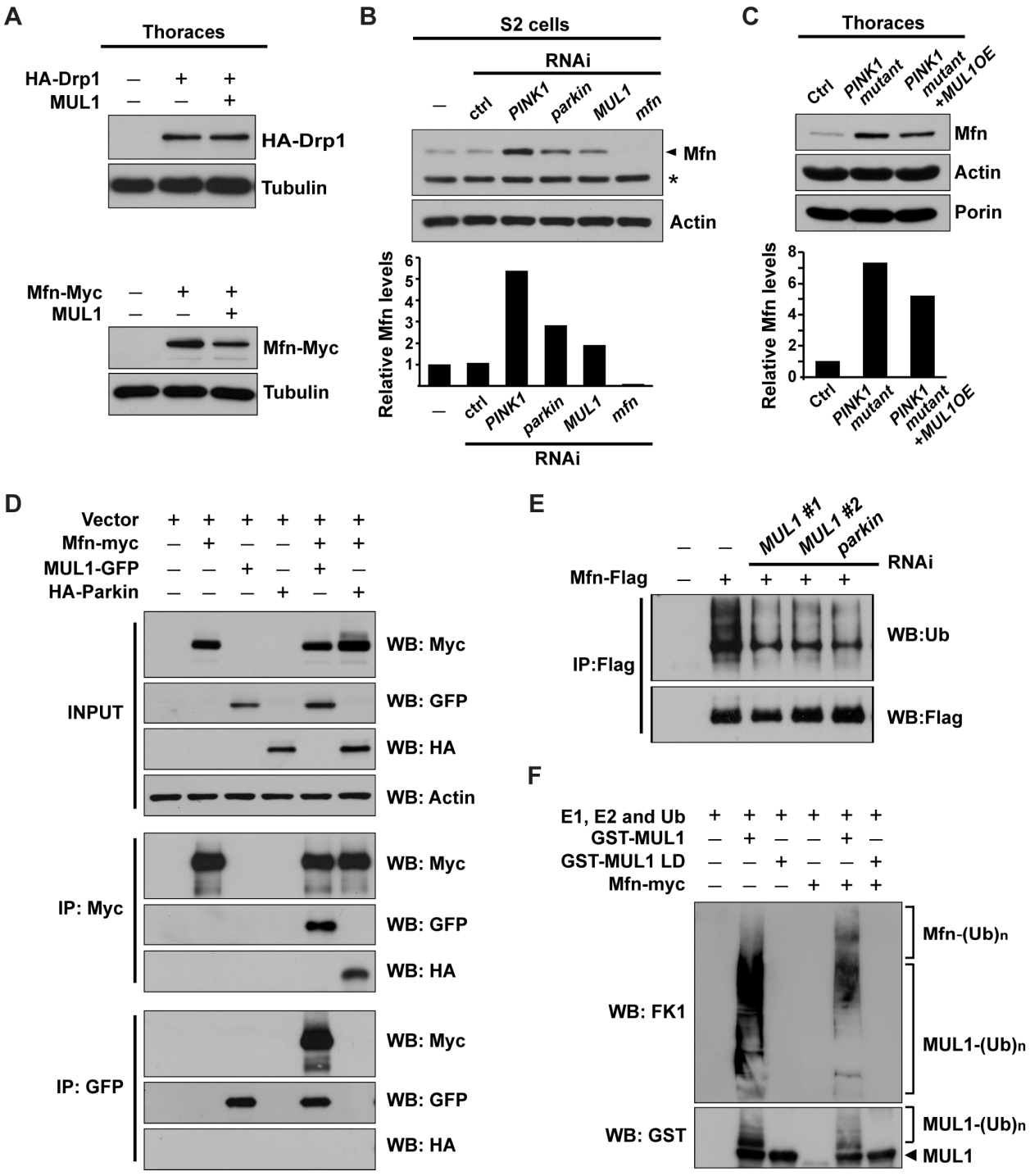

Figure 3-4. *MUL1* negatively regulates MFN through direct interaction and ubiquitination.

(A) Western blot analysis of Drp1 and MFN levels in fly thoraces. In lysates from fly thoraces, *MUL1* overexpression decreases MFN levels but fails to show any changes in Drp1 levels. (B)

S2 cells were either not treated or treated with *control, PINK1, parkin, MUL1,* or *MFN* RNAi as indicated. S2 cells were harvested and subjected to western blot. MFN specific band (indicated as an arrowhead) is disappeared in knockdown of *MFN*. Unspecific band is marked as an asterisk. Below, quantification of relative MFN levels shows increase of MFN levels in cells treated with *PINK1, parkin,* and *MUL1* RNAi. (C) MFN levels in fly thoraces. Compared to wild type, MFN levels are increased in *PINK1* mutant thoraces. When *MUL1* is overexpressed, the increased MFN levels are reduced in *PINK1* mutant thoraces. (D) Western blot analysis of co-immunoprecipitation. S2 cells were transfected with empty vector, MFN-myc, *MUL1*-GFP, or HA-Parkin as indicated. Cells were harvested and lysed, and 2% of lysates were subjected to western blot to check protein expression, shown as INPUT. For the rest of lysates, immunoprecipitations were performed with antibody against Myc or GFP, and western blots were probed with antibody against GFP, Myc, or HA. In lysates from S2 cells transfected with both *MUL1*-GFP and MFN-myc, *MUL1*-GFP was co-immunoprecipitated with MFN-myc using both anti-GFP and anti-Myc antibody. MFN-myc also co-immunoprecipitates with HA-Parkin, which serves as a positive control. (E) MFN ubiquitination levels in S2 cells. S2 cells were either not treated or treated with *MUL1, parkin*, or both RNAi and transfected with MFN-Flag. Immunoprecipitation was performed with anti-Flag antibody, and western blots were probed with anti-Ubiquitin antibody and anti-Flag antibody. In S2 cells, MFN is highly ubiquitinated without treatment of any RNAi. Treatment of *MUL1* or *parkin* RNAi reduces ubiquitnated MFN levels. (F) *In vitro* ubiquitination assay. *MUL1* and *MUL1* LD were fused to GST tag, and GST fusion proteins (GST-*MUL1* and GST-*MUL1* LD) were purified from *E. coli*.. MFN-myc was expressed in S2 cells and purified with Myc antibody bound magnetic beads. Western blot probed with FK1 antibody shows smear bands, which are only shown in reactions with GST-

MUL1. When MFN-myc is incubated together with GST-*MUL1*, there is increase in higher molecular weight bands, suggesting ubiquitinated MFN. Western blot probed with GST antibody detects unubiquitinated form of GST-*MUL1* and GST-*MUL1* LD, which are indicated as arrow head, as well as ubiquitinated form shown in bracket.

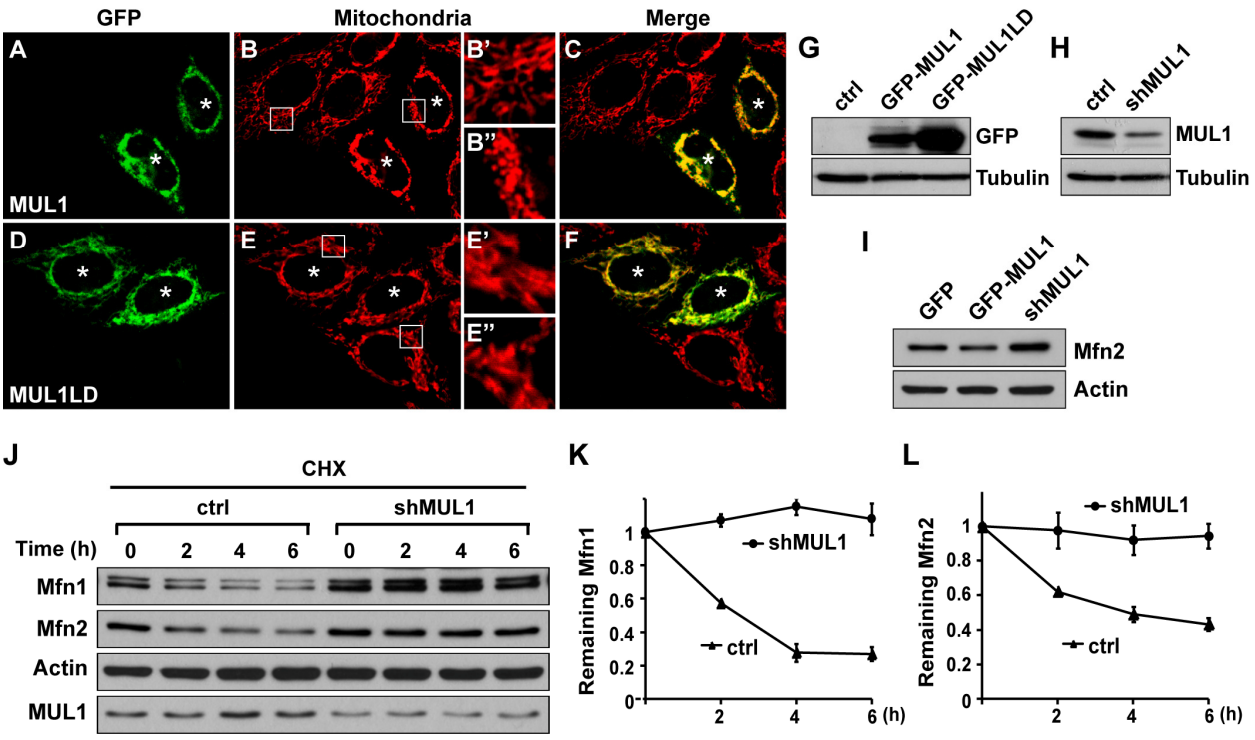

Figure 3-5. *MUL1*'s function in regulation of mitochondrial dynamics is conserved in HeLa cells. (A-F) Mitochondrial staining of HeLa cells transfected with GFP-*MUL1* or GFP-*MUL1*LD. Cells transfected with GFP-*MUL1* (A-C) or GFP-*MUL1* LD (D-F) are marked with asterisks. Mitochondria are stained with mitotracker in red (B and E). (B' and B'') blow up images of mitochondria from (B). (E' and E'') blow up images of mitochondria from (E). In cells expressing GFP-*MUL1*, mitochondria are clustered in perinuclear region (B). In addition, GFP-*MUL1* expression causes small and fragmented mitochondria, shown in detail in (B'') compared to cells not expressing GFP-*MUL1* (B'). However, GFP-*MUL1* LD does not cause peri-nuclear localization of mitochondria (E) and small and fragmented mitochondria (E'). (G) Western blot probed with GFP antibody shows expression of GFP-*MUL1* and GFP-*MUL1* LD. (H) Western blot detecting endogenous *MUL1* levels displays decreased *MUL1* levels in cells expressing

sh*MUL1*. (I) Western blot analysis of MFN2 levels in HeLa cells. *MUL1* expression causes slightly reduced levels of MFN2 while *MUL1* knockdown increases MFN2 levels. (J) Western blot analysis of MFN1 and MFN2 levels after CHX treatment. HeLa and HeLa expressing sh*MUL1* were treated with CHX for time as indicated. MFN1 and 2 levels in each time point were normalized with Actin, and relative portion of remaining MFN1 and 2 compared to time point 0 was calculated and plotted in a graph (K and L).

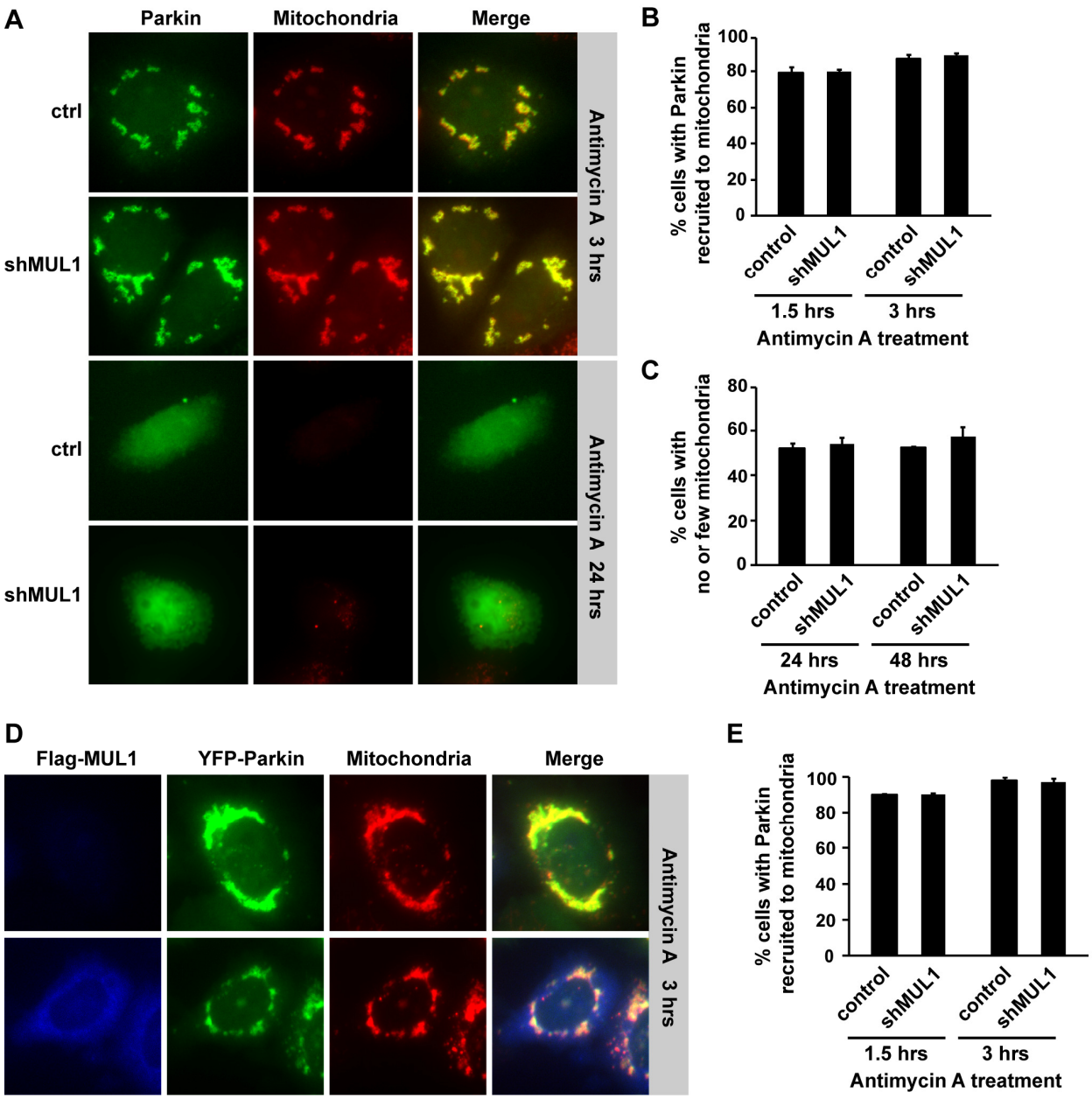

Figure 3-6. Knockdown or overexpression of *MUL1* does not affect Parkin-mediated mitophagy. (A) HeLa cells or HeLa cells stably expressing sh*MUL1* were transfected with YFP-Parkin, treated with DMSO or antimycin A, and immunostained for Parkin and mitochondria. After 3 hours of antimycin A treatment, Parkin is recruited to mitochondria, which is shown by co-localization of Parkin and mitochondrial marker. After 24 hours of anytimycin A

treatment, Parkin goes back to cytosol and mitochondrial signal disappeared. (B) Quantification of cells with Parkin recruited to mitochondria after 1.5 or 3 hour antimycin A treatment indicates no significant difference between HeLa and HeLa stably expressing sh*MUL1*. (C) Quantification of cells with no or few mitochondria after 24 or 48 hour antimycin A treatment also displays no significant difference between both cell lines. (D) HeLa cells stably expressing YFP-Parkin and mitoRFP were transfected with Flag-*MUL1*, treated with DMSO or antimycin A, and labeled for Flag, Parkin and mitochondria. 3 hour antimycin A treatment causes Parkin localization to mitochondria in cells with or without *MUL1* expression. (E) Quantification of cells with Parkin recruited to mitochondria after 1.5 or 3 hour Antimycin A treatment. Both 1.5 and 3 hour antimycin A treatments show similar percentage of Parkin recruitment to mitochondria.

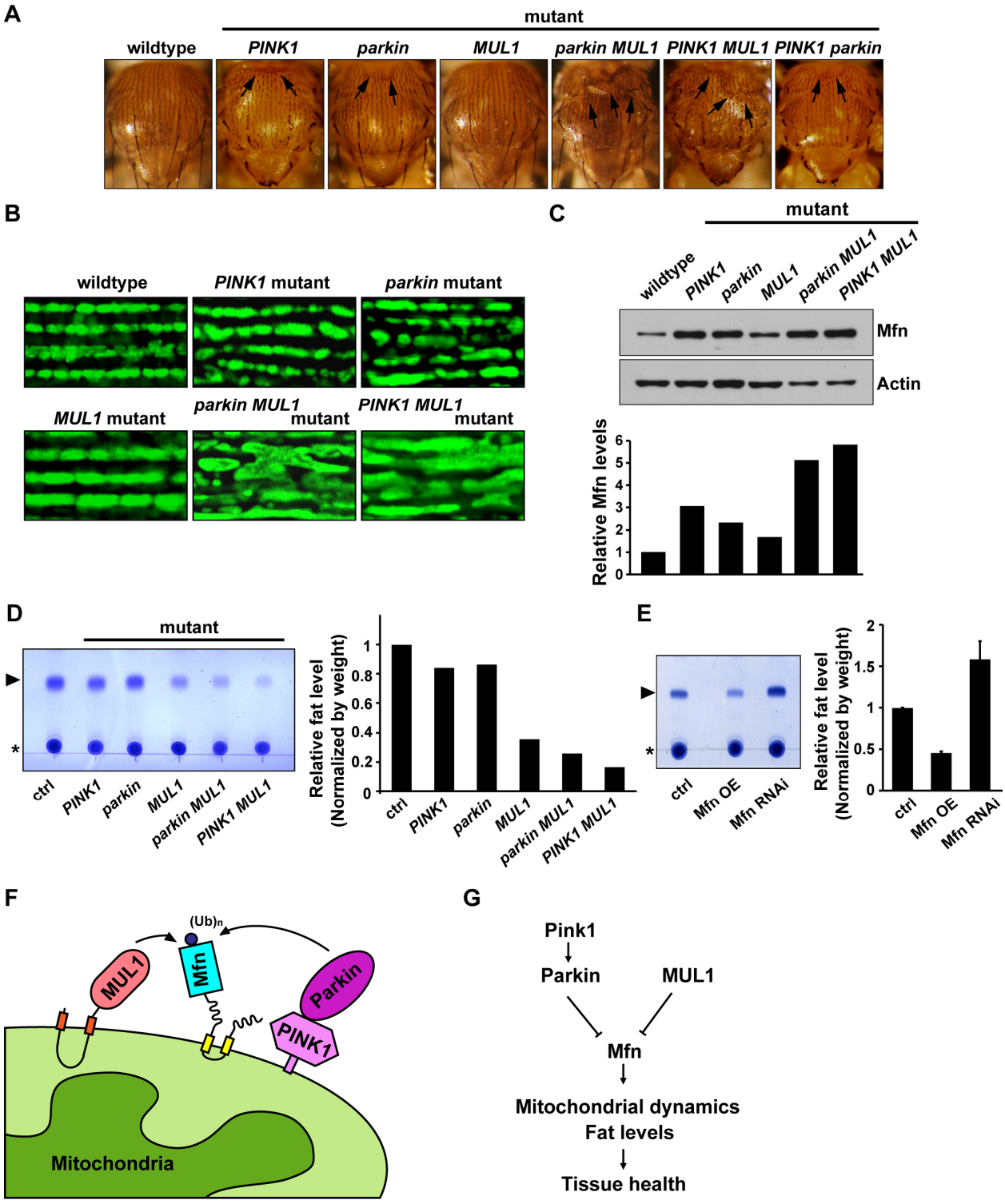

Figure 3-7. *MUL1* acts in parallel to the PINK1/Parkin pathway to regulates mitochondrial morphology, MFN levels, and fat levels. (A) Images of fly thoraces. Unlike wild type or

MUL1 mutant flies, which have normal thoraces, *PINK1* or *parkin* mutant flies show thoracic indentations due to muscle degeneration, which are pointed by arrows. While *PINK1 parkin* double null mutant flies show similar extent of thoracic indentations to *PINK1* or *parkin* mutant flies, double null mutants of *PINK1 MUL1* and *parkin MUL1* show even more severe thoracic indentations indicated by arrows. (B) Antibody staining of mitochondria in muscle fibers. Anti-ATP synthase antibody was used to label mitochondria in muscle fibers. In wild type muscle fibers, mitochondria are in regular shape and size. In contrast, mitochondrial size varies in *PINK1* or *parkin* mutant muscle fibers – small and fragmented to elongated mitochondria. *MUL1* mutants have regular sized but slightly elongated mitochondria. *PINK1 MUL1* or *Parkin MUL1* double null mutants have highly elongated and interconnected mitochondria showing further enhanced mitochondrial morphologies compared to other genotypes. (C) Western blot analysis of MFN levels *in vivo*. Lysates from *Drosophila* larvae were probed with antibody against MFN, and relative levels of MFN were calculated by normalization with Actin. For *PINK1, parkin*, or *MUL1* mutants, MFN levels were increased compared to wild type. However, MFN levels of double null mutants were higher than those of single mutants, showing further increase of MFN levels. (D-E) TLC plates and quantification of fat levels in flies. Compared to control, single null mutant flies show reduction in fat levels. The reduction is further increased in double null mutant flies (D). (E) TLC plate and quantification of fat levels in flies overexpressing *MFN* or *MFN* RNAi in indirect flight muscles. *MFN* overexpression decreases fat levels while *MFN* RNAi increases fat levels. (F) Schematic diagram shows that mitochondrially-localized *MUL1* ubiquitinates and negatively regulates MFN. Parkin recruited to mitochondria by PINK1 also shares the same regulation of MFN. (G) Schematic diagram shows that *MUL1* acts in parallel to the PINK1/Parkin pathway to regulate MFN levels and fat levels.

SUPPLEMENTARY FIGURES AND FIGURE LEGENDS

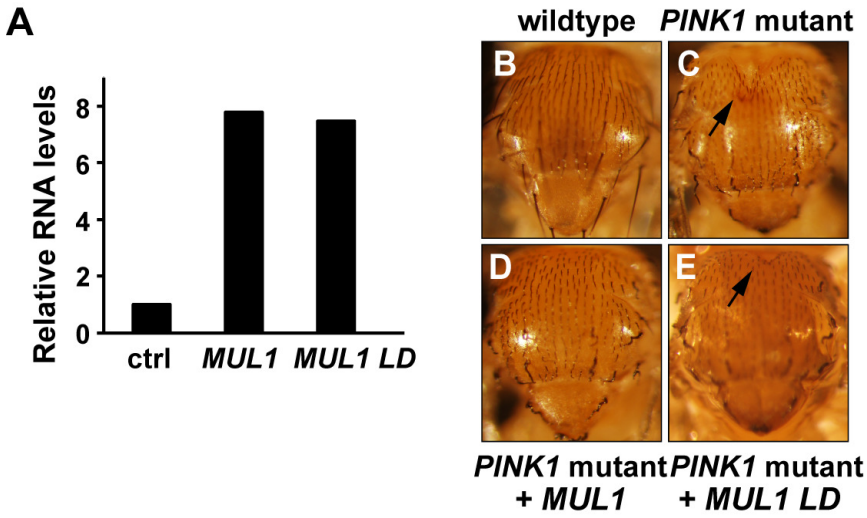

Supplementary Figure S3-1. Overexpression of wildtype *MUL1*, but not *MUL1 LD*, suppresses *PINK1* mutant thoracic indentation. (A) qPCR shows that *MUL1* and *MUL1* LD mRNA are expressed relatively similar levels in muscles. (B-E) Images of fly thoraces. Compared with wildetype (B), *PINK1* mutants have thoracic indentation due to muscle degeneration (C). *MUL1* overexpression suppresses *PINK1* mutant thoracic indentation (D) whereas *MUL1 LD* overexpression fails to suppresse the indentation.

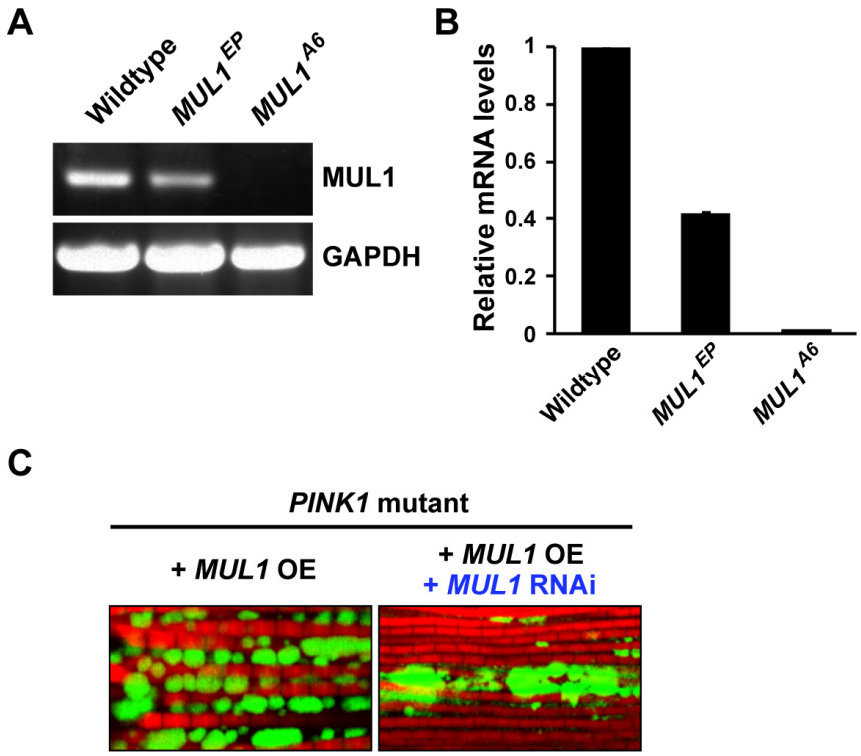

Supplementary Figure S3-2. Transcripts of *MUL1*^{EY} and *MUL1* mutant (*MUL1*^{A6}) alleles. (A) RT PCR shows that *MUL1*^{EY} allele has detectable but reduced levels of *MUL1* transcripts. However, there was no MUL transcript detected in *MUL1* mutant (*MUL1*^{A6}) alleles. (B) qPCR shows that *MUL1*^{EY} allele has approximately 60% reduction of *MUL1* transcript compared to wildtype. No *MUL1* transcript is detected in *MUL1* mutant (*MUL1*^{A6}) alleles. (C) *MUL1* RNAi line reverses the suppression of *PINK1* mutant mitochondrial phenotypes by *MUL1* overexpression.

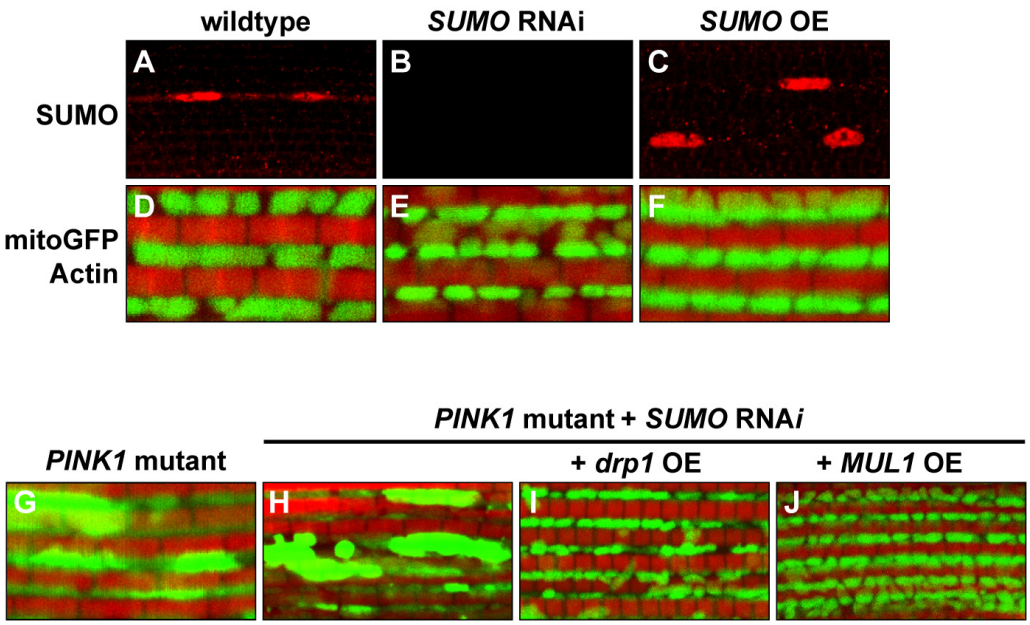

Supplementary Figure S3-3. SUMO is not essential for the *PINK1* mutant suppression by *MUL1* or Drp1. (A-C) Confocal images of muscles stained with SUMO antibody. Compare to wildtype (A), which shows antibody staining of endogenous SUMO, there is not antibody staining observed in SUMO knockdown (B). (C) In muscles overexpressing *SUMO*, SUMO staining is detected. (D-F) Confocal images of muscles. Mitochondria are labeled with mitoGFP, and Actin is labled with phalloidine in red. Compared with wildtype (D), there is no clear change of mitochondrial morphology in *SUMO* RNAi and *SUMO* overexpression (E and F). (G-J) Confocal images of muscle. Mitochondria are labeled with mitoGFP, and Actin is labled with phalloidine in red. While *PINK1* mutants and *SUMO* knockdown in *PINK1* mutants show mitochondrial morphology defects (G), overexpression of *drp1* (I) or *MUL1* (J) suppresses *PINK1* mutant mitochondrial morphology even in *SUMO* knockdown.

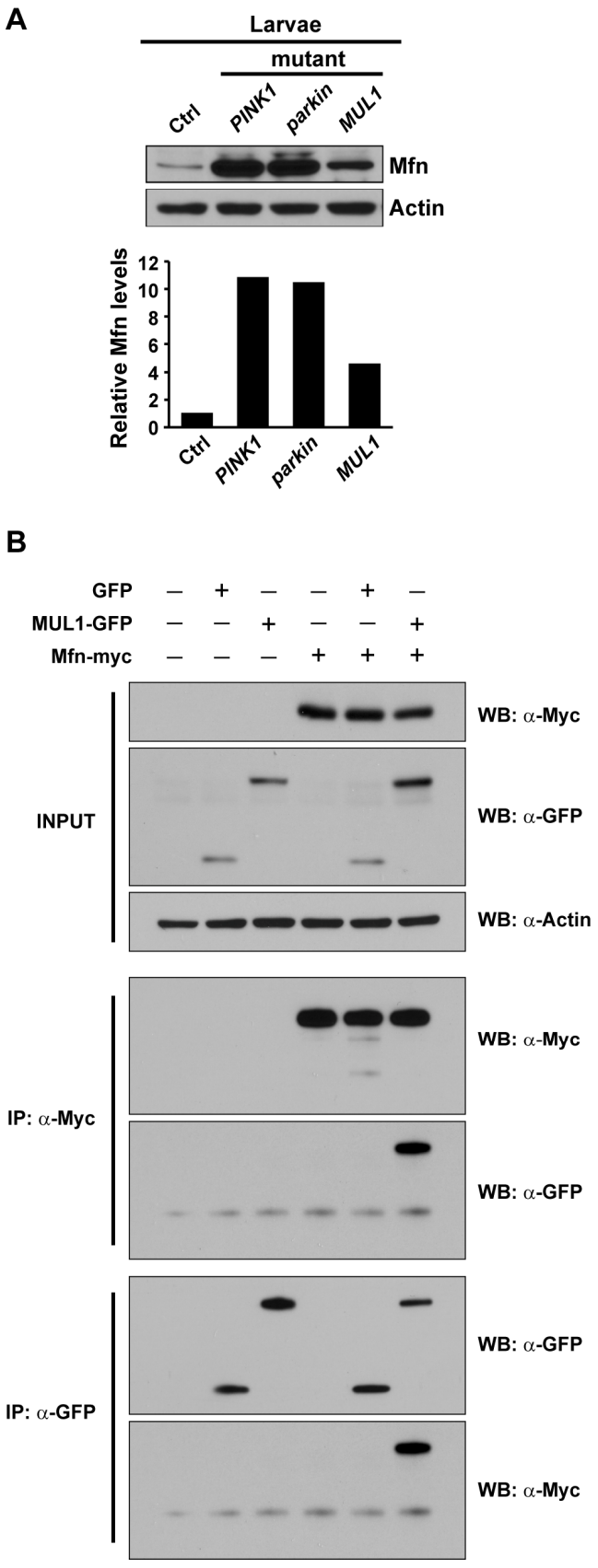
A
Larvae
mutant
Ctrl
PINK1
parkin
MUL1
Mfn
Actin
Relative Mfn levels
12
10
8
6
4
2
0
Ctrl
PINK1
parkin
MUL1
B
GFP
MUL1-GFP
Mfn-myc
INPUT
WB: α-Myc
WB: α-GFP
WB: α-Actin
IP: α-Myc
WB: α-Myc
WB: α-GFP
IP: α-GFP
WB: α-GFP
WB: α-Myc

Supplementary Figure S3-4. Western blots of mutant larvae and Co-IP control.

(A) Western blot analysis of MFN levels in mutant larvae. In larval lysates, compared with control, MFN levels are increased in *PINK1*, *parkin*, and *MUL1* mutant larvae. (B) Western blot analysis of co-immunoprecipitation. S2 cells were transfected with empty vector, MFN-myc, GFP, or *MUL1*-GFP as indicated. Cells were harvested and lysed, and 2% of lysates were subjected to western blot to check protein expression, shown as INPUT. For the rest of lysates, immunoprecipitations were performed with antibody against Myc or GFP, and western blots were probed with antibody against GFP, or Myc. In lysates from S2 cells transfected with both *MUL1*-GFP and MFN-myc, *MUL1*-GFP was co-immunoprecipitated with MFN-myc using both anti-GFP and anti-Myc antibody. However, GFP was not co-immunoprecipitated with MFN-myc.

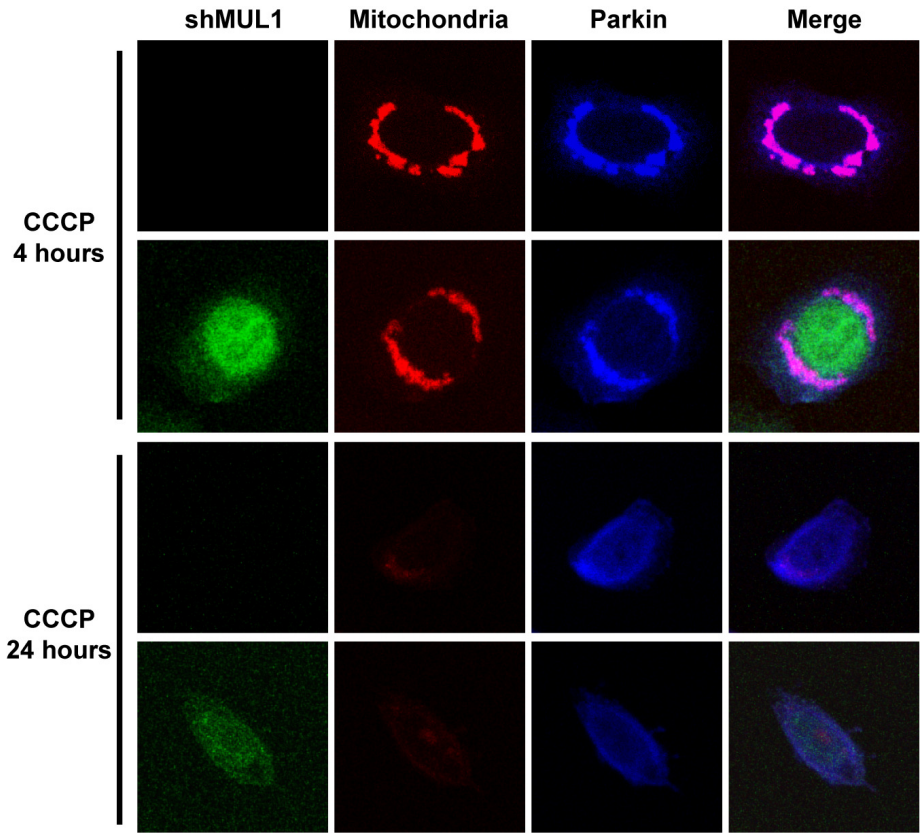

Supplementary Figure S3-5. Knockdown of *MUL1* does not affect Parkin-mediated mitophagy. (A) HeLa cells or HeLa cells stably expressing sh*MUL1* were transfected with YFP-Parkin, treated with DMSO or CCCP, and immunostained for Parkin and mitochondria. After 4 hours of CCCP treatment, Parkin is recruited to mitochondria, which is shown by co-localization of Parkin and mitochondrial marker. After 24 hours of CCCP treatment, Parkin goes back to cytosol and mitochondrial signal disappeared.

REFERENCES

Akundi, R.S., Z. Huang, J. Eason, J.D. Pandya, L. Zhi, W.A. Cass, P.G. Sullivan, and H. Bueler. 2011. Increased mitochondrial calcium sensitivity and abnormal expression of innate immunity genes precede dopaminergic defects in Pink1-deficient mice. *PLoS One*. 6:e16038.

Al-Anzi, B., V. Sapin, C. Waters, K. Zinn, R.J. Wyman, and S. Benzer. 2009. Obesity-blocking neurons in Drosophila. *Neuron*. 63:329-341.

Bae, S., S.Y. Kim, J.H. Jung, Y. Yoon, H.J. Cha, H. Lee, K. Kim, J. Kim, I.S. An, H.D. Um, I.C. Park, S.J. Lee, S.Y. Nam, Y.W. Jin, J.H. Lee, and S. An. 2012. Akt is negatively regulated by the MULAN E3 ligase. *Cell Res*. 22:873-885.

Braschi, E., V. Goyon, R. Zunino, A. Mohanty, L. Xu, and H.M. McBride. 2010. Vps35 mediates vesicle transport between the mitochondria and peroxisomes. *Curr Biol*. 20:1310-1315.

Braschi, E., R. Zunino, and H.M. McBride. 2009. MAPL is a new mitochondrial SUMO E3 ligase that regulates mitochondrial fission. *EMBO reports*. 10:748-754.

Chan, N.C., A.M. Salazar, A.H. Pham, M.J. Sweredoski, N.J. Kolawa, R.L. Graham, S. Hess, and D.C. Chan. 2011a. Broad activation of the ubiquitin-proteasome system by Parkin is critical for mitophagy. *Hum Mol Genet*.

Chan, N.C., A.M. Salazar, A.H. Pham, M.J. Sweredoski, N.J. Kolawa, R.L. Graham, S. Hess, and D.C. Chan. 2011b. Broad activation of the ubiquitin-proteasome system by Parkin is critical for mitophagy. *Hum Mol Genet*. 20:1726-1737.

Clark, I.E., M.W. Dodson, C. Jiang, J.H. Cao, J.R. Huh, J.H. Seol, S.J. Yoo, B.A. Hay, and M. Guo. 2006. Drosophila pink1 is required for mitochondrial function and interacts genetically with parkin. *Nature*. 441:1162-1166.

Costa, A.C., S.H. Loh, and L.M. Martins. 2013. Drosophila Trap1 protects against mitochondrial dysfunction in a PINK1/parkin model of Parkinson's disease. *Cell Death Dis*. 4:e467.

de Brito, O.M., and L. Scorrano. 2008. Mitofusin 2 tethers endoplasmic reticulum to mitochondria. *Nature*. 456:605-610.

Deng, H., M.W. Dodson, H. Huang, and M. Guo. 2008. The Parkinson's disease genes pink1 and parkin promote mitochondrial fission and/or inhibit fusion in Drosophila. *Proc Natl Acad Sci U S A*. 105:14503-14508.

Fernandes, C., and Y. Rao. 2011. Genome-wide screen for modifiers of Parkinson's disease genes in Drosophila. *Mol Brain*. 4:17.

Frank-Cannon, T.C., T. Tran, K.A. Ruhn, T.N. Martinez, J. Hong, M. Marvin, M. Hartley, I. Trevino, D.E. O'Brien, B. Casey, M.S. Goldberg, and M.G. Tansey. 2008. Parkin deficiency increases vulnerability to inflammation-related nigral degeneration. *J Neurosci*. 28:10825-10834.

Gareau, J.R., and C.D. Lima. 2010. The SUMO pathway: emerging mechanisms that shape specificity, conjugation and recognition. *Nat Rev Mol Cell Biol*. 11:861-871.

Gautier, C.A., T. Kitada, and J. Shen. 2008. Loss of PINK1 causes mitochondrial functional defects and increased sensitivity to oxidative stress. *Proc Natl Acad Sci U S A*. 105:11364-11369.

Gegg, M.E., J.M. Cooper, K.Y. Chau, M. Rojo, A.H. Schapira, and J.W. Taanman. 2010. Mitofusin 1 and mitofusin 2 are ubiquitinated in a PINK1/parkin-dependent manner upon induction of mitophagy. *Hum Mol Genet*. 19:4861-4870.

Gegg, M.E., and A.H. Schapira. 2011. PINK1-parkin-dependent mitophagy involves ubiquitination of mitofusins 1 and 2: Implications for Parkinson disease pathogenesis. *Autophagy*. 7:243-245.

Geisler, S., K.M. Holmstrom, D. Skujat, F.C. Fiesel, O.C. Rothfuss, P.J. Kahle, and W. Springer. 2010. PINK1/Parkin-mediated mitophagy is dependent on VDAC1 and p62/SQSTM1. *Nat Cell Biol*. 12:119-131.

Gispert, S., F. Ricciardi, A. Kurz, M. Azizov, H.H. Hoepken, D. Becker, W. Voos, K. Leuner, W.E. Muller, A.P. Kudin, W.S. Kunz, A. Zimmermann, J. Roeper, D. Wenzel, M. Jendrach, M. Garcia-Arencibia, J. Fernandez-Ruiz, L. Huber, H. Rohrer, M. Barrera, A.S. Reichert, U. Rub, A. Chen, R.L. Nussbaum, and G. Auburger. 2009. Parkinson phenotype in aged PINK1-deficient mice is accompanied by progressive mitochondrial dysfunction in absence of neurodegeneration. *PLoS One*. 4:e5777.

Glauser, L., S. Sonnay, K. Stafa, and D.J. Moore. 2011. Parkin promotes the ubiquitination and degradation of the mitochondrial fusion factor mitofusin 1. *J Neurochem*. 118:636-645.

Guo, X., K.H. Chen, Y. Guo, H. Liao, J. Tang, and R.P. Xiao. 2007. Mitofusin 2 triggers vascular smooth muscle cell apoptosis via mitochondrial death pathway. *Circ Res*. 101:1113-1122.

Harder, Z., R. Zunino, and H. McBride. 2004. Sumo1 conjugates mitochondrial substrates and participates in mitochondrial fission. *Curr Biol*. 14:340-345.

Huang, P., T. Yu, and Y. Yoon. 2007. Mitochondrial clustering induced by overexpression of the mitochondrial fusion protein MFN2 causes mitochondrial dysfunction and cell death. *Eur J Cell Biol*. 86:289-302.

Imai, Y., T. Kanao, T. Sawada, Y. Kobayashi, Y. Moriwaki, Y. Ishida, K. Takeda, H. Ichijo, B. Lu, and R. Takahashi. 2010. The loss of PGAM5 suppresses the mitochondrial degeneration caused by inactivation of PINK1 in Drosophila. *PLoS Genet*. 6:e1001229.

Jung, J.H., S. Bae, J.Y. Lee, S.R. Woo, H.J. Cha, Y. Yoon, K.S. Suh, S.J. Lee, I.C. Park, Y.W. Jin, K.H. Lee, S. An, and J.H. Lee. 2011. E3 ubiquitin ligase Hades negatively regulates the exonuclear function of p53. *Cell Death Differ*. 18:1865-1875.

Kitada, T., A. Pisani, D.R. Porter, H. Yamaguchi, A. Tscherter, G. Martella, P. Bonsi, C. Zhang, E.N. Pothos, and J. Shen. 2007. Impaired dopamine release and synaptic plasticity in the striatum of PINK1-deficient mice. *Proc Natl Acad Sci U S A*. 104:11441-11446.

Kitada, T., Y. Tong, C.A. Gautier, and J. Shen. 2009. Absence of nigral degeneration in aged parkin/DJ-1/PINK1 triple knockout mice. *J Neurochem*. 111:696-702.

Koh, H., H. Kim, M.J. Kim, J. Park, H.J. Lee, and J. Chung. 2012. Silent information regulator 2 (Sir2) and Forkhead box O (FOXO) complement mitochondrial dysfunction and dopaminergic neuron loss in Drosophila PTEN-induced kinase 1 (PINK1) null mutant. *J Biol Chem*. 287:12750-12758.

Kumar, K.R., A. Weissbach, M. Heldmann, M. Kasten, S. Tunc, C.M. Sue, M. Svetel, V.S. Kostic, J. Segura-Aguilar, A. Ramirez, D.K. Simon, P. Vieregge, T.F. Munte, J. Hagenah, C. Klein, and K. Lohmann. 2012. Frequency of the D620N Mutation in VPS35 in Parkinson Disease. *Arch Neurol*:1-5.

Lesage, S., C. Condroyer, S. Klebe, A. Honore, F. Tison, C. Brefel-Courbon, A. Durr, and A. Brice. 2012. Identification of VPS35 mutations replicated in French families with Parkinson disease. *Neurology*. 78:1449-1450.

Li, W., M.H. Bengtson, A. Ulbrich, A. Matsuda, V.A. Reddy, A. Orth, S.K. Chanda, S. Batalov, and C.A. Joazeiro. 2008. Genome-wide and functional annotation of human E3 ubiquitin ligases identifies MULAN, a mitochondrial E3 that regulates the organelle's dynamics and signaling. *PLoS One*. 3:e1487.

Liu, S., and B. Lu. 2010. Reduction of protein translation and activation of autophagy protect against PINK1 pathogenesis in Drosophila melanogaster. *PLoS Genet*. 6:e1001237.

Liu, S., T. Sawada, S. Lee, W. Yu, G. Silverio, P. Alapatt, I. Millan, A. Shen, W. Saxton, T. Kanao, R. Takahashi, N. Hattori, Y. Imai, and B. Lu. 2012. Parkinson's disease-associated kinase PINK1 regulates Miro protein level and axonal transport of mitochondria. *PLoS Genet*. 8:e1002537.

Lokireddy, S., I.W. Wijesoma, S. Teng, S. Bonala, P.D. Gluckman, C. McFarlane, M. Sharma, and R. Kambadur. 2012. The ubiquitin ligase *MUL1* induces mitophagy in skeletal muscle in response to muscle-wasting stimuli. *Cell Metab*. 16:613-624.

Matsuda, N., S. Sato, K. Shiba, K. Okatsu, K. Saisho, C.A. Gautier, Y.S. Sou, S. Saiki, S. Kawajiri, F. Sato, M. Kimura, M. Komatsu, N. Hattori, and K. Tanaka. 2010. PINK1 stabilized by mitochondrial depolarization recruits Parkin to damaged mitochondria and activates latent Parkin for mitophagy. *J Cell Biol*. 189:211-221.

Misko, A., S. Jiang, I. Wegorzewska, J. Milbrandt, and R.H. Baloh. 2010. Mitofusin 2 is necessary for transport of axonal mitochondria and interacts with the Miro/Milton complex. *J Neurosci*. 30:4232-4240.

Narendra, D., L.A. Kane, D.N. Hauser, I.M. Fearnley, and R.J. Youle. 2010a. p62/SQSTM1 is required for Parkin-induced mitochondrial clustering but not mitophagy; VDAC1 is dispensable for both. *Autophagy*. 6:1090-1106.

Narendra, D., A. Tanaka, D.F. Suen, and R.J. Youle. 2008a. Parkin is recruited selectively to impaired mitochondria and promotes their autophagy. *The Journal of Cell Biology*. 183:795-803.

Narendra, D., A. Tanaka, D.F. Suen, and R.J. Youle. 2008b. Parkin is recruited selectively to impaired mitochondria and promotes their autophagy. *J Cell Biol*. 183:795-803.

Narendra, D.P., S.M. Jin, A. Tanaka, D.F. Suen, C.A. Gautier, J. Shen, M.R. Cookson, and R.J. Youle. 2010b. PINK1 is selectively stabilized on impaired mitochondria to activate Parkin. *PLoS Biol*. 8:e1000298.

Neuspiel, M. 2008. Cargo-Selected Transport from the Mitochondria to Peroxisomes Is Mediated by Vesicular Carriers. *Current Biology*. 18:102-108.

Palacino, J.J., D. Sagi, M.S. Goldberg, S. Krauss, C. Motz, M. Wacker, J. Klose, and J. Shen. 2004. Mitochondrial dysfunction and oxidative damage in parkin-deficient mice. *J Biol Chem*. 279:18614-18622.

Park, J., S.B. Lee, S. Lee, Y. Kim, S. Song, S. Kim, E. Bae, J. Kim, M. Shong, J.M. Kim, and J. Chung. 2006. Mitochondrial dysfunction in Drosophila PINK1 mutants is complemented by parkin. *Nature*. 441:1157-1161.

Perez, F.A., W.R. Curtis, and R.D. Palmiter. 2005. Parkin-deficient mice are not more sensitive to 6-hydroxydopamine or methamphetamine neurotoxicity. *BMC Neurosci*. 6:71.

Perez, F.A., and R.D. Palmiter. 2005. Parkin-deficient mice are not a robust model of parkinsonism. *Proc Natl Acad Sci U S A*. 102:2174-2179.

Poole, A.C., R.E. Thomas, L.A. Andrews, H.M. McBride, A.J. Whitworth, and L.J. Pallanck. 2008. The PINK1/Parkin pathway regulates mitochondrial morphology. *Proc Natl Acad Sci U S A*. 105:1638-1643.

Poole, A.C., R.E. Thomas, S. Yu, E.S. Vincow, and L. Pallanck. 2010. The mitochondrial fusion-promoting factor mitofusin is a substrate of the PINK1/parkin pathway. *PLoS One*. 5:e10054.

Rakovic, A., A. Grunewald, J. Kottwitz, N. Bruggemann, P.P. Pramstaller, K. Lohmann, and C. Klein. 2011. Mutations in PINK1 and Parkin impair ubiquitination of Mitofusins in human fibroblasts. *PLoS One*. 6:e16746.

Shen, T., M. Zheng, C. Cao, C. Chen, J. Tang, W. Zhang, H. Cheng, K.H. Chen, and R.P. Xiao. 2007. Mitofusin-2 is a major determinant of oxidative stress-mediated heart muscle cell apoptosis. *J Biol Chem*. 282:23354-23361.

Tain, L.S., H. Mortiboys, R.N. Tao, E. Ziviani, O. Bandmann, and A.J. Whitworth. 2009. Rapamycin activation of 4E-BP prevents parkinsonian dopaminergic neuron loss. *Nat Neurosci*. 12:1129-1135.

Tanaka, A., M.M. Cleland, S. Xu, D.P. Narendra, D.F. Suen, M. Karbowski, and R.J. Youle. 2010. Proteasome and p97 mediate mitophagy and degradation of mitofusins induced by Parkin. *J Cell Biol*. 191:1367-1380.

Verstreken, P., C.V. Ly, K.J. Venken, T.W. Koh, Y. Zhou, and H.J. Bellen. 2005. Synaptic mitochondria are critical for mobilization of reserve pool vesicles at Drosophila neuromuscular junctions. *Neuron*. 47:365-378.

Vilarino-Guell, C., C. Wider, O.A. Ross, J.C. Dachsel, J.M. Kachergus, S.J. Lincoln, A.I. Soto-Ortolaza, S.A. Cobb, G.J. Wilhoite, J.A. Bacon, B. Behrouz, H.L. Melrose, E. Hentati, A. Puschmann, D.M. Evans, E. Conibear, W.W. Wasserman, J.O. Aasly, P.R. Burkhard, R. Djaldetti, J. Ghika, F. Hentati, A. Krygowska-Wajs, T. Lynch, E. Melamed, A. Rajput, A.H. Rajput, A. Solida, R.M. Wu, R.J. Uitti, Z.K. Wszolek, F. Vingerhoets, and M.J. Farrer. 2011. VPS35 mutations in Parkinson disease. *Am J Hum Genet*. 89:162-167.

Vo, S.H., M. Butzlaff, S.K. Pru, R.A. Ni Charthaigh, P. Karsten, A. Lankes, S. Hamm, M. Simons, B. Adryan, J.B. Schulz, and A. Voigt. 2012. Large-scale screen for modifiers of ataxin-3-derived polyglutamine-induced toxicity in Drosophila. *PLoS One*. 7:e47452.

Yang, Y., S. Gehrke, Y. Imai, Z. Huang, Y. Ouyang, J.W. Wang, L. Yang, M.F. Beal, H. Vogel, and B. Lu. 2006. Mitochondrial pathology and muscle and dopaminergic neuron degeneration caused by inactivation of Drosophila Pink1 is rescued by Parkin. *Proc Natl Acad Sci U S A*. 103:10793-10798.

Yang, Y., Y. Ouyang, L. Yang, M.F. Beal, A. McQuibban, H. Vogel, and B. Lu. 2008. Pink1 regulates mitochondrial dynamics through interaction with the fission/fusion machinery. *Proc Natl Acad Sci U S A*. 105:7070-7075.

Zhang, B., J. Huang, H.-L. Li, T. Liu, Y.-Y. Wang, P. Waterman, A.-P. Mao, L.-G. Xu, Z. Zhai, D. Liu, P. Marrack, and H.-B. Shu. 2008. GIDE is a mitochondrial E3 ubiquitin ligase that induces apoptosis and slows growth. *Cell Research*. 18:900-910.

Zimprich, A., A. Benet-Pages, W. Struhal, E. Graf, S.H. Eck, M.N. Offman, D. Haubenberger, S. Spielberger, E.C. Schulte, P. Lichtner, S.C. Rossle, N. Klopp, E. Wolf, K. Seppi, W. Pirker, S. Presslauer, B. Mollenhauer, R. Katzenschlager, T. Foki, C. Hotzy, E. Reinthaler, A. Harutyunyan, R. Kralovics, A. Peters, F. Zimprich, T. Brucke, W. Poewe, E. Auff, C. Trenkwalder, B. Rost, G. Ransmayr, J. Winkelmann, T. Meitinger, and T.M.

Strom. 2011. A mutation in VPS35, encoding a subunit of the retromer complex, causes late-onset Parkinson disease. *Am J Hum Genet*. 89:168-175.

Ziviani, E., R.N. Tao, and A.J. Whitworth. 2010. Drosophila parkin requires PINK1 for mitochondrial translocation and ubiquitinates mitofusin. *Proc Natl Acad Sci U S A*. 107:5018-5023.

CHAPTER 4

CONCLUSIONS AND FUTURE DIRECTIONS

The PINK1/Parkin pathway and Omi

Omi/HtrA2 encodes a serine protease that localizes to the mitochondrial inter membrane space. In cultured cells, *Omi* expression causes apoptotic cell death (Hegde et al., 2002; Martins et al., 2002; van Loo et al., 2002; Verhagen et al., 2002). *mnd2* (motor neuron degeneration 2) mice that have a mutation in *Omi* abolishing protease activity reported muscle wasting and neurodegenerative phenotypes similar to parkinsonism (Jones et al., 2003). Later studies have further linked PD and *Omi/HtrA2* (Bogaerts et al., 2008; Strauss et al., 2005). Omi/HtrA2 G399S mutation was found in sporadic PD patients. Furthermore, a study in cultured cells reported that Omi/HtrA2 binds to PINK1 and gets phosphorylated by the serine-threonine kinase p38 in PINK1-dependent manner (Plun-Favreau et al., 2007). This study suggests that *Omi/HtrA2* functions downstream of *PINK1,* with PINK1 positively regulating Omi/HtrA2. Based on these series of evidence, *Omi/HtrA2* was designated as *Parkinson disease-13* locus (*PARK13*). However, our work in *Drosophila* fails to show any genetic interaction between *PINK1* and *Omi/HtrA2*. First, *Omi* mutants do not share *PINK1* mutant mitochondrial phenotypes in testes and muscles as well as dopaminergic neuronal cells. Second, *Omi* overexpression or *Omi* mutation fails to modify *PINK1* mutant phenotypes in testes and muscles. Third, localization of Omi does not change in *PINK1* mutants. Fourth, PINK1 levels or processing are not affected in *Omi* mutants. Taken together, our work concludes that there is no genetic interaction between *Omi* and *PINK1*, suggesting that *Omi/HtrA2* is not in the PINK1/Parkin pathway. The discrepancies might be due to difference between *in vivo* and *in vitro* systems. It is also possible

that *Omi* shows genetic interactions with *PINK1* in mitochondrial function. ConcOmitant with submission of our manuscript, two studies with larger sample size than previous ones reported that no clear association of *Omi/HtrA2* with PD was observed, indicating that G399S allele is not disease mutation (Ross et al., 2008; Simon-Sanchez and Singleton, 2008). However, another study provides evidence that Omi cleaves Parkin in mammalian cells (Park et al., 2009). So far, it remains if *Omi* is associated with PD. Further studies are needed to address these questions.

The PINK1/Parkin pathway and *MUL1*

Parkin binds to and ubiquitinates MFN in several systems (Gegg et al., 2010; Gegg and Schapira, 2011; Poole et al., 2008; Ziviani et al., 2010) (Rakovic et al., 2011). Consistently, *PINK1* or *parkin* deficiency in *Drosophila* causes dramatically increased MFN levels (Poole et al., 2008; Ziviani et al., 2010). However, it remains unclear if increased MFN is responsible for defects observed in *PINK1* or *parkin* mutants. Our work shows that *MFN* overexpression displays strikingly similar phenotypes to *PINK1* and *parkin* mutants such as mitochondrial morphology defects, muscle degeneration, and muscle cell death. This indicates that an increase in MFN levels is sufficient to cause *PINK1* or *parkin* mutant phenotypes, suggesting a direct link between increased MFN levels and pathology. The exact mechanism how increased MFN levels causes the pathology needs to be further elucidated. However, several speculations can be made from existing literature. *MFN* overexpression causes perinuclear clustering of mitochondria, which leads to mitochondrial dysfunction including reduced mitochondrial membrane potential, release of cytochorome C, and apoptotic cells death (Huang et al., 2007). *MFN* overexpression also causes cell death via inhibition of Akt signaling, activation of caspases, and increased Bax levels (Guo et al., 2007; Shen et al., 2007). As MFN regulates ER-mitochondrial interactions (de

Brito and Scorrano, 2008), ER dysfunction might also contribute to the pathology. Furthermore, MFN's function in mitochondrial transport in neuronal cells (Misko et al., 2010) poses the possibility that altered mitochondrial transport is an underlying cause of vulnerability toward neuronal cell death.

Our seeking for suppressors of *PINK1* mutant mitochondrial morphology defects in muscles resulted in the identification of *MUL1*, a mitochondrial ubiquitin E3 ligase, as a novel suppressor. *MUL1* overexpression suppresses several *PINK1* mutant phenotypes including muscle degeneration and dopaminergic neuronal phenotypes. *MUL1* also suppresses *parkin* mutant and *MFN* overexpression pathology. In contrast to wildtype *MUL1*, the ligase dead form of *MUL1* fails to suppress *PINK1* and *parkin* mutant phenotypes, suggesting that ligase activity is crucial for the suppression. This series of observations - increased MFN levels in *PINK1* or *parkin* mutants, suppression of the *PINK1* or *parkin* mutant phenotypes by *MUL1*, and crucial E3 ligase activity for the suppression of *PINK1* mutant phenotypes - strongly suggest the possibility that the suppression is achieved through negative regulation of MFN levels by *MUL1*. Indeed, immunoprecipitation and ubiquitination assays indicate that *MUL1* interacts with and ubiquitinates MFN. Consistent with our finding, a recent study reported that *MUL1* binds to and ubiquitinates MFN upon muscle wasting stimuli (Lokireddy et al., 2012). That *MUL1* suppresses *PINK1* and *parkin* mutant phenotypes through regulation of MFN levels evokes an interesting question – Do other previously identified *PINK1* mutant suppressors rescue the phenotypes by modulation of MFN levels? Although there are several *PINK1* mutant suppressors identified (Costa et al., 2013; Fernandes and Rao, 2011; Imai et al., 2010; Liu and Lu, 2010; Tain et al., 2009; Vo et al., 2012), no study so far has checked the modulation of MFN levels by these

suppressors. The answers to this question may reveal differences in suppressors and mechanisms of the suppression.

In addition to a role in mitochondrial dynamics, the PINK1/Parkin pathway mediates mitophagy (Matsuda et al., 2010; Narendra et al., 2008; Narendra et al., 2010) (Chan et al., 2011; Tanaka et al., 2010). Although *MUL1* suppresses *PINK1* and *parkin* mutant phenotypes, *MUL1* does not affect Parkin-mediated mitophagy. Both knockdown and overexpression of *MUL1* do not disrupt recruitment of Parkin to mitochondria or clearance of mitochondria. It is interesting to point out that even though *MUL1* and Parkin share MFN as their target, *MUL1* does not seem to have role in Parkin-induced mitophagy. Furthermore, this indicates that modulation of MFN levels is sufficient to suppress *PINK1* mutant pathology. However, a recent study provides evidence that *MUL1* promotes mitophagy (Lokireddy et al., 2012). This discrepancy could be explained by difference in systems and methods used. Our study used the mitophagy assay that Richard Youle's group established (Narendra et al., 2008) and assesses Parkin recruitment to mitochondria and clearance of mitochondria. The other group overexpressed *MUL1* and measured emission of mitochondrial fluorescent protein that changes color in an acidic environment like lysosome. Whether *MUL1* has a function in mitophagy should be further elucidated.

That *MUL1* does not affect Parkin-mediated mitophagy suggests that *MUL1* acts in a different pathway from the PINK1/Parkin pathway. Genetic epistasis studies in *Drosophila* provide strong evidence that *MUL1* acts in parallel to the PINK1/Parkin pathway to regulate mitochondrial morphology and body fat levels. Our studies suggest that this is achieved by regulation of MFN. However, it is entirely possible that *MUL1* and Parkin have other shared

target molecules such as Miro. Finding other shared targets will increase our understanding on the parallel pathways and the contexts of regulation. The parallel pathways raise several exciting questions. What other molecules are in the *MUL1* pathway? Although several molecules have been reported as direct substrates of *MUL1* (Bae et al., 2012; Braschi et al., 2009; Jung et al., 2011), it is not clear if they are regulated only by *MUL1* or by both *MUL1* and the PINK1/Parkin pathways. Only upstream molecule that is reported is FOXO. In response to muscle wasting stimuli, increased FOXO upregulates *MUL1* expression (Lokireddy et al., 2012). It is interesting to note that FOXO is also shown to suppress *PINK1* and *parkin* mutant phenotypes in *Drosophila* (Koh et al., 2012; Tain et al., 2009). Based on the suppression, the authors suggest that *FOXO* acts as a downstream of *PINK1*(Koh et al., 2012). However, one cannot exclude the possibility that FOXO suppresses *PINK1* mutants through the upregulation of *MUL1*. Another important question is "Would the parallel pathways explain weak phenotypes in *PINK1* or *parkin* deficient mice?" In contrast to PD patients with *PINK1* or *parkin* mutations, *PINK1* or *parkin* deficient mice, or even *PINK1*, *parkin*, and *DJ-1* triple knockout mice bear only subtle phenotypes (Palacino et al., 2004) (Akundi et al., 2011; Frank-Cannon et al., 2008; Gautier et al., 2008; Gispert et al., 2009; Kitada et al., 2007; Kitada et al., 2009; Perez et al., 2005; Perez and Palmiter, 2005). It remains unclear why these mice do not show robust phenotypes similar to *Drosophila* and humans. It has been speculated that there might be a compensation mechanism in mice. The work presented here suggests that *MUL1* acting in a parallel pathway might compensate some of phenotypes in the mice. It is of great interest to ask if double knockout mice of *PINK1 MUL1* or *parkin MUL1* show robust phenotypes.

A direct link between *MUL1* and PD has not been explored yet. Based on phenotypes of PD mouse model and the possibility of parallel pathways as discussed above, it is worth studying

if patients with *PINK1* or *parkin* mutations have polymorphisms in *MUL1* gene that potentially affect *MUL1* expression or activity. Interestingly, a study reports that *MUL1* forms a complex with VPS35 and VPS26 (Braschi et al., 2010). *VPS35* has been recently identified as a PD gene in that mutations in *VPS35* cause PD (Kumar et al., 2012; Lesage et al., 2012; Vilarino-Guell et al., 2011; Zimprich et al., 2011). Whether this interaction is interrupted in PD patients with *VPS35*, *PINK1*, or *parkin* mutations would be interesting to study. Taken together, circumstantial evidence points to the possibility of *MUL1*'s relevance to PD.

Taken together, our work suggests *MUL1* as a potential therapeutic target to rescue PD pathology. Further studies on *MUL1* would greatly expand our understanding of PD.

REFERENCES

Akundi, R.S., Z. Huang, J. Eason, J.D. Pandya, L. Zhi, W.A. Cass, P.G. Sullivan, and H. Bueler. 2011. Increased mitochondrial calcium sensitivity and abnormal expression of innate immunity genes precede dopaminergic defects in Pink1-deficient mice. *PLoS One*. 6:e16038.

Bae, S., S.Y. Kim, J.H. Jung, Y. Yoon, H.J. Cha, H. Lee, K. Kim, J. Kim, I.S. An, H.D. Um, I.C. Park, S.J. Lee, S.Y. Nam, Y.W. Jin, J.H. Lee, and S. An. 2012. Akt is negatively regulated by the MULAN E3 ligase. *Cell Res*. 22:873-885.

Bogaerts, V., K. Nuytemans, J. Reumers, P. Pals, S. Engelborghs, B. Pickut, E. Corsmit, K. Peeters, J. Schymkowitz, P.P. De Deyn, P. Cras, F. Rousseau, J. Theuns, and C. Van Broeckhoven. 2008. Genetic variability in the mitochondrial serine protease HTRA2 contributes to risk for Parkinson disease. *Hum Mutat*. 29:832-840.

Braschi, E., V. Goyon, R. Zunino, A. Mohanty, L. Xu, and H.M. McBride. 2010. Vps35 mediates vesicle transport between the mitochondria and peroxisomes. *Curr Biol*. 20:1310-1315.

Braschi, E., R. Zunino, and H.M. McBride. 2009. MAPL is a new mitochondrial SUMO E3 ligase that regulates mitochondrial fission. *EMBO reports*. 10:748-754.

Chan, N.C., A.M. Salazar, A.H. Pham, M.J. Sweredoski, N.J. Kolawa, R.L. Graham, S. Hess, and D.C. Chan. 2011. Broad activation of the ubiquitin-proteasome system by Parkin is critical for mitophagy. *Hum Mol Genet*. 20:1726-1737.

Costa, A.C., S.H. Loh, and L.M. Martins. 2013. Drosophila Trap1 protects against mitochondrial dysfunction in a PINK1/parkin model of Parkinson's disease. *Cell Death Dis*. 4:e467.

de Brito, O.M., and L. Scorrano. 2008. Mitofusin 2 tethers endoplasmic reticulum to mitochondria. *Nature*. 456:605-610.

Fernandes, C., and Y. Rao. 2011. Genome-wide screen for modifiers of Parkinson's disease genes in Drosophila. *Mol Brain*. 4:17.

Frank-Cannon, T.C., T. Tran, K.A. Ruhn, T.N. Martinez, J. Hong, M. Marvin, M. Hartley, I. Trevino, D.E. O'Brien, B. Casey, M.S. Goldberg, and M.G. Tansey. 2008. Parkin deficiency increases vulnerability to inflammation-related nigral degeneration. *J Neurosci*. 28:10825-10834.

Gautier, C.A., T. Kitada, and J. Shen. 2008. Loss of PINK1 causes mitochondrial functional defects and increased sensitivity to oxidative stress. *Proc Natl Acad Sci U S A*. 105:11364-11369.

Gegg, M.E., J.M. Cooper, K.Y. Chau, M. Rojo, A.H. Schapira, and J.W. Taanman. 2010. Mitofusin 1 and mitofusin 2 are ubiquitinated in a PINK1/parkin-dependent manner upon induction of mitophagy. *Hum Mol Genet*. 19:4861-4870.

Gegg, M.E., and A.H. Schapira. 2011. PINK1-parkin-dependent mitophagy involves ubiquitination of mitofusins 1 and 2: Implications for Parkinson disease pathogenesis. *Autophagy*. 7:243-245.

Gispert, S., F. Ricciardi, A. Kurz, M. Azizov, H.H. Hoepken, D. Becker, W. Voos, K. Leuner, W.E. Muller, A.P. Kudin, W.S. Kunz, A. Zimmermann, J. Roeper, D. Wenzel, M. Jendrach, M. Garcia-Arencibia, J. Fernandez-Ruiz, L. Huber, H. Rohrer, M. Barrera, A.S. Reichert, U. Rub, A. Chen, R.L. Nussbaum, and G. Auburger. 2009. Parkinson

phenotype in aged PINK1-deficient mice is accompanied by progressive mitochondrial dysfunction in absence of neurodegeneration. *PLoS One*. 4:e5777.

Guo, X., K.H. Chen, Y. Guo, H. Liao, J. Tang, and R.P. Xiao. 2007. Mitofusin 2 triggers vascular smooth muscle cell apoptosis via mitochondrial death pathway. *Circ Res*. 101:1113-1122.

Hegde, R., S.M. Srinivasula, Z. Zhang, R. Wassell, R. Mukattash, L. Cilenti, G. DuBois, Y. Lazebnik, A.S. Zervos, T. Fernandes-Alnemri, and E.S. Alnemri. 2002. Identification of Omi/HtrA2 as a mitochondrial apoptotic serine protease that disrupts inhibitor of apoptosis protein-caspase interaction. *J Biol Chem*. 277:432-438.

Huang, P., T. Yu, and Y. Yoon. 2007. Mitochondrial clustering induced by overexpression of the mitochondrial fusion protein MFN2 causes mitochondrial dysfunction and cell death. *Eur J Cell Biol*. 86:289-302.

Imai, Y., T. Kanao, T. Sawada, Y. Kobayashi, Y. Moriwaki, Y. Ishida, K. Takeda, H. Ichijo, B. Lu, and R. Takahashi. 2010. The loss of PGAM5 suppresses the mitochondrial degeneration caused by inactivation of PINK1 in Drosophila. *PLoS Genet*. 6:e1001229.

Jones, J.M., P. Datta, S.M. Srinivasula, W. Ji, S. Gupta, Z. Zhang, E. Davies, G. Hajnoczky, T.L. Saunders, M.L. Van Keuren, T. Fernandes-Alnemri, M.H. Meisler, and E.S. Alnemri. 2003. Loss of Omi mitochondrial protease activity causes the neuromuscular disorder of mnd2 mutant mice. *Nature*. 425:721-727.

Jung, J.H., S. Bae, J.Y. Lee, S.R. Woo, H.J. Cha, Y. Yoon, K.S. Suh, S.J. Lee, I.C. Park, Y.W. Jin, K.H. Lee, S. An, and J.H. Lee. 2011. E3 ubiquitin ligase Hades negatively regulates the exonuclear function of p53. *Cell Death Differ*. 18:1865-1875.

Kitada, T., A. Pisani, D.R. Porter, H. Yamaguchi, A. Tscherter, G. Martella, P. Bonsi, C. Zhang, E.N. Pothos, and J. Shen. 2007. Impaired dopamine release and synaptic plasticity in the striatum of PINK1-deficient mice. *Proc Natl Acad Sci U S A*. 104:11441-11446.

Kitada, T., Y. Tong, C.A. Gautier, and J. Shen. 2009. Absence of nigral degeneration in aged parkin/DJ-1/PINK1 triple knockout mice. *J Neurochem*. 111:696-702.

Koh, H., H. Kim, M.J. Kim, J. Park, H.J. Lee, and J. Chung. 2012. Silent information regulator 2 (Sir2) and Forkhead box O (FOXO) complement mitochondrial dysfunction and dopaminergic neuron loss in Drosophila PTEN-induced kinase 1 (PINK1) null mutant. *J Biol Chem*. 287:12750-12758.

Kumar, K.R., A. Weissbach, M. Heldmann, M. Kasten, S. Tunc, C.M. Sue, M. Svetel, V.S. Kostic, J. Segura-Aguilar, A. Ramirez, D.K. Simon, P. Vieregge, T.F. Munte, J. Hagenah, C. Klein, and K. Lohmann. 2012. Frequency of the D620N Mutation in VPS35 in Parkinson Disease. *Arch Neurol*:1-5.

Lesage, S., C. Condroyer, S. Klebe, A. Honore, F. Tison, C. Brefel-Courbon, A. Durr, and A. Brice. 2012. Identification of VPS35 mutations replicated in French families with Parkinson disease. *Neurology*. 78:1449-1450.

Liu, S., and B. Lu. 2010. Reduction of protein translation and activation of autophagy protect against PINK1 pathogenesis in Drosophila melanogaster. *PLoS Genet*. 6:e1001237.

Lokireddy, S., I.W. Wijesoma, S. Teng, S. Bonala, P.D. Gluckman, C. McFarlane, M. Sharma, and R. Kambadur. 2012. The ubiquitin ligase *MUL1* induces mitophagy in skeletal muscle in response to muscle-wasting stimuli. *Cell Metab*. 16:613-624.

Martins, L.M., I. Iaccarino, T. Tenev, S. Gschmeissner, N.F. Totty, N.R. Lemoine, J. Savopoulos, C.W. Gray, C.L. Creasy, C. Dingwall, and J. Downward. 2002. The serine protease

Omi/HtrA2 regulates apoptosis by binding XIAP through a reaper-like motif. *J Biol Chem*. 277:439-444.

Matsuda, N., S. Sato, K. Shiba, K. Okatsu, K. Saisho, C.A. Gautier, Y.S. Sou, S. Saiki, S. Kawajiri, F. Sato, M. Kimura, M. Komatsu, N. Hattori, and K. Tanaka. 2010. PINK1 stabilized by mitochondrial depolarization recruits Parkin to damaged mitochondria and activates latent Parkin for mitophagy. *J Cell Biol*. 189:211-221.

Misko, A., S. Jiang, I. Wegorzewska, J. Milbrandt, and R.H. Baloh. 2010. Mitofusin 2 is necessary for transport of axonal mitochondria and interacts with the Miro/Milton complex. *J Neurosci*. 30:4232-4240.

Narendra, D., A. Tanaka, D.F. Suen, and R.J. Youle. 2008. Parkin is recruited selectively to impaired mitochondria and promotes their autophagy. *J Cell Biol*. 183:795-803.

Narendra, D.P., S.M. Jin, A. Tanaka, D.F. Suen, C.A. Gautier, J. Shen, M.R. Cookson, and R.J. Youle. 2010. PINK1 is selectively stabilized on impaired mitochondria to activate Parkin. *PLoS Biol*. 8:e1000298.

Palacino, J.J., D. Sagi, M.S. Goldberg, S. Krauss, C. Motz, M. Wacker, J. Klose, and J. Shen. 2004. Mitochondrial dysfunction and oxidative damage in parkin-deficient mice. *J Biol Chem*. 279:18614-18622.

Park, H.M., G.Y. Kim, M.K. Nam, G.H. Seong, C. Han, K.C. Chung, S. Kang, and H. Rhim. 2009. The serine protease HtrA2/Omi cleaves Parkin and irreversibly inactivates its E3 ubiquitin ligase activity. *Biochem Biophys Res Commun*. 387:537-542.

Perez, F.A., W.R. Curtis, and R.D. Palmiter. 2005. Parkin-deficient mice are not more sensitive to 6-hydroxydopamine or methamphetamine neurotoxicity. *BMC Neurosci*. 6:71.

Perez, F.A., and R.D. Palmiter. 2005. Parkin-deficient mice are not a robust model of parkinsonism. *Proc Natl Acad Sci U S A*. 102:2174-2179.

Plun-Favreau, H., K. Klupsch, N. Moisoi, S. Gandhi, S. Kjaer, D. Frith, K. Harvey, E. Deas, R.J. Harvey, N. McDonald, N.W. Wood, L.M. Martins, and J. Downward. 2007. The mitochondrial protease HtrA2 is regulated by Parkinson's disease-associated kinase PINK1. *Nat Cell Biol*. 9:1243-1252.

Poole, A.C., R.E. Thomas, L.A. Andrews, H.M. McBride, A.J. Whitworth, and L.J. Pallanck. 2008. The PINK1/Parkin pathway regulates mitochondrial morphology. *Proc Natl Acad Sci U S A*. 105:1638-1643.

Rakovic, A., A. Grunewald, J. Kottwitz, N. Bruggemann, P.P. Pramstaller, K. Lohmann, and C. Klein. 2011. Mutations in PINK1 and Parkin impair ubiquitination of Mitofusins in human fibroblasts. *PLoS One*. 6:e16746.

Ross, O.A., A.I. Soto, C. Vilarino-Guell, M.G. Heckman, N.N. Diehl, M.M. Hulihan, J.O. Aasly, S. Sando, J.M. Gibson, T. Lynch, A. Krygowska-Wajs, G. Opala, M. Barcikowska, K. Czyzewski, R.J. Uitti, Z.K. Wszolek, and M.J. Farrer. 2008. Genetic variation of Omi/HtrA2 and Parkinson's disease. *Parkinsonism & related disorders*.

Shen, T., M. Zheng, C. Cao, C. Chen, J. Tang, W. Zhang, H. Cheng, K.H. Chen, and R.P. Xiao. 2007. Mitofusin-2 is a major determinant of oxidative stress-mediated heart muscle cell apoptosis. *J Biol Chem*. 282:23354-23361.

Simon-Sanchez, J., and A.B. Singleton. 2008. Sequencing analysis of OMI/HTRA2 shows previously reported pathogenic mutations in neurologically normal controls. *Hum Mol Genet*.

Strauss, K.M., L.M. Martins, H. Plun-Favreau, F.P. Marx, S. Kautzmann, D. Berg, T. Gasser, Z. Wszolek, T. Muller, A. Bornemann, H. Wolburg, J. Downward, O. Riess, J.B. Schulz,

and R. Kruger. 2005. Loss of function mutations in the gene encoding Omi/HtrA2 in Parkinson's disease. *Hum Mol Genet*. 14:2099-2111.

Tain, L.S., H. Mortiboys, R.N. Tao, E. Ziviani, O. Bandmann, and A.J. Whitworth. 2009. Rapamycin activation of 4E-BP prevents parkinsonian dopaminergic neuron loss. *Nat Neurosci*. 12:1129-1135.

Tanaka, A., M.M. Cleland, S. Xu, D.P. Narendra, D.F. Suen, M. Karbowski, and R.J. Youle. 2010. Proteasome and p97 mediate mitophagy and degradation of mitofusins induced by Parkin. *J Cell Biol*. 191:1367-1380.

van Loo, G., M. van Gurp, B. Depuydt, S.M. Srinivasula, I. Rodriguez, E.S. Alnemri, K. Gevaert, J. Vandekerckhove, W. Declercq, and P. Vandenabeele. 2002. The serine protease Omi/HtrA2 is released from mitochondria during apoptosis. Omi interacts with caspase-inhibitor XIAP and induces enhanced caspase activity. *Cell Death Differ*. 9:20-26.

Verhagen, A.M., J. Silke, P.G. Ekert, M. Pakusch, H. Kaufmann, L.M. Connolly, C.L. Day, A. Tikoo, R. Burke, C. Wrobel, R.L. Moritz, R.J. Simpson, and D.L. Vaux. 2002. HtrA2 promotes cell death through its serine protease activity and its ability to antagonize inhibitor of apoptosis proteins. *J Biol Chem*. 277:445-454.

Vilarino-Guell, C., C. Wider, O.A. Ross, J.C. Dachsel, J.M. Kachergus, S.J. Lincoln, A.I. Soto-Ortolaza, S.A. Cobb, G.J. Wilhoite, J.A. Bacon, B. Behrouz, H.L. Melrose, E. Hentati, A. Puschmann, D.M. Evans, E. Conibear, W.W. Wasserman, J.O. Aasly, P.R. Burkhard, R. Djaldetti, J. Ghika, F. Hentati, A. Krygowska-Wajs, T. Lynch, E. Melamed, A. Rajput, A.H. Rajput, A. Solida, R.M. Wu, R.J. Uitti, Z.K. Wszolek, F. Vingerhoets, and M.J. Farrer. 2011. VPS35 mutations in Parkinson disease. *Am J Hum Genet*. 89:162-167.

Vo, S.H., M. Butzlaff, S.K. Pru, R.A. Ni Charthaigh, P. Karsten, A. Lankes, S. Hamm, M. Simons, B. Adryan, J.B. Schulz, and A. Voigt. 2012. Large-scale screen for modifiers of ataxin-3-derived polyglutamine-induced toxicity in Drosophila. *PLoS One*. 7:e47452.

Zimprich, A., A. Benet-Pages, W. Struhal, E. Graf, S.H. Eck, M.N. Offman, D. Haubenberger, S. Spielberger, E.C. Schulte, P. Lichtner, S.C. Rossle, N. Klopp, E. Wolf, K. Seppi, W. Pirker, S. Presslauer, B. Mollenhauer, R. Katzenschlager, T. Foki, C. Hotzy, E. Reinthaler, A. Harutyunyan, R. Kralovics, A. Peters, F. Zimprich, T. Brucke, W. Poewe, E. Auff, C. Trenkwalder, B. Rost, G. Ransmayr, J. Winkelmann, T. Meitinger, and T.M. Strom. 2011. A mutation in VPS35, encoding a subunit of the retromer complex, causes late-onset Parkinson disease. *Am J Hum Genet*. 89:168-175.

Ziviani, E., R.N. Tao, and A.J. Whitworth. 2010. Drosophila parkin requires PINK1 for mitochondrial translocation and ubiquitinates mitofusin. *Proc Natl Acad Sci U S A*. 107:5018-5023.